INFORMATION TO USERS

This manuscript has been reproduced from the microfilm master. UMI films the text directly from the original or copy submitted. Thus, some thesis and dissertation copies are in typewriter face, while others may be from any type of computer printer.

The quality of this reproduction is dependent upon the quality of the copy submitted. Broken or indistinct print, colored or poor quality illustrations and photographs, print bleedthrough, substandard margins, and improper alignment can adversely affect reproduction.

In the unlikely event that the author did not send UMI a complete manuscript and there are missing pages, these will be noted. Also, if unauthorized copyright material had to be removed, a note will indicate the deletion.

Oversize materials (e.g., maps, drawings, charts) are reproduced by sectioning the original, beginning at the upper left-hand corner and continuing from left to right in equal sections with small overlaps. Each original is also photographed in one exposure and is included in reduced form at the back of the book.

Photographs included in the original manuscript have been reproduced xerographically in this copy. Higher quality 6" x 9" black and white photographic prints are available for any photographs or illustrations appearing in this copy for an additional charge. Contact UMI directly to order.

UMI

A Bell & Howell Information Company
300 North Zeeb Road, Ann Arbor MI 48106-1346 USA
313/761-4700 800/521-0600

THE DESIGN AND SYNTHESIS OF MACROCYCLES FOR USE AS COMPONENTS OF ION TRANSPORTERS

by

Lynn Michele Cameron
B.Sc., Saint Mary's University, 1986
M.Sc., McMaster University, 1990

A Dissertation Submitted in Partial Fulfillment of the
Requirements for the Degree of

DOCTOR OF PHILOSOPHY

in the Department of Chemistry

We accept this thesis as conforming to the required standard

Dr. T.M. Fyles, Supervisor (Department of Chemistry)

Dr. A. McAuley, Departmental Member (Department of Chemistry)

Dr. P.C. Wan, Departmental Member (Department of Chemistry)

Dr. J.N. Owens, Outside Member (Department of Biology)

Dr. L. Weiler, External Examiner (University of British Columbia)

University of Victoria

Supervisor: Dr. T.M. Fyles

ABSTRACT

The thesis describes the development of a new set of macrocycles that could be used as part of an existing modular set of components, that when assembled, probe the structure-activity relationship of ion transporters. A property directed synthesis approach was adopted in which the properties, rather than the specific chemical makeup of the final target, guide the synthetic path. This allows for incorporation of the favorable properties and avoidance of the troublesome aspects of the current set of macrocycles into the synthetic design of the new modular components. As components in a modular set, the macrocycles are required in sufficient yield, so the property directed synthesis must provide an economical and efficient route to the targets. Molecular mechanics was used as a tool to estimate the length and rigidity of the macrocyclic systems. The design was also dictated by the need to incorporate high yielding methods for macrocyclization into the synthesis. All targets are formally meta cyclophanes involving overall axial symmetry to limit regioisomerism.

The syntheses of **23**, **25**, **27**, and **28** were based on the macrocyclization of bis-α-halo amides with bis-nucleophiles. Target **22** incorporated the bis-chloroamide of *meta*-phenylene diamine and a diol **23** derived from 1,3 bisbromomethyl benzene and butane diol. Conditions sufficient to deprotonate **23** apparently resulted in concomitant deprotonation of the amides leading to complex mixtures of products. Based on these observations the secondary amides of **23** were replaced with the homologous N-Me tertiary amides to give target **25**. As anticipated, macrocyclization

of **23** and the bis chloramide of N,N' dimethyl metaphenylene diamine gave **25a** in a yield of 7%.

The design requires additional functional groups at the 5 and 5' positions of the cyclophane. The chemistry leading to combinations of nitro and *t*-Boc protected amino groups in these positions was explored. Additional side reactions of the alkoxide nucleophile with nitro substituted aromatics precluded the desired macrocyclization reactions, and in all cases complex product mixtures were obtained.

Additionally, the diol component **23** was replaced with a diol **26** of similar length in which the ether linkages were replaced by secondary amides. This gave a further target **27**. In this series as well the side reaction of alkoxide with the nitro aromatic resulted in destruction of starting materials without production of product macrocycle. A corresponding target incorporating a dithiol in place of the diol **23** was explored in a preliminary fashion, but the physical properties of the dithiol complicated the purification of the precursor.

The synthesis of a series of tetraester macrocycles derived from isophthalic acid and diols was explored. Direct condensation of 5-nitro isophthaloyl chloride and 1,8-octanediol gave a series of symetrical 2+2, 3+3, and 4+4 tetraesters in high conversion. A step-wise synthesis from the mono-tetrahydropyranyl derivative of 1,8-octane diol gave the 2+2 macrocycle **67** substituted with nitro and *t*-Boc protected amino in the 5 and 5' positions in an overall yield of 16%.

The efficiency of the synthesis of **67** is analysed using plan graphs as initially described by Hendrickson for natural products synthesis. The synthesis plan is compared with the actual performance in terms of reagent consumption, total weight manipulated, and the time for the synthesis. These results are compared with the synthesis of a comparable target in the existing series of macrocycles. Although tetraester **67** is somewhat less efficiently prepared than earlier examples, it is better functionalized to lead to candidate ion transporters.

Examiners:

Dr. T.M. Fyles, Supervisor (Department of Chemistry)

Dr. A. McAuley, Departmental Member (Department of Chemistry)

Dr. P.C. Wan, Departmental Member (Department of Chemistry)

Dr. J.N. Owens, Outside Member (Department of Biology)

Dr. L. Weiler, External Examiner (University of British Columbia)

TABLE OF CONTENTS

LIST OF TABLES

LIST OF FIGURES

LIST OF SCHEMES

LIST OF ABBREVIATIONS

Ar	aromatic
DMA	N,N′-dimethylacetamide
DMF	N,N′-dimethylformamide
DMSO	dimethylsulfoxide
IR	infrared
Me	methyl
mp	melting point
ms	mass spectrum
nmr	nuclear magnetic resonance
t-Boc	*tert*-butyloxy carbonyl
THF	tetrahydrofuran
Thp	tetrahydropyranyl
TLC	thin layer chromatography

ACKNOWLEDGEMENTS

I would like to thank my supervisor Dr. T. Fyles for his patience, guidance and encouragement throughout this work. Thanks are extended to Scott Buckler for preparing many of the starting materials and to Danny Lau for help with the sulfur chemistry. I wish to thank the chemistry department staff and faculty, in particular Mrs. Christine Greenwood and Dr. David McGillivray. I thank K.E.Laidig and fellow graduate students especially B.Cameron, L.Clouston, K.Coulter, R.Hooper, D.Loock, P.Montoya-Pelaez, X.Zhou and B.Zeng for insightful discussions throughout the course of this work. Financial assistance from the University of Victoria was much appreciated.

CHAPTER 1

INTRODUCTION TO ION TRANSPORT

1.1 Ion Transport

Biological membranes are necessary to separate cells and cell compartments, but in order to maintain the complex biological processes, the cells must communicate with each other. Communication between the cell components occurs through the exchange of ions or molecules and these substances must pass through the membrane barrier. In general, membranes are impermeable to ions because of the high energy barrier that must be overcome to traverse the bilayer. Thus transporters act as catalysts by lowering this energy barrier and discriminantly allow ions to pass. With few exceptions, most natural channels are large proteins or protein aggregates, the structures of which are still being investigated [1,2,3]. Little is known on the molecular level of the structure and control of ion channels[4] so through the study of artificial model systems that mimic the function of the more complex system, insight into the biological process may be obtained. Of those few exceptions mentioned above, smaller natural products such as gramicidin A or amphotericin B have been widely studied and provide the basis for much of the structural design of the mimics[5,6,7].

For as many ion transporters exist, there are probably as many mechanisms for transport to occur. The two extremes are shown in Figure 1. These two basic mechanisms for transport are the channel mechanism or carrier mechanism. The structural requirements for a transporter vary depending on the mechanism. For instance, a channel must span the thickness of the bilayer. A carrier may be envisioned

as complexing the ion, diffusing through the bilayer and releasing the ion on the other side. It is often difficult to distinguish between the two modes of action but the transport kinetics may provide some insight. Ions may flow through a channel unhindered at a rate of 10^7 s^{-1}, as in the case for gramicidin, whereas carriers typically move less than 10^3 ions s^{-1} because the ion-carrier complex must diffuse through the lipid. Carriers have been widely studied and there are several reviews on the subject[8].

This thesis deals with the design and synthesis of artificial transporters of alkali metal cations via channels across lipid membranes. A detailed discussion of ion channel transporters was published by Fyles and van Straaten-Nijenhuis[9]. A short, but concise review has recently been published by Gokel[10]. This chapter introduces the structure and mechanism of some natural transporters that provide the basis for the design rationale and synthesis of artificial channels. This is followed by a short review of synthetic transporters.

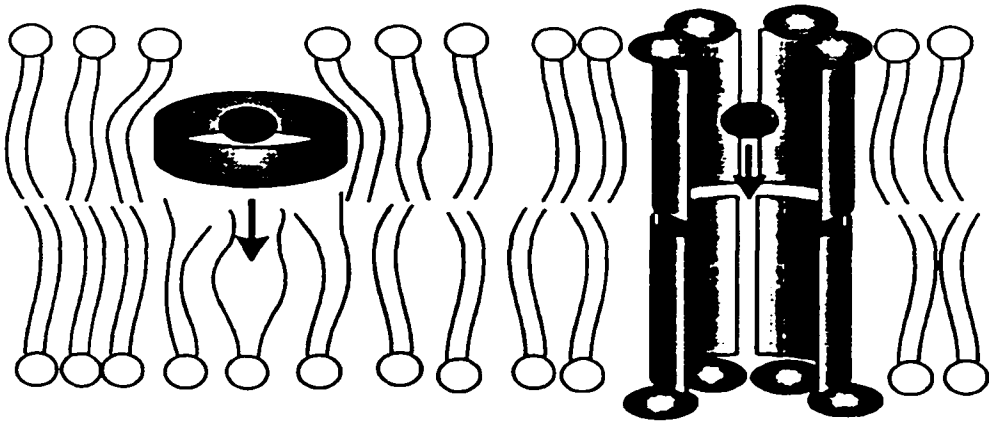

Figure 1. Mechanisms for Ion Transport

1.2 Examples of Low Molecular Weight Channel Forming Compounds

1.2.1 Gramicidin A

Gramicidin A is a cation selective transporter. The active form of the transporter is a peptide dimer consisting of 15 alternating D- and L- amino acid residues each, linked through hydrogen bonds at the N terminus. The polypeptide forms a β-helix 26Å long with a pore diameter of 4Å (Figure 2)[11]. It is believed that the carbonyl groups line the inside of the pore creating a hydrophilic environment suitable for water and cations, while the hydrophobic side chains interact favourably with the lipophilic membrane.

1.2.2 Amphotericin B

Amphotericin B is an example of a small non-peptidic transporter. It is a macrocycle composed on one face of hydrophobic polyene and on the other face of a hydrophilic poly alcohol. It is believed that 12-20 molecules of amphotericin aggregate to form a pore[12] in such a fashion that the hydrocarbon face interacts with the lipid and the alcohols orient inwards to line the pore. The alcohols thus create a polar opening through which the cations may flow. There is a high degree of organization involved with amphotericin as two aggregates must dimerize to form a channel (Figure 2).

a)

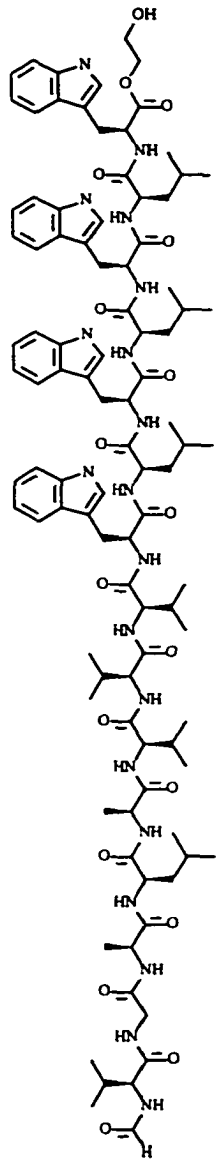

b)

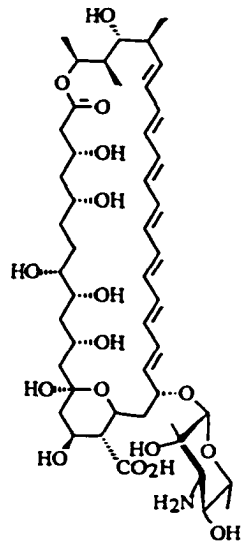

Figure 2: a)Gramicidin, b)Amphotericin

1.3 Artificial Ion Channels

1.3.1 Design Criteria

Artificial channels are functional mimics and most often do not resemble the natural systems in composition, but rather possess the same physical qualities that allow them to perform their function. The design criteria for artificial ion channels are: 1) the assembled channel must span the thickness of the bilayer, 2) there must be a polar group at the bilayer interface, 3) there must be a complementary balance of polar and apolar groups, 4) they must incorporate into the membrane and then adopt the correct orientation once inserted and 5) from a practical standpoint, they must be synthetically feasible. The extent to which points 1-4 are important is unknown, hence the need for further investigation.

The remaining sections of this chapter will be divided into three sections of ion channel design. The first section describes a family of molecules that are believed to dimerize to form a channel. In general these molecules are designed to span half the thickness of the bilayer. The second section is dedicated to the group of molecules which aggregate to form a pore through the bilayer These molecules are often characterized by the intermolecular interactions which force them to self-assemble. The third section is dedicated to those which are believed to operate as single molecule channels, that is, the molecule forms a tunnel and is designed to span the width of the bilayer. These are typically large synthetic molecules, on the scale of 4000 daltons. It is difficult to separate the molecules into these groups and the authors referenced

herein often only speculate on the mechanism. To date only two groups (Fyles[7,13], Gokel[14]) have undertaken a structure-activity study which is necessary to investigate the sensitivity of the channels to changes in structure and to gain a better understanding of the channel property design criteria.

The synthetic transporters are studied in biomimetic membranes which consist of suspensions of lipids in water to form vesicles or planar bilayers that are formed by painting the lipid across a teflon plate with a small hole[15]. Kinetics from vesicles provide information on overall activity, while planar bilayers focus on rates of ion transport through single active channels[16].

1.3.2 Channels Formed From Dimers

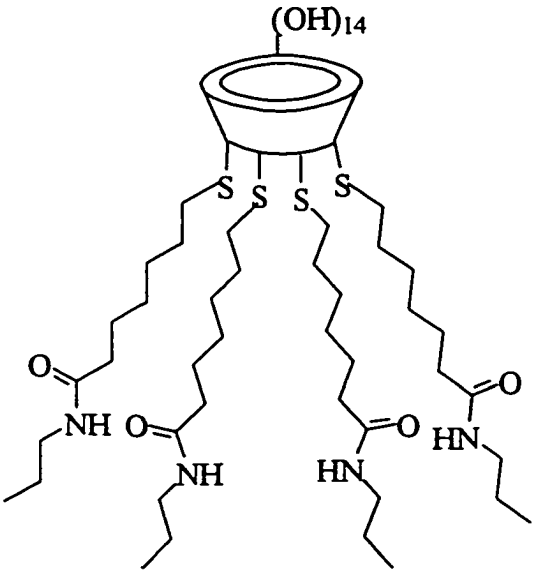

Figure 3: Tabushi's Cyclodextrin channel[17]

The earliest artificial transporters were dimer channels based on a tetrasubstituted β-cyclodextrin published by Tabushi[17] and coworkers in 1982, shown in Figure 3. The cyclodextrins are cyclic cone shaped molecules made up of 6, 7 and 8 α-D-glucose units, referred to as α-, β- and γ-cyclodextrin respectively, and the diameter of the hole in each is approximately 4.5, 7.0 and 8.5 Å respectively. The β-cyclodextrin having a pore diameter of 7 Å would then allow the passage of alkali metal cations, hydrated cations and some small molecules. The 14 hydroxyls of the secondary face of the cyclodextrin serve as the polar head group and would be expected to locate at the membrane/aqueous interface. The total length of the dimer is

estimated to be about 38Å. The thioethers and amides provide ionophilic sites to move the Ca^{2+} / Cu^{2+} ions along the channel.

Kobuke's channels[18] are similar in design (Figure 4) but the pore size is governed by a calix-4-arene. There are 4 alkyl (C_{17}) chains which would be long enough to span half the thickness of the bilayer. They propose dimer formation where the phenolic hydroxyls are the polar head groups. The compound had to be applied to

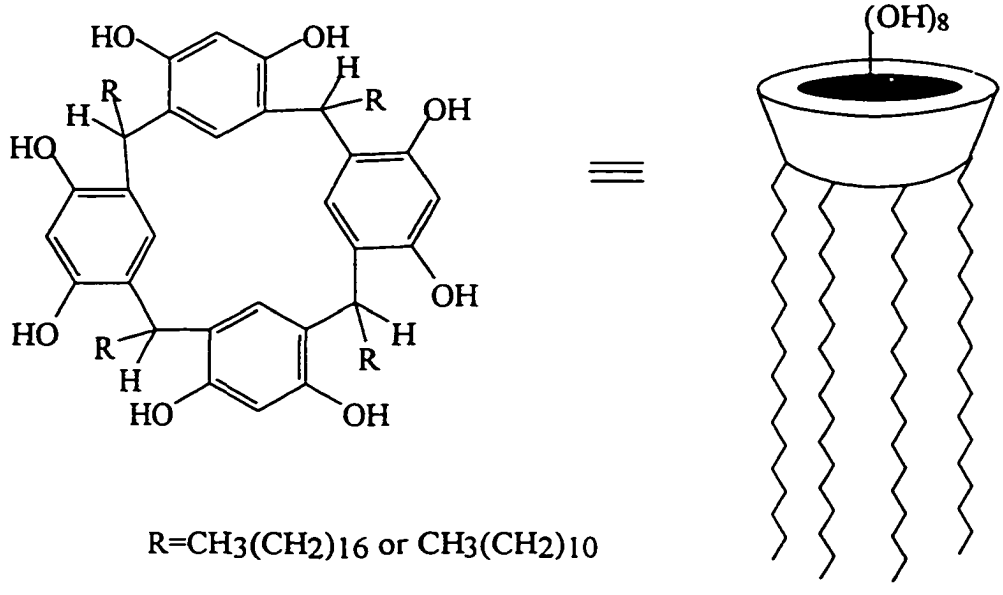

Figure 4: Kobuke's Calixarene Based Channel[18]

both sides of the bilayer in order to exhibit any activity and rationalization for this was the compound could not easily diffuse through the membrane. The channel was investigated as a transporter for both Na^+ and K^+ ions and was shown to be selective for K^+. It is important to note that a shorter alkyl chain (C_{11}) did not support stable ion transport. An explanation for this is that it is too short to span the bilayer.

Woolley et al.[19] demonstrated structural control over ion transport by modifying the widely studied gramicidin channel to investigate the regulatory effects of positively charged substituents and different conformational isomers at the mouth of the channel. Ethylene diamine, propylamine or piperazine were bound at the C terminus via a carbamate linkage and it was shown that the positively charged groups as well as the cis-trans isomerization of the carbamate controlled the flow of cations through the channel.

1.3.3 Aggregate Pores

Fyles et al. have adopted a modular synthetic approach to both the pore formers[7,20] and single molecule channels[13,21,22]. Both are composed of polar head groups , wall units and core linkers as depicted in Figure 5. The same wall units and polar head groups can in principle be used as building blocks in the pore formers and in the unimolecular channels. A structure-activity relationship was published in 1994[20] in which 14 of the possible 24 bolaamphiphiles were assembled using the modular approach and investigated for transport activity. Conclusions were drawn concerning the structural requirements for efficient ion transport. Macrocyclic wall units were chosen to impart internal rigidity (structural control) to the system. It was hypothesized that differences in the lipophilicity of the wall units, in the hydrogen bonding capability of the spacers and in the head group size and charge were important. Of the wall units investigated, **1**, **2** and **3**, vary in their degree of hydrophobicity in the order **3**<**2**<**1**. As evidenced by the transport activity, they found

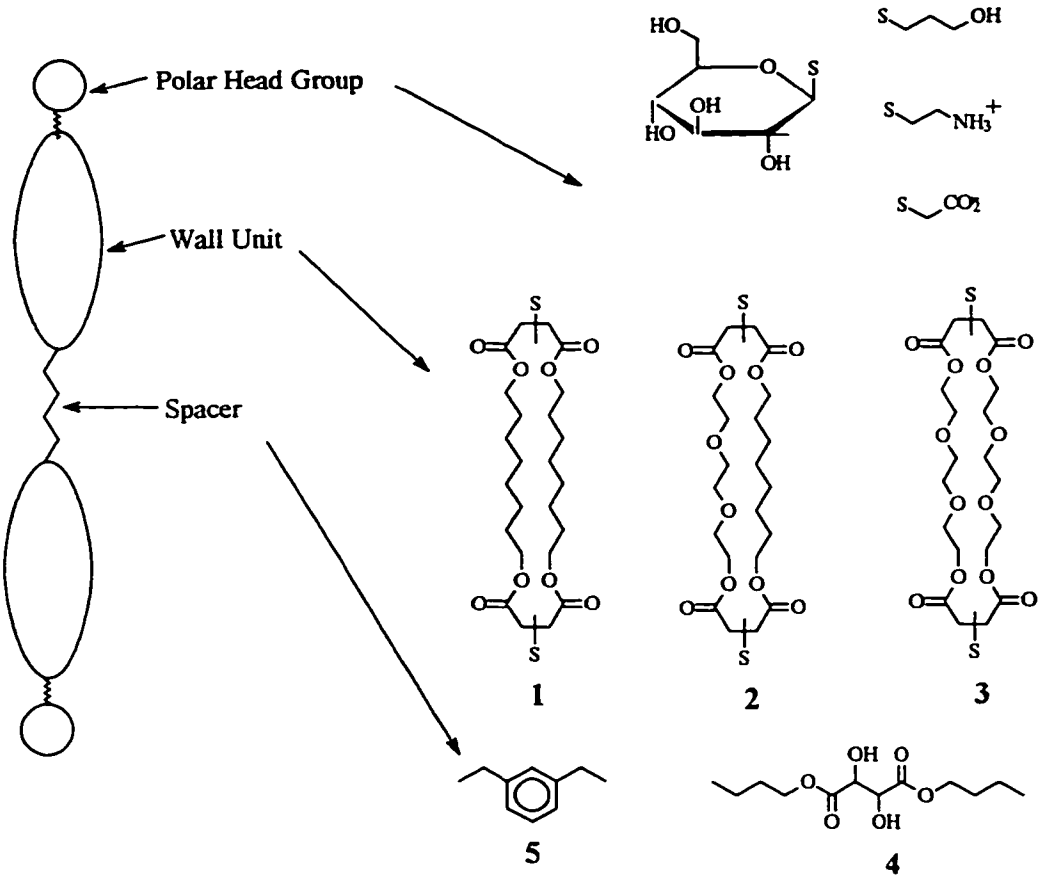

Figure 5: Fyles Suite of Pore Formers[7,20]

that wall units **1** and **2** were similar but more active than **3** and that in general the spacer with the hydrogen bonding capability **4**, was a better spacer than **5**.

Perhaps the most simple channel to date, from a synthetic perspective, has been achieved by Menger[5]. The channels have the general structure $RO(CH_2CH_2O)_nR'$ where R, n, and R′ are varied. The best results are obtained when $R=CH_3(CH_2)_{10}C=O$, n=5, and $R'=-CH_2Ph$. Because the "ion-conducting segment", the poly(oxyethylene), is only long enough to span half the bilayer a minimum of 2 molecules would be required for transport. It does not require a huge leap of the imagination to see that this transporter vaguely resembles the amphotericin structure although the authors do not allude to this possibility. Transport was lost if

R=R′=dodecanoyl or if R=R′=Bz or if R=$CH_3(CH_2)_4C$=O and the activity was impaired if n=3. The authors conclude that the benzyl group is necessary to interact with the membrane polar head groups (quaternary N) by ion -dipole interaction. It would be interesting to know what the effect would be if it were substituted by a hydrogen.

Kobuke[23] describes an ion channel that is composed of aggregates of the ion pairs of a poly(oxybutylene) with a carboxylate group at one end , and a quaternary ammonium group disubstituted with two long alkyl chains (C_{18}) (Figure 6). The two lengths investigated, n=2 and n=3, resulted in overall lengths of 24 and 30Å respectively and both were equally active. The long alkyl chains on the ammonium nitrogen provided the hydrophobic regions for incorporation into the membrane. They propose the ion pair was incorporated into the bilayer followed by self-assembly where the polar groups formed a pore through which the ions could pass (Figure 6). The channels were selective for cations. Substituting the carboxylate head group for a phosphate[24] opened the possibilities for a voltage gated channel.

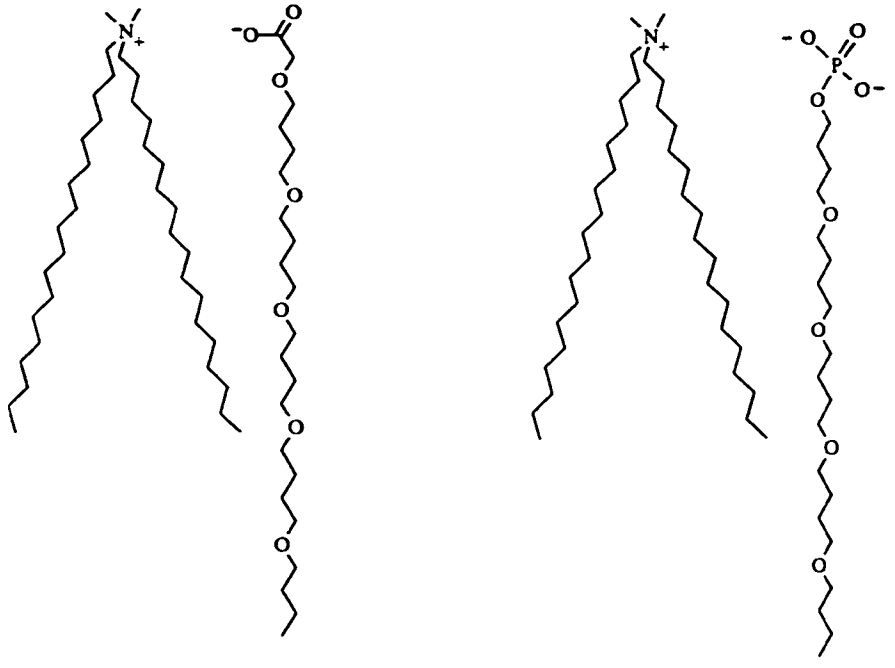

Figure 6: Kobuke's Ion Pair Aggregates[23,24]

In 1993 Ghadiri reported[25,26,27] a self-assembling nanotubular array of cyclic peptides capable of ion transport (Figure 7). The macrocyclic peptides were composed of 8 alternating D- and L- amino acids which formed a flat ring that would stack one on top of the other and would be held in place by 8 alternating donor / acceptor hydrogen bonds to each face. The amide backbone is perpendicular to the plane of the ring with the R groups of the amino acids anchoring the assembled channel in the lipid. These channels were reported to transport Na^+ and K^+ almost 3 times faster than gramicidin A. When 8 amino acid residues were used, a pore diameter of approximately 7.5 Å was formed. The properties of the resulting channel may be altered according to the number and type of amino acids used[28]. A molecular dynamics study[29] has shown the aggregate to be fairly rigid and upon minimization the

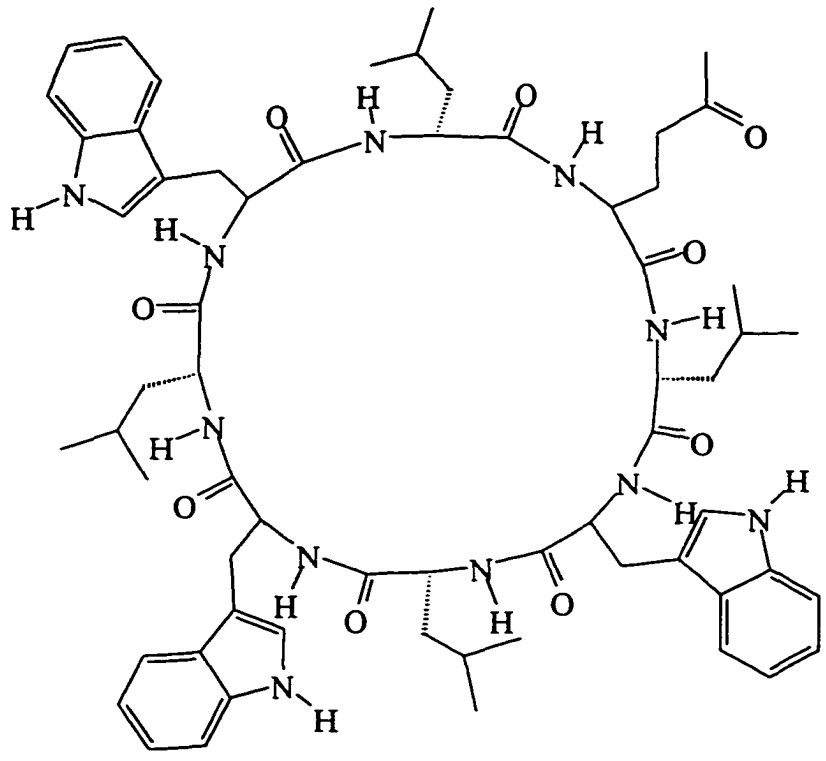

Figure 7: Ghadiri's Cyclic Peptide[26]

tube-like structure does not rearrange. Simulations also found that water molecules placed inside the cavity did not compete for the hydrogen bonding sites.

Regen has designed a steroid based amphotericin mimic[6]. The steroid has two side chains composed of poly(oxyethylene) subunits (Figure 8). The steroid moiety is expected to enter the bilayer, incorporating at least one of the hydrophilic chains (Scheme 1). This structure resembles amphotericin in principle by possessing a lipophilic face and a hydrophilic face. In fact, the activity was less than that for amphotericin.

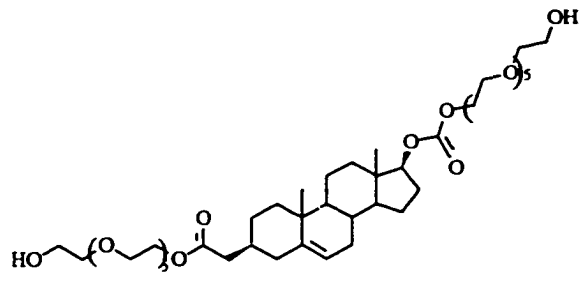

Figure 8: Regen's Steroid Based Transporter[6]

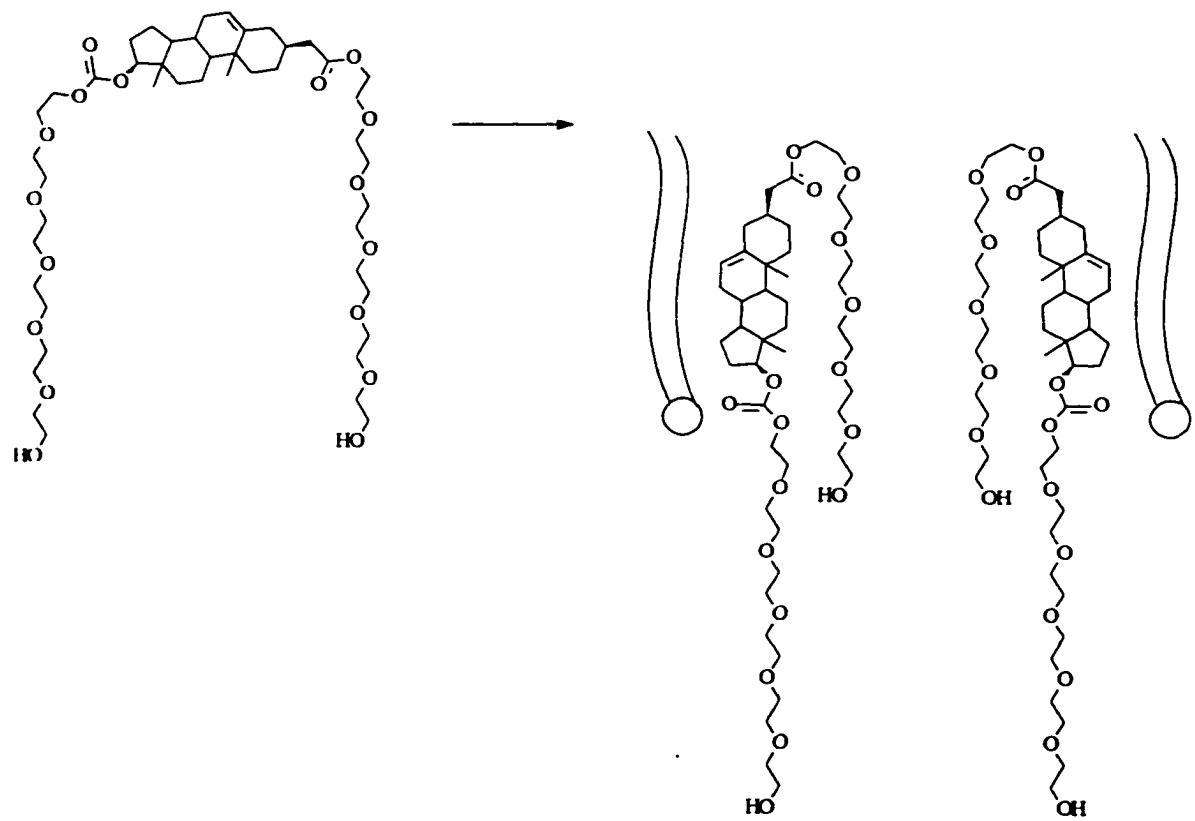

Scheme 1: Regen's Steroid Incorporated Into Lipid[6]

1.3.4 Single Molecule Channels

All single molecule channels to date have had two characteristics in common. First, as stated above, they must span the thickness of the bilayer. Second, each end of these channels are sufficiently hydrophilic to interact with the aqueous medium on either side of the bilayer thus anchoring the channel in place. The importance of the other design criteria are less straightforward to explore and have as yet to be resolved. However, as with the dimers and aggregate pores, it is believed that the interior of the channel must provide both hydrophilic (to complex with ions and allow their passage) and hydrophobic (to interact with lipid) regions.

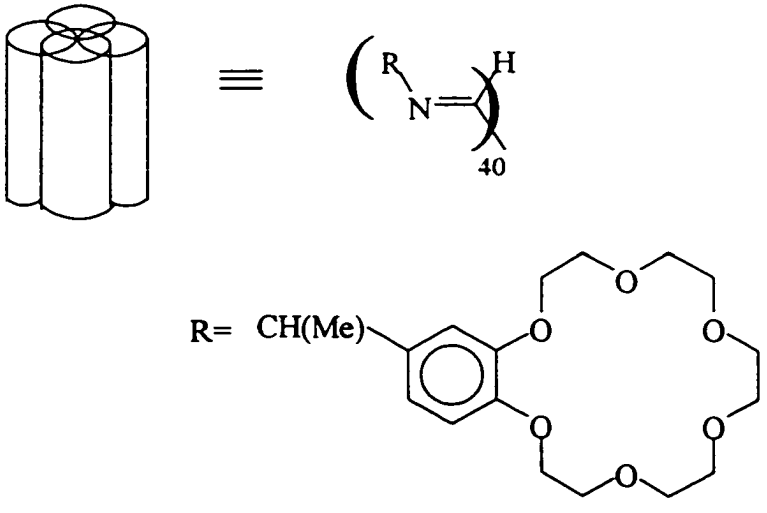

Figure 9: Nolte's Isocyanide Polymer[30]

The first non-peptidic single molecule channel was prepared by Nolte et al[30,31]. The isocyanide polymer, substituted at each residue with a crown ether, could potentially have 4 functioning channels per molecule. The polymer adopts a helical conformation completing one full turn every 4 residues. They built structures composed of 40 monomers resulting in a length of approximately 40 Å (Figure 9).

The most complete structure-activity study of single molecule channels to date has been accomplished by the Fyles group[13,21,22]. The ion channels were assembled having the basic structure as shown in Figure 10 which was a hexa-, tetra- or di-substituted 18-crown-6 ether (18-C-6) prepared from **10**. The channel consisted of a core acid. This 18-C-6 could act as the filter. In other words, ion transport selectivity could be governed by the crown ether and display a similar trend to cation selectivity in ion binding. Structural control was also investigated by changing the stereochemistry at the core, ie. **6** vs **7** and **8** vs **9**. Linked to the core were a variety of possible macrocyclic wall unit structures that were varied in their hydrophobic/hydrophilic content and in their length. The polar head groups investigated were the same as those used in the pore formers[7,20]. Using a modular approach cores, walls, and head groups could be mixed and matched to properly assess the demands of a functioning channel and optimize those requirements. Twenty-one of the possible one hundred compounds were prepared. Careful interpretation of the data revealed that some of the subunits routinely displayed poor activity; these are the wall units **14** which possibly are too long and **12** which may be too hydrophilic. They also demonstrated that all components of the channel are necessary by testing partially built modules for transport. The most active wall units appeared to be **10** and **11**. It is these wall units from which the designs in this thesis take root.

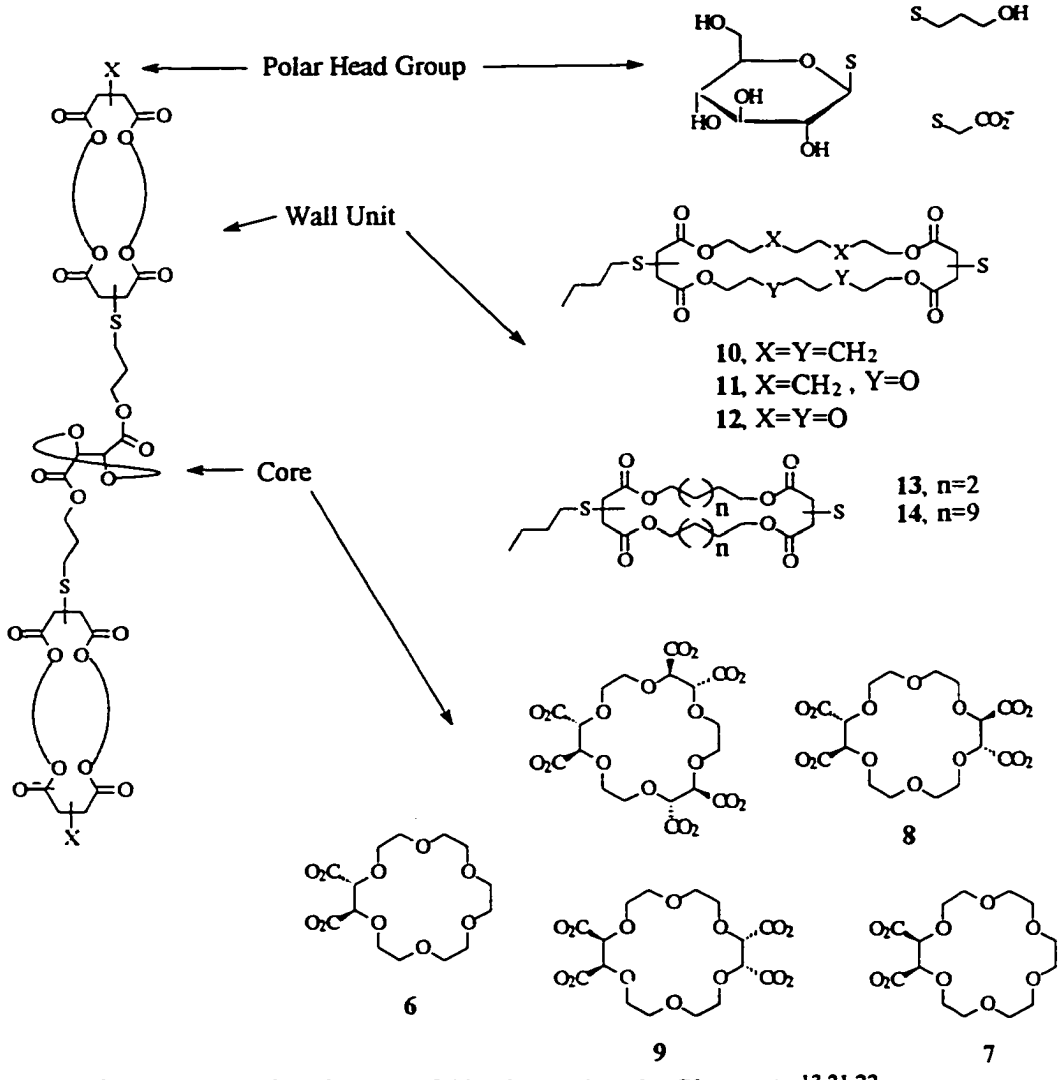

Figure 10: Fyles Group of Single Molecule Channels [13,21,22]

Jullien and Lehn have designed a channel[32] (Figure 11a) in analogy to the Fyles' channels. The basic design may be thought of in the same way with an 18-C-6 core and four wall units oriented axially from the core. It acts as both a hydrophilic complexation site for the cations as well as serving to select the cations that may pass. The poly(oxyethylene) chains also provide binding sites for cations. The length of the chains is again governed by the thickness of the bilayer. The wall units contain phenyl

groups that provide some rigidity for the system and also serve as a chromophore for easy UV detection in the membranes. The amides provide increased rigidity and the n-butyl group of the tertiary amides increase the lipophilicity. Carboxylate anions provide good anchors by interacting with the aqueous medium at each end of the channel and should ensure the molecule spans the bilayer. Molecular modelling suggests the fully extended length of the molecule is 45-50 Å.

Lehn further investigated this type of structure but changed the 18-C-6 core by replacing it with a β-cyclodextrin (Figure 11b). In Lehn's design[33,34] the wall units are attached via an ester linkage to seven primary hydroxyls on the narrow rim and to seven of the available fourteen secondary hydroxyl's on the wide mouth of the cavity. This provides a total of fourteen wall units (seven up and seven down). Carboxylate serves as the polar head group and either poly(oxyethylene) units or polymethylene units make up the rest of the arm. The phenyl groups are present for rigidity and as a UV chromophore. The total length of the channel was estimated to be approximately 50 Å in length. When tested for transport activity[35] the poly(oxyethylene) was very similar to the polymethylene analogue. These results are similar to the results obtained with the Fyles suite of wall units[13]. As far as Na^+ and Li^+ transport is concerned there was no significant difference in any of the molecules. All transport rates were very slow, on the order of 10^{-3} min^{-1}. The smaller molecules that were not long enough to span the bilayer were confirmed carriers. This is in accordance with the design.

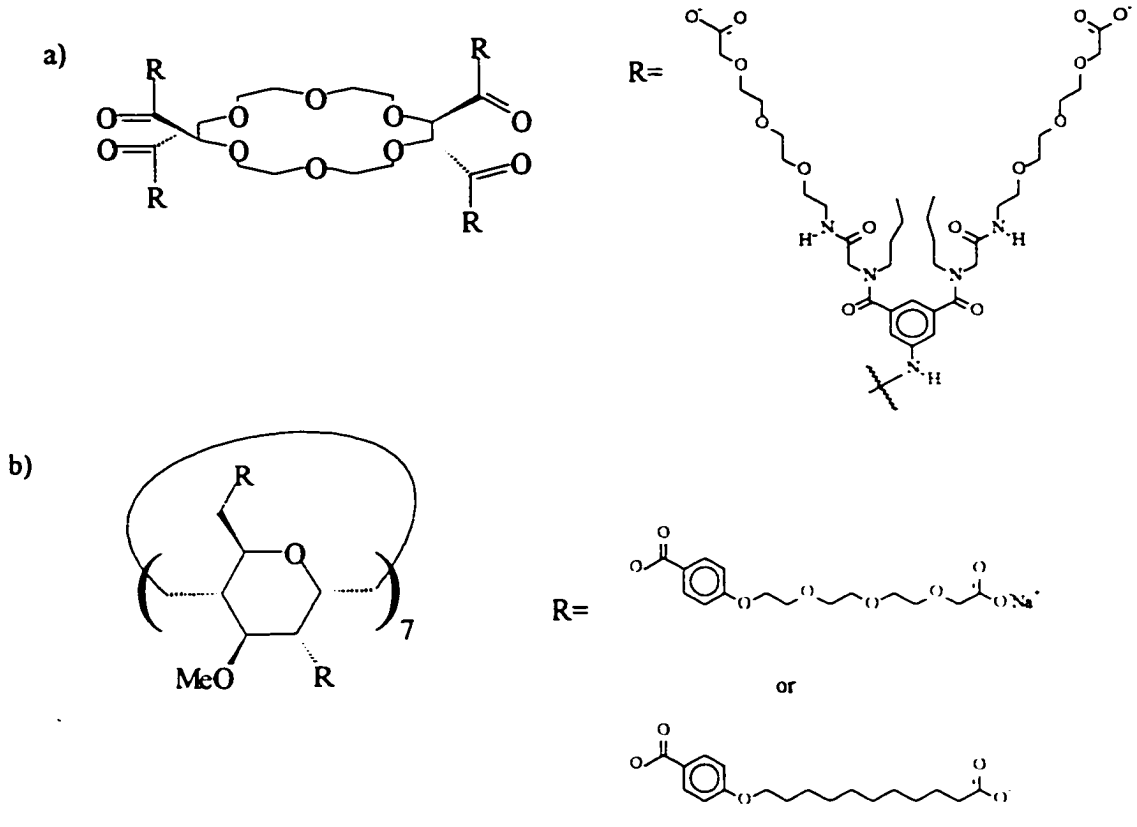

Figure 11: Lehn's Channels, a)18-Crown-6 Based Structure[32]. b)Cyclodextrin Based Structure[33,34]

Gokel et al[36] designed a channel (Figure 12) based on three diazacrown subunits. They propose that a hydrophilic crown at both ends would fix the channel in the bilayer. Another crown at the midpoint would provide a hydrophilic site for complexation of the cations. The length of the spacers and sidearms between the crowns correspond to the thickness of the bilayer. The hydrophobic sidearms and spacers also ensure the incorporation of the transporter into the hydrophobic lipid bilayer. Transport of Na^+ was approximately 4 fold less active than gramicidin A.

Starting from the active compound **15**, Gokel investigated the structure-activity relationship[14] by testing compounds that vary in one of the structural units. If compound **15** is viewed as having the basic structure as shown in Figure 12 then to test the design criteria they varied the sidearms, R (Bn, H, cholesterol-ether linked, and cholesterol-ester linked). One of the variations was to change the spacer from the hydrophobic polymethylene subunit **15** to a poly(oxyethylene) subunit **16**. It was thought that the more hydrophilic oxygens may help move the cations along. In fact, the more active transporter was **15**, the more hydrophobic compound.

Functional groups may be incorporated into the subunits to impart some control over channel openings. For example, two other structural variations of the channel **15** were to incorporate groups into the spacer so as to act as a gated channel. Instead of the channel remaining open, the cis-trans geometry of an amide **17** may open and close the channel. Also by incorporating an anthraquinone spacer unit **18** which is capable of accepting 1 or 2 electrons to form a stable anion, cation flow may be stopped due to the "blockage" of the channel. The central unit was changed from a diazacrown to a poly(oxyethylene) chain. The structural significance of the crown was also investigated using a smaller crown (15 membered). The sidearms were changed to benzyl groups to investigate the effect of aryl groups on transport. Compound **15** was found to be the best transporter when analyzed using fluorescence methods while compounds **16**, **17**, and **18** were comparable to gramicidin. The conclusion from this study was that a too hydrophilic interior is detrimental to transport. The reason is still unknown. One explanation may be the low solubility of

the more hydrophilic molecule in the lipid. The authors conclude that the channels require the component parts of **15** due to the lack of activity when parts are missing.

In order to address the question of whether the transporter is incorporated into the lipid the octanol-water partition coefficients were determined. Fortunately, all of the compounds were found to be completely soluble in the octanol. In an attempt to categorize the transporters as carriers or channels Gokel et al.[37] have compared the rate of transport across bulk $CHCl_3$ relative to the carrier valinomycin and with the rate of transport across a bilayer membrane relative to the channel gramicidin. Since the distance across the $CHCl_3$ layer was too great for a channel to span, then the fast rate in $CHCl_3$ and the slow rate in the bilayer was interpreted to be indicative of a carrier. It was previously postulated[14] that the transporter **19** acted as a channel and the benzyl ring stabilized the head groups by interaction with the polar head groups of the bilayer. They postulate that if the crowns are head groups through which the ions pass then changes in the electron density of the benzyl group should influence transport activity. Derivatives **20** and **21** were prepared and the electron withdrawing NO_2 group in **20** reduces the transport while the electron donating methoxy **21** in enhances the rate[37].

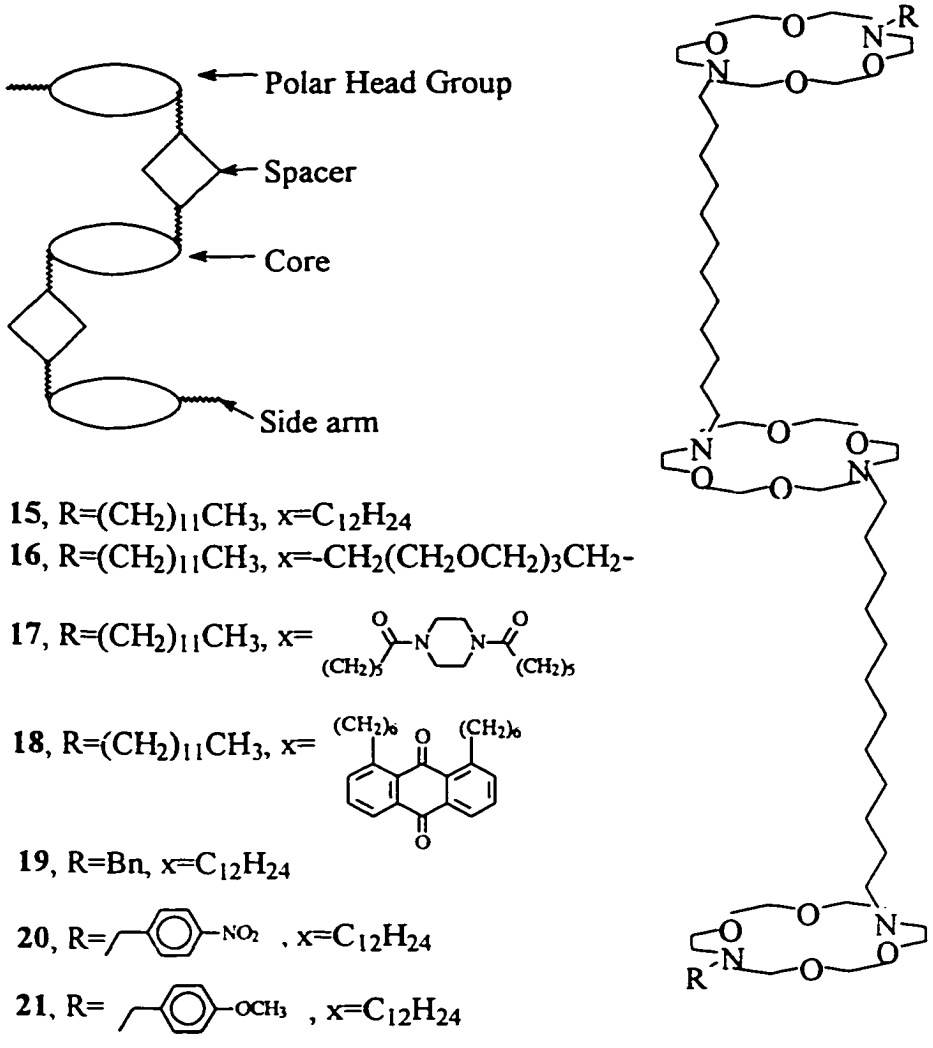

Figure 12: Gokel's Family of Single Molecule Transporters [14,36,37]

Similar to Nolte's helical crowns, Voyer recently exploited the helix forming ability of L-leucine and combined it with L-phenylalanine substituted with a 21-crown-7 moiety (Crown)[38]. The peptide sequence is *t*BOC-N(Leu-Crown-Leu-Leu-Leu-Crown-Leu)$_3$OMe. The crown ether phenylalanine residues are strategically placed so the crowns appear stacked, forming a crown ether pore adjacent to the helix as shown

in Figure 13. The N terminus is protected with a *t*-butyloxycarbonyl group and the C terminus is protected as the methyl ester. These protecting groups decrease the hydrophilic character of the helix and probably serve to increase the solubility of the compound into the lipid. Presumably the crown ethers interact with the aqueous medium outside the bilayer.

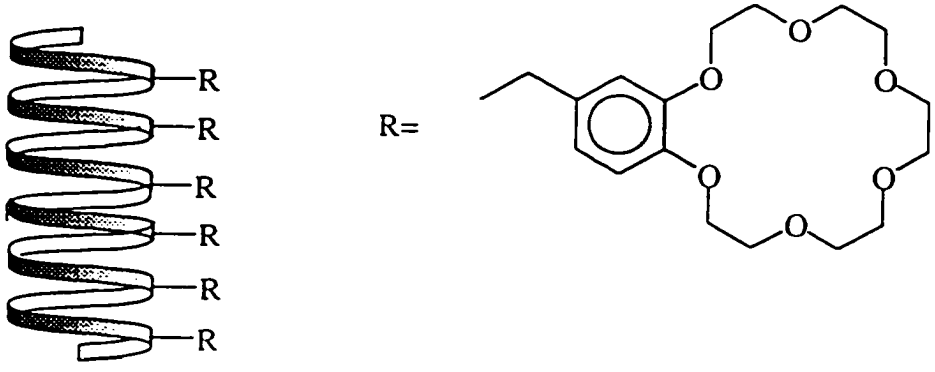

Figure 13: Voyer's Stacked Crowns[38]

1.4 Rationale for Synthetic Study

To summarize, a wide range of compounds facilitate transport. Channels may be categorized as two or more molecules that aggregate, as dimers, and as large single molecules Yet, these compounds have some properties in common; they all have a similar length, they all have polar head groups and they all have amphiphilic character. But the structure-activity studies are far from over. For example, most of the structural issues pertaining to mechanism remain unresolved. The needed structural and functional investigations will require the efficient synthesis of a wide variety of ion

channel mimics. Consequently, we need to explore facile, efficient synthetic pathways to ion channels.

CHAPTER 2

INTRODUCTION TO DESIGN AND SYNTHESIS

2.1 Design of Ion Transporters Via a Modular Assembly Approach

The modular approach to assembling ion transporters provides an efficient method for assessing the structural requirements for an active ion channel. As discussed in the introduction, the Fyles group has synthesized a number of macrocyclic wall units for this purpose. These wall units have been incorporated in both single molecule channels and in pore former molecules. Synthetically, the wall units are the most complex of the building blocks, especially in the aggregate pore family of molecules. For this reason, an efficient and easily modified method for obtaining macrocyclic wall units is desirable. The remainder of this dissertation is dedicated to the design and synthesis of macrocycles that can be used as wall units. The macrocycles discussed are not identical to those previously studied but are designed to preserve desireable features while also improving the efficiency of the synthesis. This will eventually lead to a new modular set for synthesis of new candidates for evaluation by structure-activity studies.

2.2 Strengths and Weaknesses of the Previous Wall Units

The previous set of macrocycles was designed to investigate the optimum length and lipophilic compatibility. A short-hand nomenclature consistent with the modular assembly was developed[39] to assist in identifying each structure. The wall

units all have the same basic structure shown in Figure 14. The label Trg represents triethylene glycol, the numbers 5, 8 and 12 represent the length of the methylene chain and the subscript 2 indicates both sides of the wall are the same. Of the wall units investigated, 5_2, 8_2 and 12_2 serve to investigate the length criteria. The wall units 8_2 and 8Trg were the most active of this set and were estimated to be 13.5 and 14.0 Å long respectively. This length will be incorporated into the design of the new systems. Conversely, the macrocycles 8_2, 8Trg and Trg_2 are all roughly the same length but vary in their degree of hydrophobicity. The most active transporters contained the 28 membered macrocycles 8_2 and 8Trg. The building block Trg_2 did not support transport and a rationalization is that it is too hydrophilic.

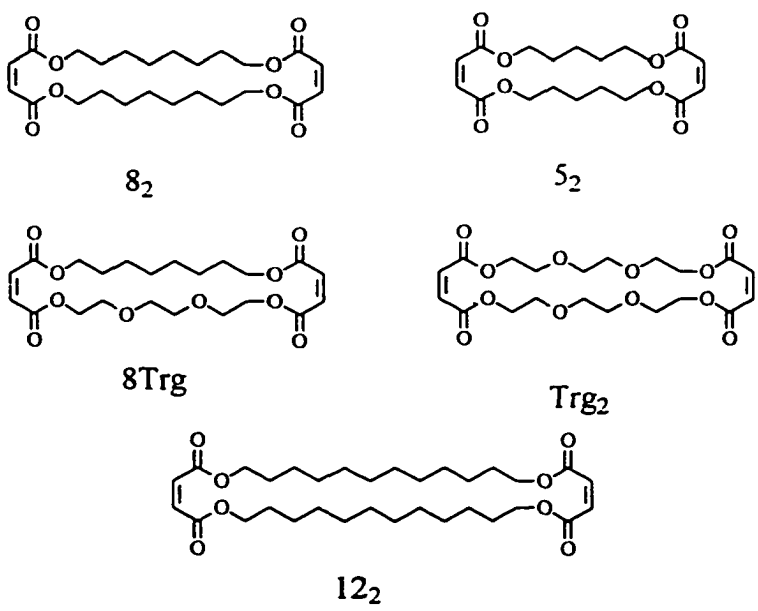

Figure 14: Previous Set of Wall Units

The yields of the more active macrocycles 8_2 and 8Trg from commercial precursors are 12% and 6.4% respectively[39]. In a second generation modular set it is

desirable to have much higher yielding macrocyclization reactions. Therefore, the new set of macrocycles should be designed to include methods capable of high yielding macrocyclization.

The most active linkers of the previous set of pore formers were derived from tartaric acid[20] and it was believed the hydrogen bonding capability of the linker may assist in the aggregation. Current work within the group[40] questions this conclusion but does not alter the basic goal of this dissertation. New wall units should be designed that may incorporate a variety of functionality so that investigation of hydrogen bonding capability in the wall units can be done. Functionality also could be incorporated to investigate rigidity or further investigate polarity and functionality issues.

An inherent flaw in the design of the previous set of wall units arises in the addition of cores or linkers and polar head groups. Although James[41] describes the Michael addition as being rather simple chemistry, there is no regio- or stereochemical control of the Michael addition of the sulfur nucleophiles to the maleate esters (Figure 15). In the case of 8Trg, where x and y are different, the addition of the head group and linker gives rise to 16 possible isomers. So when the wall units are incorporated into a transport molecule, for example, a pore former where there are two moles of macrocycle for every mole of transporter, then there are 16^2=256 possible structures. In the simpler case, 8_2, where there is a plane of symmetry (x=y), the number of possible isomers is 8. This is less than 8Trg but once two molecules are linked together then the number of possible structures for the transporter is still 8^2=64.

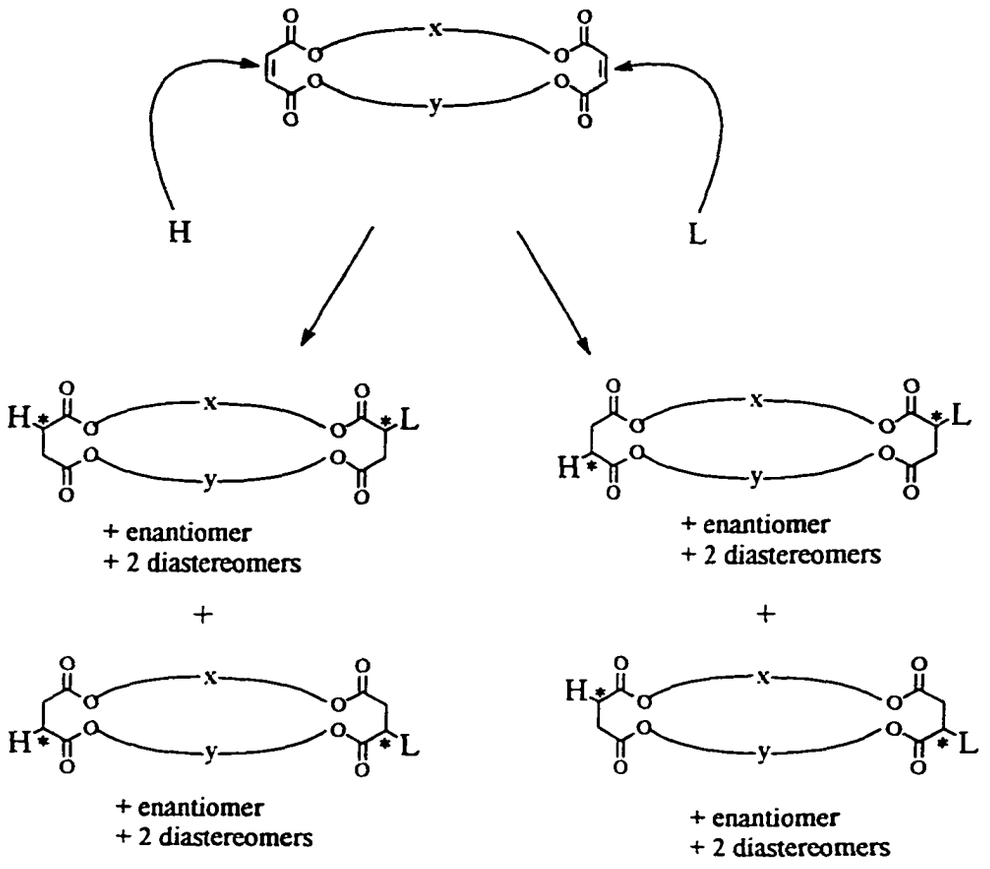

Figure 15: Stereo- and Regio- Isomers From Previous Set of Wall Units

This is a potential problem when drawing conclusions about the effect of the structure on the transport activity since it is possible to argue that of the multiple compounds present, perhaps only a fraction are active. The only way to tell is to separate and purify each compound. Obviously this is not a reasonable option as there are too many compounds with similar physical properties to perform even a crude separation. The numerous isomers appear to be very similar by nuclear magnetic resonance and gel permeation chromatography but the potential problem remains. The new wall units must avoid this problem by producing single isomers of the final targets.

2.3 Property Directed Synthesis

The approach taken in this thesis is the property directed synthesis approach as outlined by Gokel[42]. A property directed synthesis differs from a natural products or target directed synthesis in that the exact target is not dictated by structure but by function. This permits the "target" to be modified by the demands of the synthesis and so as long as it performs the desired function, the synthesis will have been achieved. Scheme 2 is a flow chart that demonstrates the typical sequence of events in a property directed synthesis. First a target is identified. In the context of this dissertation the target is a wall macrocycle of a certain length (between 15 and 17 Å) and sufficiently rigid so that it does not fold. This target should have a complementary balance of hydrophobic and hydrophilic subunits, and should have the potential to incorporate a variety of functionality to investigate the different properties (hydrogen bonding, rigidity requirements). In order that the transporters can be studied in detail, they must have an efficient, facile synthesis.

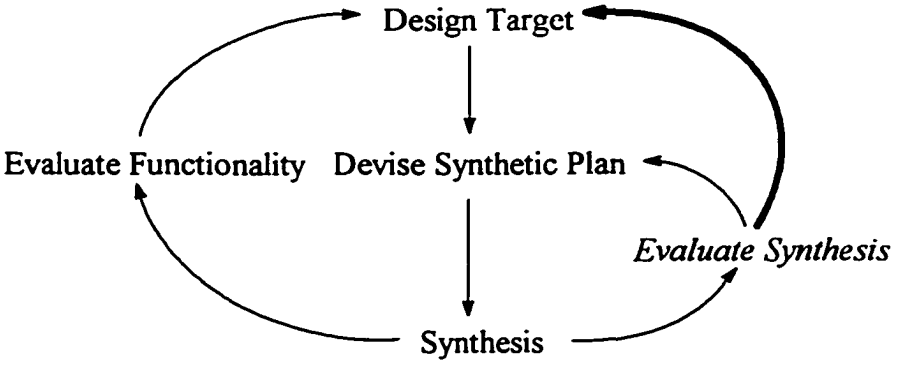

Scheme 2: Property Directed Synthesis

Once a target has been designed one must then devise a synthetic plan. In this case macrocycles are the target. When preparing the synthetic plan it should include methods that produce high yielding reactions so bulk material is available and readily incorporated as a building block into a transporter molecule. As with the synthesis of a previously unknown compound, the synthesis is constantly being evaluated and revised throughout the course of carrying out the plan.

Property directed synthesis differs from target directed synthesis such that not only can the synthetic plan be modified but also the structure of the target molecule may be changed in response to synthetic setbacks. This is possible because it does not matter what the actual structure is, only that it meets the predetermined requirements and performs the desired function. In this manner the synthetic path to a target will be optimized and a macrocycle will be obtained. The macrocycle will be assessed on the basis of structural properties and synthetic efficiency. Once a macrocycle is realized it may then be incorporated as a building block into potential transporter molecules, using a variety of linkers or cores and head groups, and the properties of the transporter may be evaluated. From this knowledge new macrocycles possessing different properties may be designed, synthesized and tested.

In practice then , we are using a property directed modular assembly approach to study ion transport. The flow chart in Scheme 2 is applied first in designing macrocyclic wall units, as in this dissertation, and then it may be subsequently applied to the actual transporters.

To summarize, the desired properties of the target wall units are that they be macrocycles available in high yield, preferably crystalline solids so they may be investigated structurally by X-ray crystallography, of a length between 15 and 17 Å, and that they in principle could incorporate a variety of functionality.

2.3.1 Introduction to Synthetic Efficiency

Typically in natural product synthesis a synthetic pathway is judged based on an overall yield from a defined starting material. If the overall yield is high, or higher than a competing route to the same molecule, then the synthesis is said to be efficient. The overall yield can be misleading because it takes into account the yields of the reaction starting from only one of the reagents. A paper published by Hendrikson in 1977[43] discusses the concept of efficiency more generally by examining the nature of the synthetic sequence, the number of steps, which is effectively a discussion of yields, the time required for each step including purification, and the cost and amounts of starting materials and reagents.

2.3.1.1 Nature of the Synthetic Sequence

The nature of the synthetic sequence pertains to the order in which the reactions are done and to the type of connections made. In order to examine this Hendrikson[43] uses a plan graph. Every dot on the graph represents an isolable intermediate and the dots are connected by lines that are indicative of the type of reaction. The different types of reactions are those that build the target skeleton and then there are extra steps which refunctionalize, protect and deprotect.

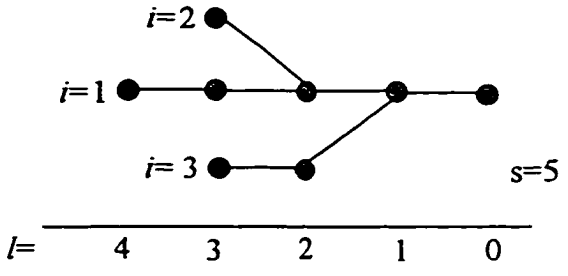

Figure 16: Example of a Plan Graph

Figure 16 is an example of the plan graph. There are *i* starting materials and on the graph they are labeled from *i*=1, 2, 3,...and up. They are assigned a rank, *l*, which corresponds to the number of steps they are away from the target. Horizontal lines connecting dots are counted as steps in the synthesis while diagonal lines are used to converge the synthesis. Figure 16 shows a plan for a synthesis from 3 starting materials that is completed in 5 steps. The target is at rank *l*=0 and the first starting material has the largest rank because it is furthest away from the target. The horizontal line containing *i*=1 is known as the main line. The 5 steps are a result of the four steps along the main line plus the step for starting material *i*=3 from rank *l*=3 to

l=2. Instead of calculating an overall yield which would presumably arise from the starting material with the largest rank, we calculate the total amount of starting material used (W). The overall yield from one starting material is the inverse of the amount of the starting material required to yield a mole of final product. For example, if an overall yield is 3% then 1/.03=33.33 moles of starting material is needed to produce 1 mole of target. In this analysis we take into account the amounts required of all the starting materials.

For the purposes of the analysis, one assumes an average yield of 80% per step, with the inverse of the factor 0.80 being 1.25. This means that in a one step reaction, 1.25 moles of starting material is needed to obtain 1 mole of product. If the reaction is a two step process then 1/(0.80 x 0.80)=1/0.64=1.56 moles of starting material is required. Since we are using an average, then steps known to give low yields may be treated as extra steps. For example, a monoprotection of a symmetrical precursor may be treated as 3 steps (0.80 x 0.80 x 0.80 = 0.51) since the statistical maximum yield is 50%. In some cases there are methods to get around this problem (for example, as the product forms it may be removed from the reaction mixture by distillation). If such methods are possible then higher yields are expected. Table 1 provides the calculated yields, y, inverse yields, x, and sum of inverse yields, S_l, for an average 80% yield at each step, l. Of course, if the real yields are known, then the actual performance can be calculated in the same way.

Table 1; Tabulation of predicted yields, inverse yields, and sum of inverse yields.

l	y	x	S_l
1	0.800	1.25	1.25
2	0.640	1.56	2.81
3	0.512	1.95	4.77
4	0.410	2.44	7.21
5	0.328	3.05	10.26
6	0.262	3.81	14.07
7	0.210	4.77	18.84
8	0.168	5.96	24.80
9	0.134	7.45	32.25
10	0.107	9.31	41.57
11	0.086	11.6	53.2
12	0.069	14.6	67.8
13	0.055	18.2	85.9
14	0.044	22.7	108.7
15	0.035	28.4	137.1
16	0.028	35.5	172.6
17	0.023	44.4	217.0
18	0.018	55.5	272.6
19	0.014	69.4	341.9
20	0.012	86.7	428.7

2.3.1.2 Materials

The weight (W_i) of the starting material (i) required to obtain 1 mole of target is $W_i=M_ix^{li}=Fn_ix^{li}$. F is a constant used to facilitate comparisons between different syntheses where all the details are not yet resolved. It is estimated to be 14 which is the weight of a CH_2 group or N. Oxygen atoms are underrepresented because their weight is 16 but the error is small and should be fairly consistent in the comparisons. The total weight of all starting materials (W_o) is given by $W_o=F\sum n_ix^{li}$, where n_i is the number of structural and heavy atoms in starting material i. Since F is a constant we can leave it out and discuss the relative weights obtained from $W=\sum n_ix^{li}$.

2.3.1.3 Reagents

In estimating the amounts of reagents used we work in molar amounts. Assuming a 1:1 stoichiometry of starting materials:reagents, a rough estimate may be produced. This is probably only useful if little is known of the synthesis. To do this the main line is taken as the line with the highest ranking starting material. A convergent plan has sublines that merge with the main line. In order that each intermediate is assigned to only one starting material , *i*, which passes through it, a new term (*l'*) is introduced. Each subline begins at rank *l* and ends at rank *l'* which is the rank of the last independent intermediate before it joins the main line. So the sum, $S_l=\sum x$, corresponds to the molar amounts of starting materials or reagents since we assume a 1:1 stoichiometry. So that we only count the reagents once, we need to take the sum of the difference of the molar amounts, which leaves the total number of moles of reagent as, $R=\sum \Delta S$.

2.3.1.4 Time

In general the time required for a reaction depends on the number of steps, s, and the amount of material manipulated. If we assume that the reaction times average out to a time, T_o, then the time, T, to reach a target may be written as, $T=sT_ou$ where u is an upscaling factor taking into account the weight. Hendrikson uses the exponential scaling factor that was used by Powers[44]. Powers found that $T \propto W^z$ where $z=0.3$. This is equivalent to saying that it takes twice as long to manipulate ten times the amount. So to calculate the time we need to know the weight of each synthon

each time it is part of an intermediate used in a reaction. The total weight manipulated, TW, becomes $F\sum n_i S_{li}$ but again F is a constant and can thus be ignored as we are comparing only the relative weights and the equation becomes, $TW=\sum n_i S_{li}$. The total weight TW divided by the number of steps, s, gives an average weight. This substituted into Powers' equation gives $T\propto(TW/s)^{0.3}$. So, substituted into Hendrikson's equation we get the approximate time ,$T=s(TW/s)^{0.3}$. Time is a relative measure and is useful in comparing two or more syntheses.

These ideas will be developed for the specific syntheses of this dissertation in Chapter 4. We will develop the corresponding synthetic graphs and calculate the actual W, T, etc. and then compare them to a current building block[45] in the modular set.

2.4 Macrocyclization Techniques

Chemists have been challenged by the preparation of macrocycles and it is only in the past 30 years have they been attainable in appreciable yield[46]. The following section presents some of the challenges for efficient macrocyclization.

A retrosynthetic analysis of any macrocycle **C** would first involve the design of the bifunctionalized precursor **BFC** that could then react intramolecularly (Scheme 3). Compound **BFC** could then be obtained from the bifunctionalized reactants **A** and **B**. For synthetic simplicity, the reactants are usually symmetrical with the same functionality at each end of the chain[47]. This design avoids the added complexity of multiple products. A one pot synthesis is possible since the same chemistry is used to join the fragments as to close the ring, resulting in maximum yields. The chains may vary but must be non-reactive under the conditions of **A**+**B**.

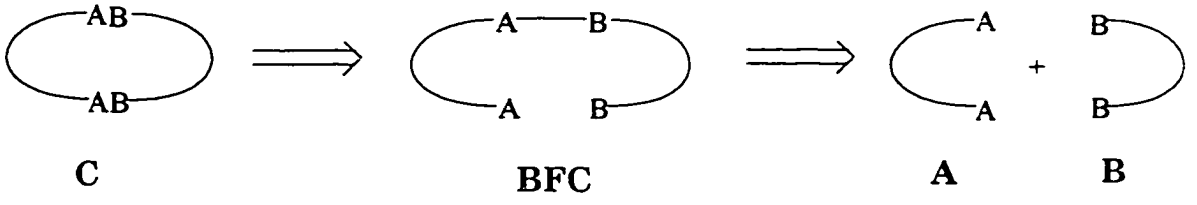

Scheme 3: Retrosynthetic Analysis of a Macrocycle

There are several possible reaction pathways (Scheme 4). The concerted double reaction (path a) leads to the desired macrocycle but it is not a likely mechanism from a thermodynamic or kinetic stand point. More likely, one end reacts first (path a.1), leading to the bifunctional chain (**BFC**). Several pathways are available to this molecule. It may cyclize (path a.2) to afford what is known as the 1+1 product. Two **BFC** may react (path b.1) yielding what is referred to as the 2+2

product. This product may also be obtained by the stepwise reactions of a **BFC** with a strand **A** molecule (path b.2) followed by a strand **B** molecule (path b.3) or vice versa, and subsequently, ring closure. This is sometimes the molecule of interest but, the main competing reaction is polymerization. The **BFC** can react with another **A** or **B** strand, etc. to yield polymers of varying lengths. It is the problem of polymerization that demands the most attention.

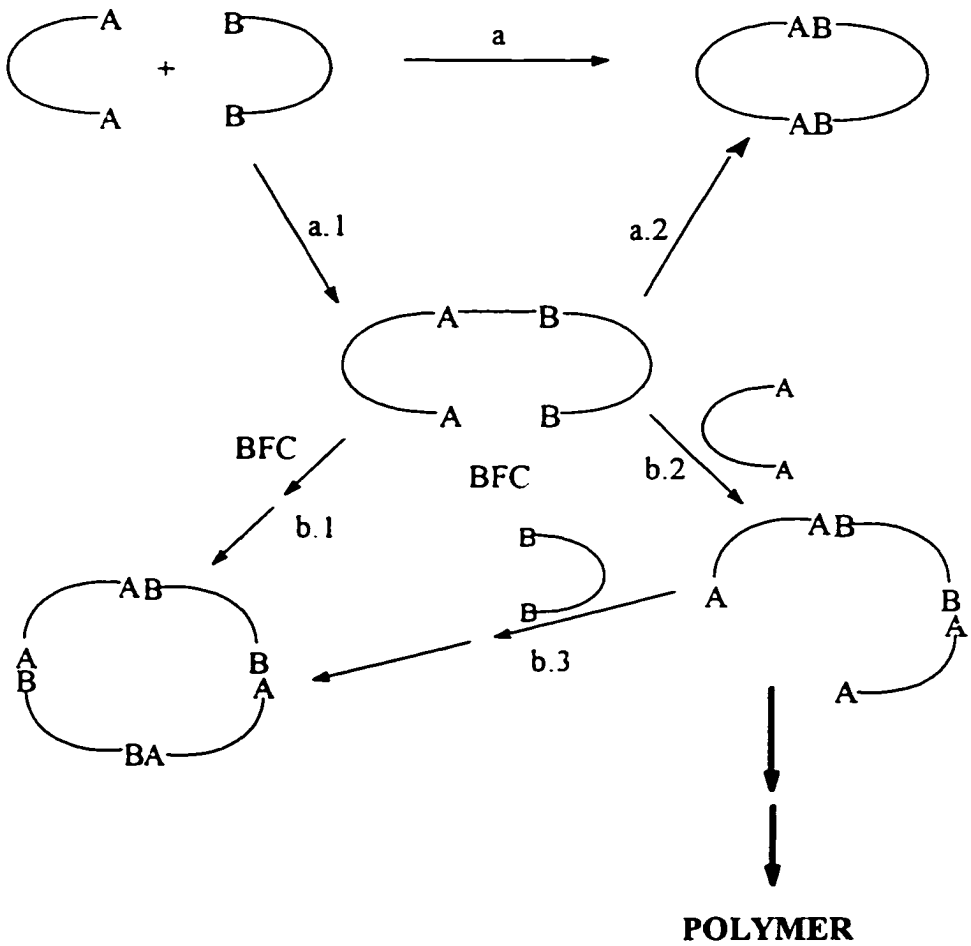

Scheme 4: Competing Pathways (Cyclization or Polymerization)

The factor controlling polymerization is the effective molarity (E.M.)[48]. Referring to Scheme 4, this is defined as k_{intra}/k_{inter}, where k_{intra} is the rate of the intramolecular reaction a.2 and k_{inter} is the rate of the intermolecular reaction b.2, assuming all react ions are irreversible. The first A-B bond is formed as one expects of the unifunctionalized compounds to form the BFC. Now, whether the molecule cyclizes or polymerizes depends on the relative rates of the inter (path a.2) and intramolecular (path b.2) processes. The rates of the reactions depend on the relative free energy of activation ($\Delta G^{\ddagger}$) of the polymerization reaction with respect to the intramolecular reaction. One must consider the activation enthalpy ($\Delta H^{\ddagger}$) and the probability for the intramolecular encounter of A and B (which relates to $\Delta S^{\ddagger}$). The primary enthalpy difference will lie in the strain energy on ring formation; a larger strain energy will result in a positive, unfavourable $\Delta H^{\ddagger}$. These strains may be caused by imperfect staggering, bond angle deformation or transannular interactions (repulsive interactions across the ring). These effects are usually greater for medium sized rings [48a], however in general they tend to decrease as ring size increases. The entropy ($\Delta S^{\ddagger}$) of the system dictates the probability of end to end encounters. It is easy to imagine that the frequency of such encounters decrease as the chain length is increased. A disordered open chain that must undergo rearrangement to form an ordered ring loses the rotational freedom and results in a negative and therefore unfavorable $\Delta S^{\ddagger}$.

There are several methods devised to favor intramolecular reaction. The most general and widely used technique follows Ziegler's high dilution principle [49]. The

E.M. is not changed , but the concentration of the substrates is very low in comparison to E.M. The purpose of this technique is to keep the concentration of the reacting species low so that the probability of a B group encountering an A group is higher intramolecularly than intermolecularly. High dilution typically refers to a final concentration on the order of 10^{-3}- 10^{-4} M. The high dilution technique requires each of the reagents to be dissolved in the appropriate solvent. Then they are added separately but simultaneously very slowly via a syringe pump device into a round bottom flask that already contains some of the solvent and possibly the other necessary reagents. Addition times vary from a few hours to several days and often additional reaction time is needed. This approach has been successfully applied to many systems but due to the large volume of solvent needed, the lengthy reaction time, and need for specialized equipment, other methods have been sought.

In an effort to develop general methods where high dilution is not necessary, the following techniques have been demonstrated: templated reaction, rigid group syntheses, and the use of high pressure. The first two methods change the E.M. so the intramolecular reaction is favoured even at "normal" concentrations while high pressure is effective for the same reasons as is high dilution (vide infra). In this dissertation both the high dilution and rigid group methods are employed.

The rigid group method refers to control of the geometry of the reactants, namely that they are already in a suitable conformation conducive to cyclization. Rigid group implies that solvent would have minimal effects on the geometries of the reactants because the preorganization is inherent in the design of the reactants. One

example is in the preparation of Schiff base macrocycles where the condensation reaction between linked benzaldehydes and amines afford yields as high as 94%.[50]

2.5 Molecular Modeling

Two of the desired properties of the macrocycles are that the length be between 15 and 17 Å and that the structure be sufficiently rigid that it will not fold or crumple on itself. The length assessment is straight forward in that the distance is measured from end to end in the low energy conformers. Rigidity is difficult to assess so molecular mechanics and dynamics were used. In the first step, we are interested in the geometry of the molecule at the global minimum so we perform molecular mechanics[51]. Since mechanics only seeks out the local minimum then we perform dynamics as a second step to explore flexibility. The computer simulations assess the relative geometric rigidity of the macrocycles to thermal excitation. Molecular dynamics imparts random velocities to each atom based upon the temperature, (i.e., heats the molecule) so it can escape a local minimum, and then follows each atom over a period of time steps. Assuming that the total time period is long enough and that we sample the collection of geometries (the trajectory) properly, we can assume that the molecule can statistically sample the potential energy surface available to it at a given temperature. The geometries found during the simulation are not minima or stationary points on the potential surface, but are just snapshots of the molecule during its trajectory. If a given macrocycle can, at a given temperature, readily achieve a large number of distinct, low energy structures, we can safely conclude that the macrocycle

is not rigid with respect to thermal excitation. If, on the other hand, the macrocycle leaves the low energy regime of the starting point and finds only higher regions over a long time period, perhaps finding another low energy region some time later, we may conclude that the macrocycle is relatively rigid to thermal excitation. To assess the length of the macrocycle it is necessary to sample some of the snapshots along the dynamics trajectory and then minimize those using molecular mechanics. The larger the sample size, the greater chance of finding the global minimum. Both mechanics and dynamics results will be discussed as the target designs are refined.

2.6 Target Evolution

2.6.1 General Strategy

The purpose of this thesis is to improve on the existing set of wall units used in the modular set. Specifically, the goals are to obtain macrocycles in high yield, to eliminate the regio and stereochemical problems, and to broaden the understanding of ion transport via the addition of a wide variety of functional groups. The basic design of the new wall units is to replace the maleate esters thus avoiding the formation of multiple regio and stereoisomers. In principle, we could work from chiral precursors to ensure single isomers result in the target. Rather we chose to use a plane of symmetry at all connection points to make achiral wall units. Thus, 1,3,5-trisubstituted benzenes are placed at either end of the macrocycle where two of the substituents are the same (A or B) and the other is

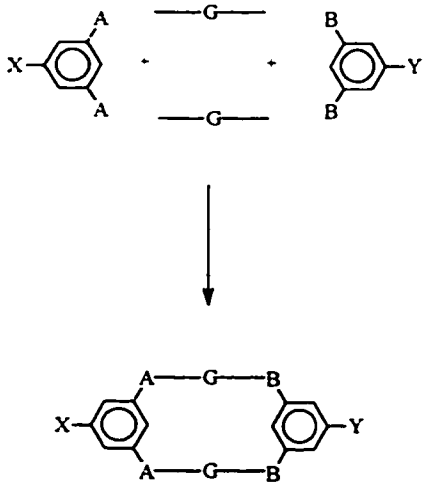

Scheme 5: General Design of New Wall Units

different (X or Y) (Scheme 5). The sides of the macrocycle (G) could be the same, or could incorporate different functionality. The phenyl ring at each end additionally imposes some rigidity on the system. This chapter discusses the evolution of the

targets in general, although many of the decisions were based on the detailed chemistry to be presented in chapter 3. Some of those results are briefly stated in this section simply to indicate the rationale. A detailed discussion of the results is deferred to chapter 3.

2.6.2 Design of Macrocycles Based on α-Heteroamides[52,53]

Nature uses peptide linkages to impose structural order using the rigidity of the amide link and we will use amide bonds for this same reason, to ensure rigidity of the system. CPK models and molecular mechanics were used to determine the overall shapes and energies of the structures, ie. whether the macrocycle had the desired length and rigidity. Secondary amides would be an ideal functional group in that they not only have a high barrier to rotation, but they possess a hydrogen atom that is capable of hydrogen bonding to another member of the ring system[47,54].

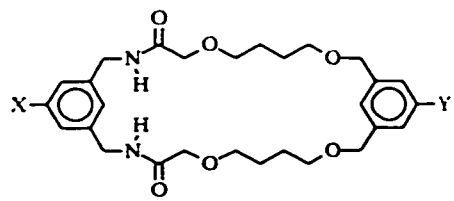

22
a, X=Y=H

Figure 17: Target 1, Macrocycle **22**

A structure that seemed favourable from both structural and synthetic points of view is **22** (Figure 17). Substituents X and Y could be different and could be any one of a variety of functional groups, such as $-NO_2$ or $-NH_2$. At this stage, the exact chemical

functional groups are not particularly important, except that they allow a convenient chemical link between a head group at one end and a linker at the other end. For reasons including cost and simplicity, the model compound **22a** was targeted to examine the chemistry and the overall structure of the macrocycle. Molecular modelling predicted the length between the 5 and 5′ positions of the two benzene rings to be approximately 13.5 Å. A retrosynthetic analysis of **22a** (Scheme 6) shows that the

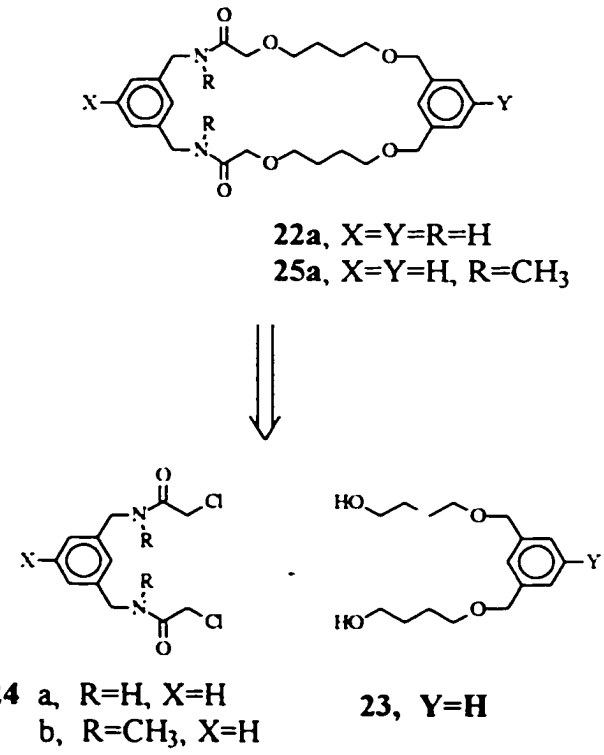

Scheme 6: Retrosynthetic Analysis of Targets **22** and **25**

structure could result from the reaction of diol **23** and the bis chloroamide **24a**, which is believed to behave as a rigid group[52,53]. The bis chloroamides supposedly form a rigid, claw-like type structure[52,53] (Scheme 7), conducive to macrocyclization. For this reason, low dilution techniques may be used. Bradshaw and co-workers report excellent yields for

macrocyclizations involving bis chloroamides and diamines or tosyl amides (approx. 50%)[52,53]. The bis chloroamides are easily prepared from the reaction of an amine with chloroacetyl chloride (Scheme 7). Thus the alluring characteristics of this approach are that the chemistry is relatively simple and the starting materials are readily available and inexpensive.

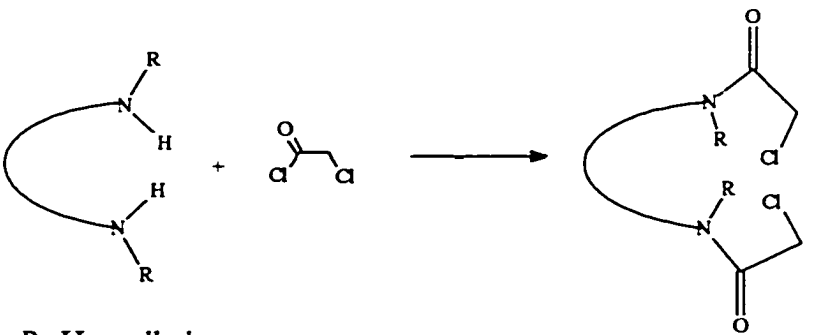

R=H or alkyl

Scheme 7: Preparation of Bis Chloroamides

As discussed in the subsequent chapter, repeated attempts at the macrocyclization of diol **23** and bischloroamide **24a** proved futile. A strong base, NaH, was used to generate the bis alkoxide which was intended to displace chloride in an S_N2 reaction to yield macrocycle **22a**. Several different solvent systems (DMA, DMF, THF, 20% DMSO in THF) were used but the desired target was never isolated. Instead, as observed by TLC, many (>11) different compounds were produced.

It was concluded from these studies that the amide hydrogens were too acidic, having pK_a's in the range of 14-16, which is similar to the pK_a for a primary alcohol[55]. At least some of the products are likely the result of deprotonating the amide. The secondary amide **22** was changed to the tertiary amide **25** (Figure 18) to eliminate this problem.

Macrocycle **25a** is a conservative modification of **22a**, differing only by an N-Me in **25a** in place of an N-H in **22a**. The retrosynthetic analysis shown in scheme 6 shows that both of these macrocycles can be prepared from α-heteroamides. Cyclization of bischloroamide **24b** with diol **23** should yield macrocycle **25a**.

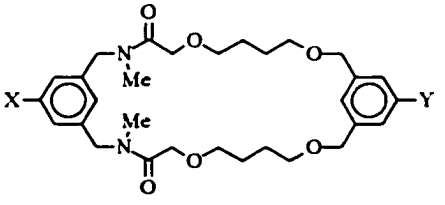

25 a, X=Y=H
b, X=NO_2, Y=NH*t*-Boc
c, X=NH*t*-Boc, Y=NO_2

Figure 18: Target 2, Macrocycle **25**

Molecular mechanics[51] estimates the distance between the 5 and 5′ positions of the benzene moieties of **25** to be approximately 13.9 Å. Using molecular dynamics, **25** was found to be much more rigid than **22**, due to the presence of the methyl group on the amide nitrogen. This was confirmed by inspection of the structures along the trajectory which showed that the N-methyl end of **25** began to deform from the preferred orientation only in the high energy regime, some 100 kcal mol^{-1} above the low energy regime. The macrocycle formed a bowed-boat conformation in most cases, with the rigid end piece forming one end and the rest of the macrocycle contorting in order to fit this conformation. In contrast, **22** readily achieved a number of different conformations about the N-H end. As an example, two representative low energy snapshots of **22** and **25** are shown in Figure 19 and Figure 20 respectively.

As discussed later, the N-Me macrocycle **25a** was prepared in low yield (7.5%) as an oil from diol **23** and bis chloroamide **24a** using THF and 10% DMSO as the solvent.

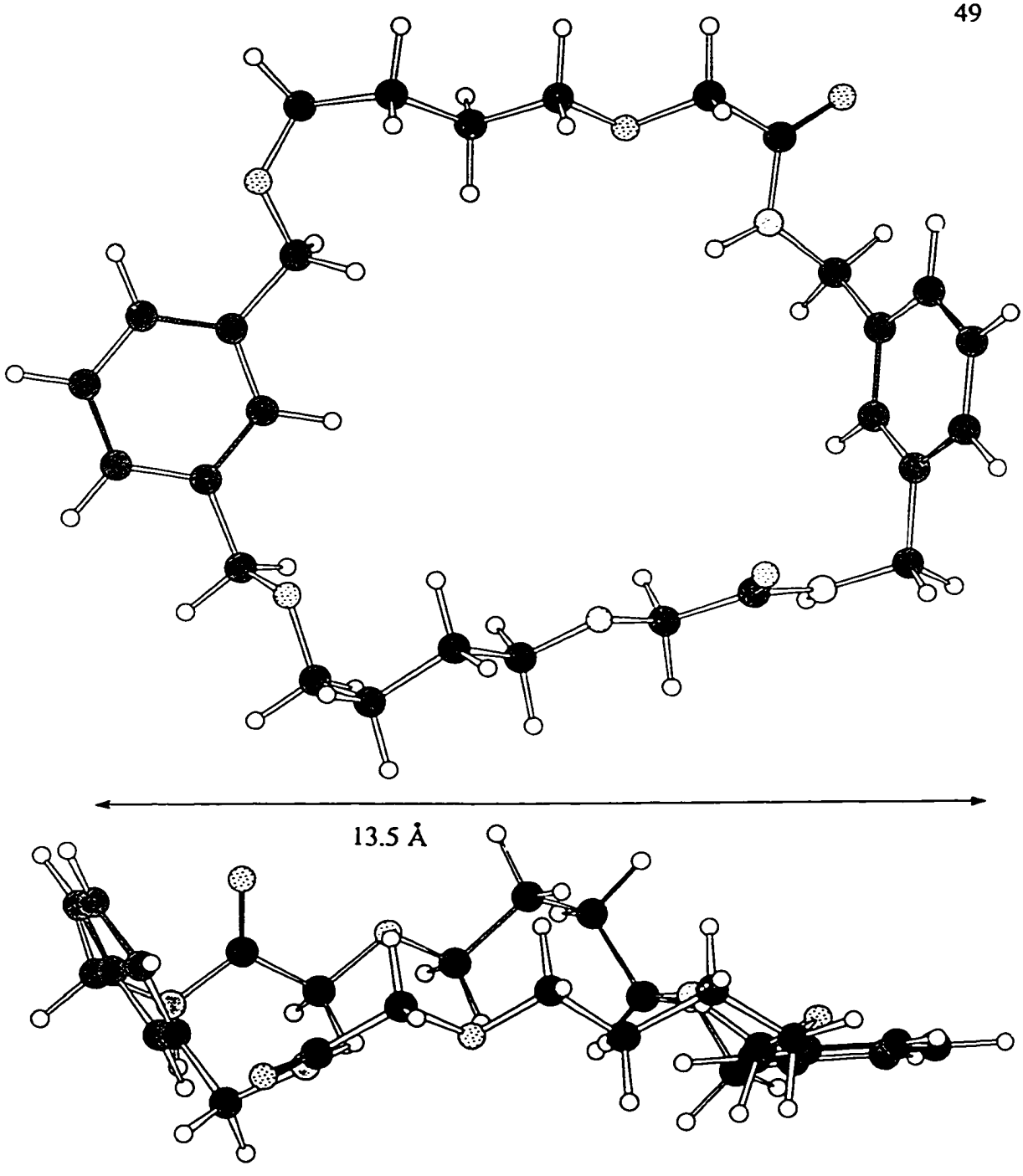

Figure 19: A Representative Snapshot of a Low Energy Conformation of Macrocycle22a

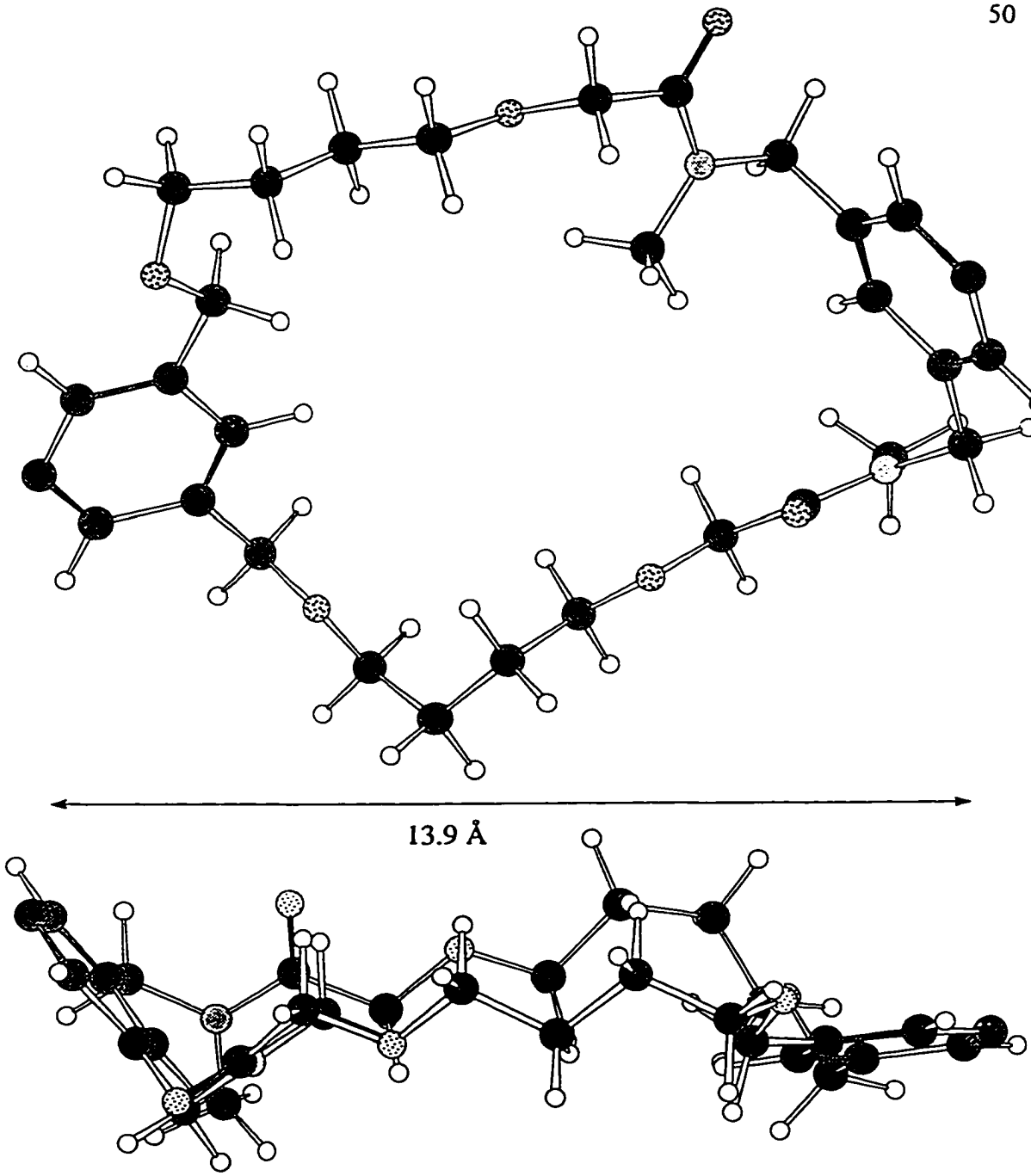

Figure 20: A Representative Snapshot of a Low Energy Conformation of Macrocycle25a

Given moderate success with the model compound **25a** the synthesis of macrocycle **25b** or **25c** where X,Y≠H was attempted. A small selection of starting materials, where 1,3,5-trisubstituted benzenes had two different substituents, dictated the synthesis. 5-Nitroisophthalic acid (Figure 21) purchased from Aldrich[56] at $71.10/500 g proved a satisfactory starting point. The nitro group linkers could terminate as NH_2's allowing amide linkages to connect the head and core to the wall.

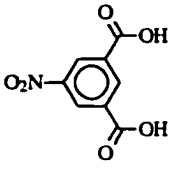

Figure 21: 5-Nitroisophthalic acid

The reduction of the nitro groups could, in theory, be done at any number of stages throughout the synthesis and it would not matter which end was protected, so **25b** and **25c** are equally desirable targets (Figure 18, p. 47). Unfortunately, neither targets **25b** nor **25c** were obtained. The macrocyclization step led to numerous products, none of which were the targets. The leaving group Cl^- was changed to I^- in hopes that alkoxide would displace the better leaving group. This turned out not to be the case.

Additionally, the synthesis of the diol was cumbersome. Purification of the oil was tedious and time consuming so while work was continuing with target **25** we began to search for a replacement diol, ideally a solid The new diol would not necessarily have to maintain the ether linkage, but it could involve amides as well. The diol **26** (Figure 22) was

prepared in good yield from 5-nitroisophthaloyl dichloride and 3-aminopropanol and proved to be the desired solid.

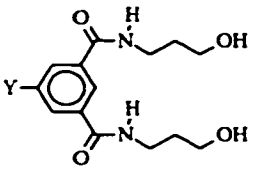

26, Y=H
Y=NH*t*-Boc

Figure 22: Modified Diol **26**

Target 3 (Figure 23) evolved where the diol **23** component was replaced by diol **26**. Coupling **24b** with diol **26** should lead to macrocycle **27**. The length was estimated to be approximately 13.5 Å using molecular modeling (Figure 24).

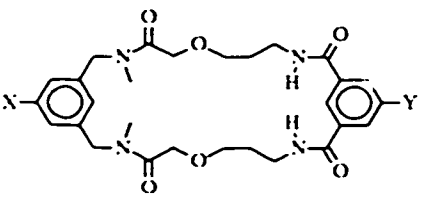

27 X=Y=H

Figure 23: Target 3, Macrocycle **27**

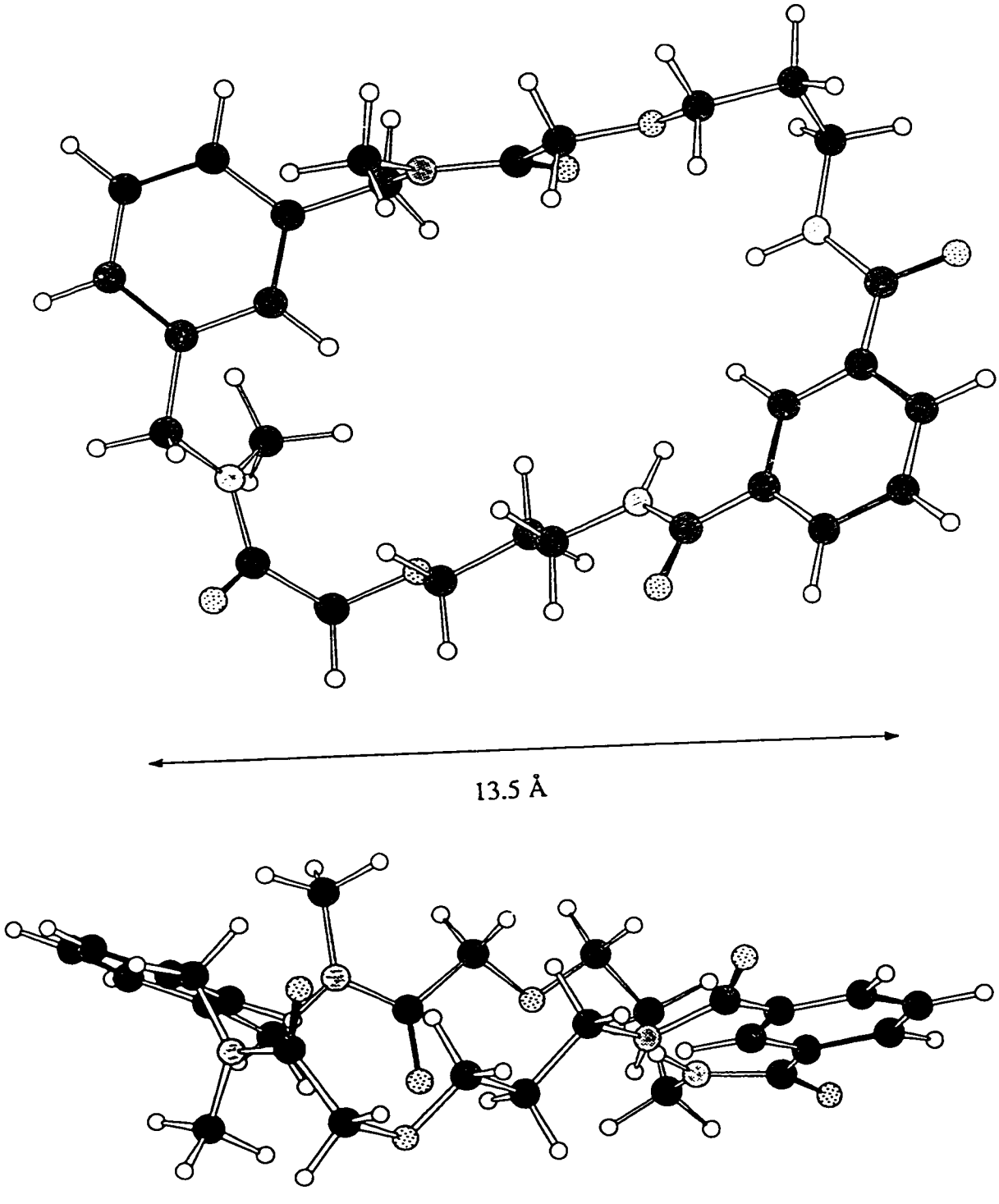

Figure 24: A Representative Snapshot of a Low Energy Conformation of Macrocycle27

Problems encountered in this synthesis were similar to those mentioned for targets **22** and **25**. The macrocyclization does not successfully compete with the side reactions necessitated by the use of an alkoxide nucleophile. The conclusions reached from studying these targets that require the nucleophile to be alkoxide are that the nucleophile must be changed in such a way that the conditions are conducive to cyclization. If ROH is changed to RSH where -SH or $-S^-$ is the nucleophile then the conditions (ie. solvent, base) may be changed. For example, CH_3CN could be used as the solvent as opposed to DMA or DMF and a mild base such as Na_2CO_3 could be used in the place of NaH. The reaction should also be faster. All of these points should result in a higher yield of macrocycle. The resulting new target **28** is shown in Figure 25 and the lower energy conformers were estimated to be approximately 13.8 Å in length (Figure 26).

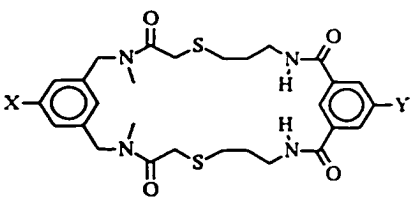

28 ,X=Y=H

Figure 25: Target 4, Macrocycle **27**

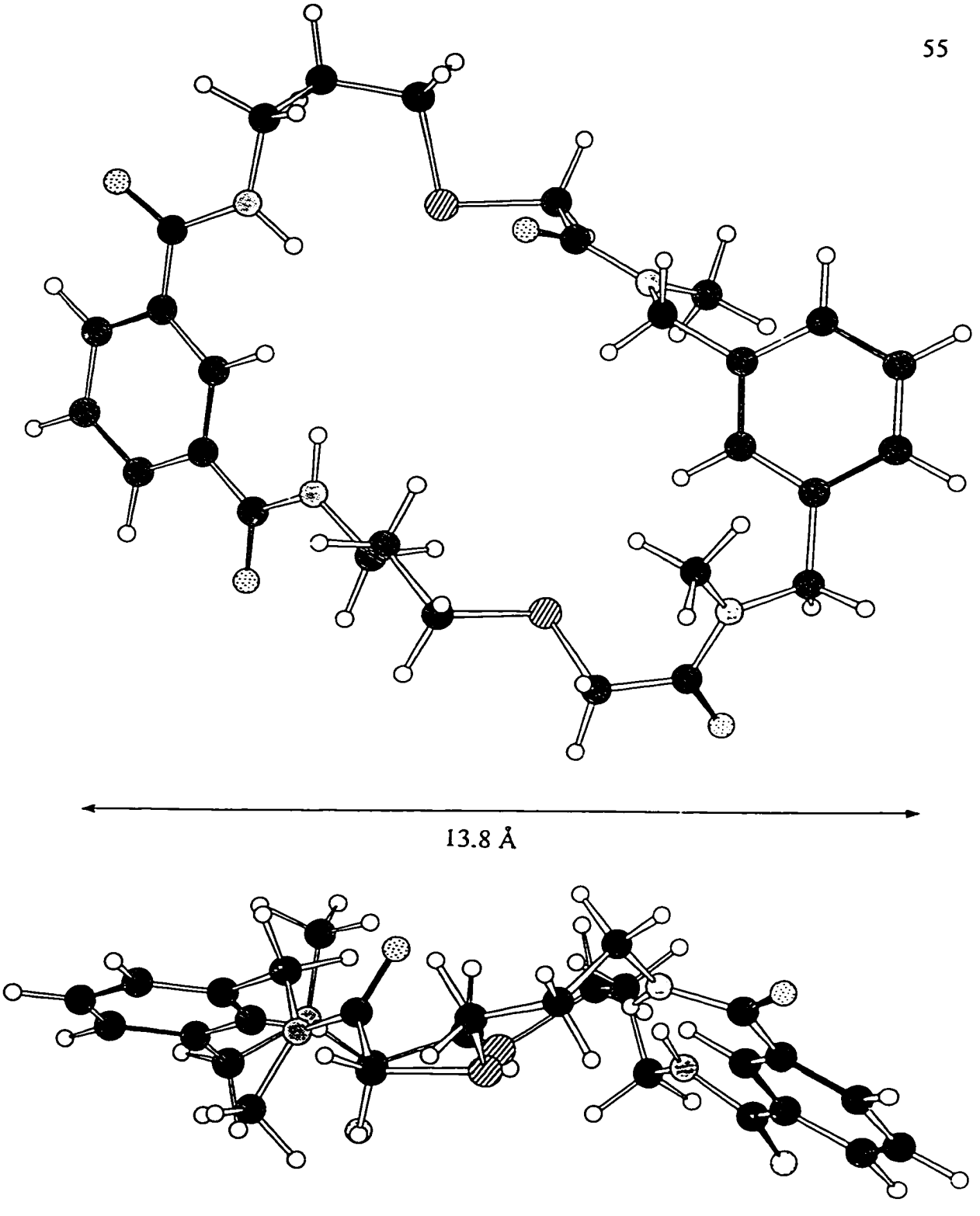

Figure 26: A Representative Snapshot of a Low Energy Conformation of Macrocycle28

2.4.4 Design of Tetraester Macrocycles

A more conservative modification of the previous set of wall units is also possible. Wall unit 8_2 was one of the more active subunits in the previous set. 1,8-Octanediol proved to be a satisfactory length and the four ester groups provided sufficient hydrophilic character. The problem was that it was prepared in low yields with the ends the same and that many isomers were obtained when adding the core and linker. We thought a similar target (Figure 27) was possible using our general design in Scheme 5 (page 43). Groups A and B are esters that can come from 5-nitroisophthalic dichloride and the group G arises from the synthon 1,8-octanediol. Ends X and Y would be different, X=NH_2 and Y=NH*t*Boc and these ends may be differentiated either before or after cyclization. If the differentiation takes place after cyclization then the step becomes a monoprotection and the yield has a statistical maximum of 50%.

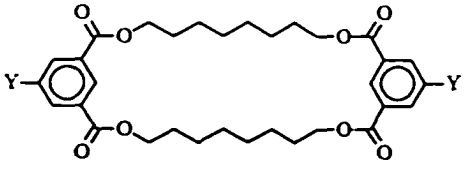

29 a, X=Y=H
b, X=NH_2, Y=NH*t*-Boc

Figure 27: Target 5, Macrocycle **29**

The molecular modeling demonstrated the length of **29** varied slightly between 15.8 and 16.9 Å but the energies of the representative snapshots were all the same (between 11.7 and 12.9 kcal/mol, Figure 28). By the same technique, macrocycle 8_2 was found to be slightly shorter at 13.5-13.7 Å.

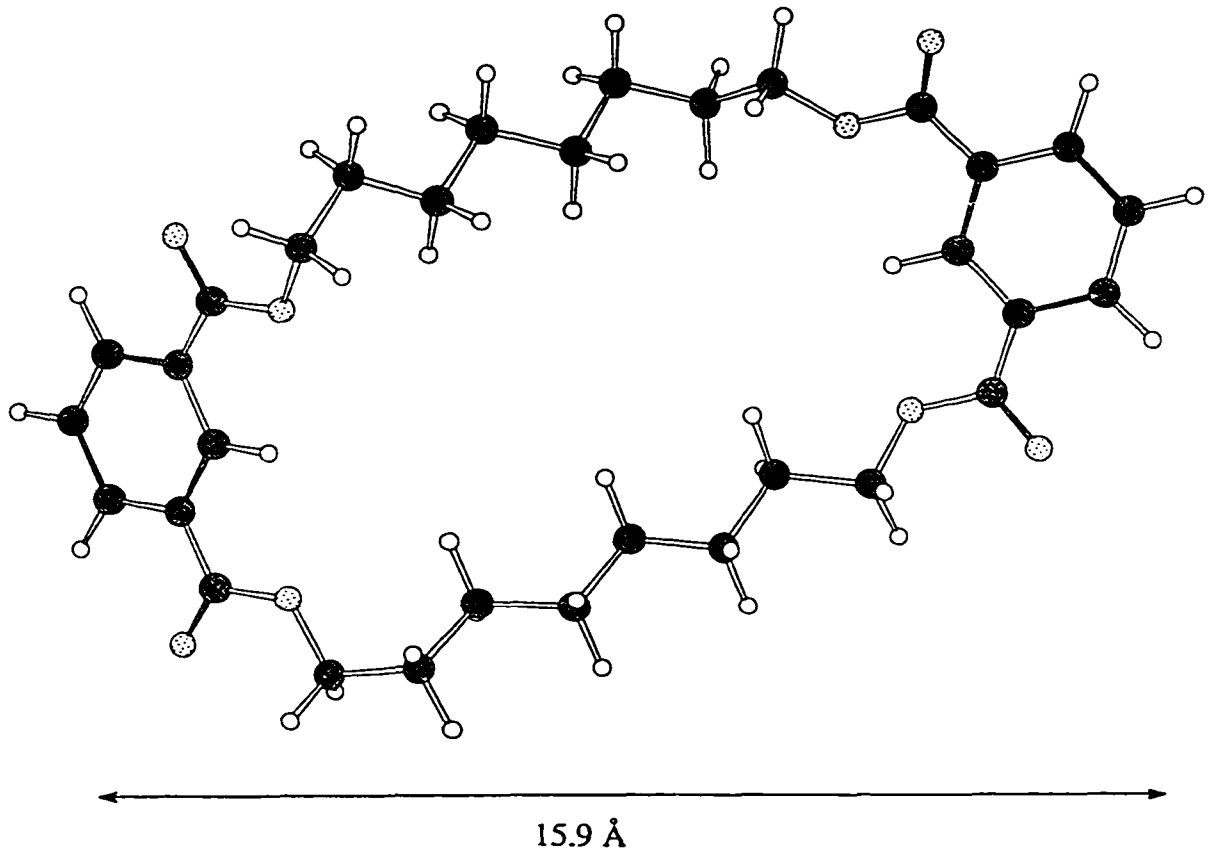

Figure 28: A Representative Snapshot of a Low Energy Conformation of Macrocycle **29**

CHAPTER 3

SYNTHESIS AND DISCUSSION

3.1 Towards the Synthesis of the Diamide Macrocycles 22 and 25

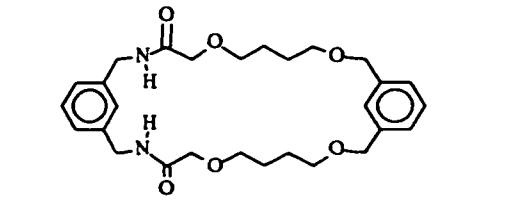

22a

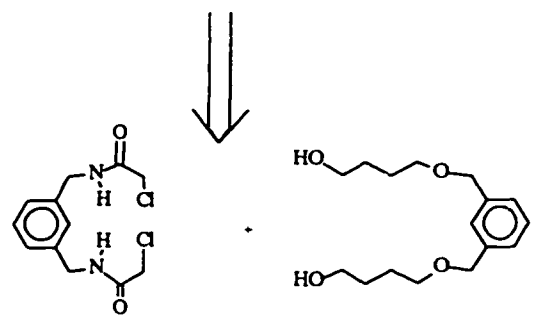

24a 23

Scheme 8: Retrosynthetic Analysis of Target 1

As discussed in chapter 2, we believed the target macrocycle **22a** could be obtained from the diol **23** and the bischloroamide **24a** (Scheme 8). Compound **24a** was prepared as shown in Scheme 9. Even though *m*-xylylenediamine **32** is commercially available, it was prepared by the route given in order to investigate the chemistry associated with the process as the acid chloride **30** would be the starting point for a target with linkers in the 5 position of the benzene ring. The acid chloride **30** was reacted with ammonium hydroxide to yield the primary amide **31** quantitatively. The ^{13}C nmr is consistent with the assigned

structure. The amide **31** was reduced using lithium aluminum hydride ($LiAlH_4$) to afford *m*-xylylenediamine **32** in 60% yield. Nmr assignments were consistent with literature results[59]. Reaction of the diamine **32** with chloroacetyl chloride under Schotten-Baumann conditions as described by Bradshaw[53] gave the bischloroamide **24a** in 33% yield.

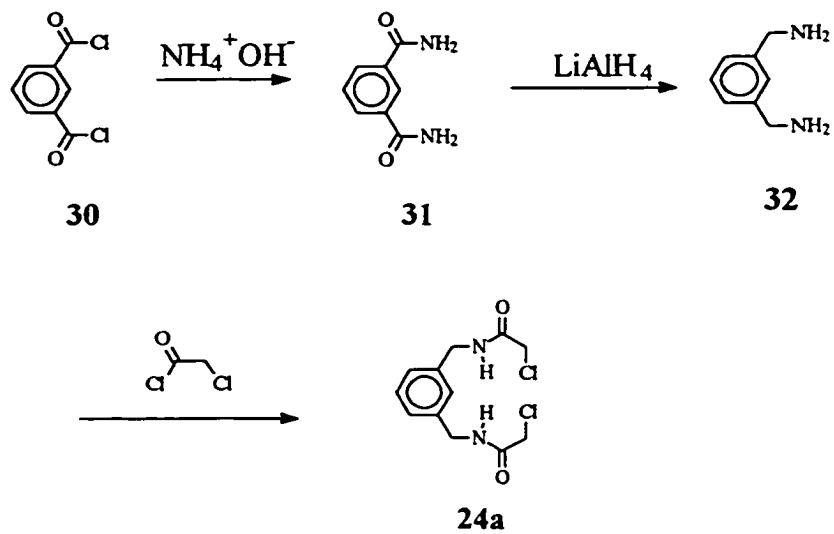

Scheme 9: Synthesis of Bischloroamide **24a**

The bischloroamide **24a** was previously prepared[59] in 1947. The ^{13}C nmr (Figure 29) shows two signals at 42.6 and 43.6 ppm that correspond to the benzyl CH_2 and the $-CH_2Cl$ carbons respectively. There are four peaks in the aromatic region although the peaks at 127.1 and 127.2 ppm appear to overlap. The amide carbonyl is characteristically found at 165.9 ppm.

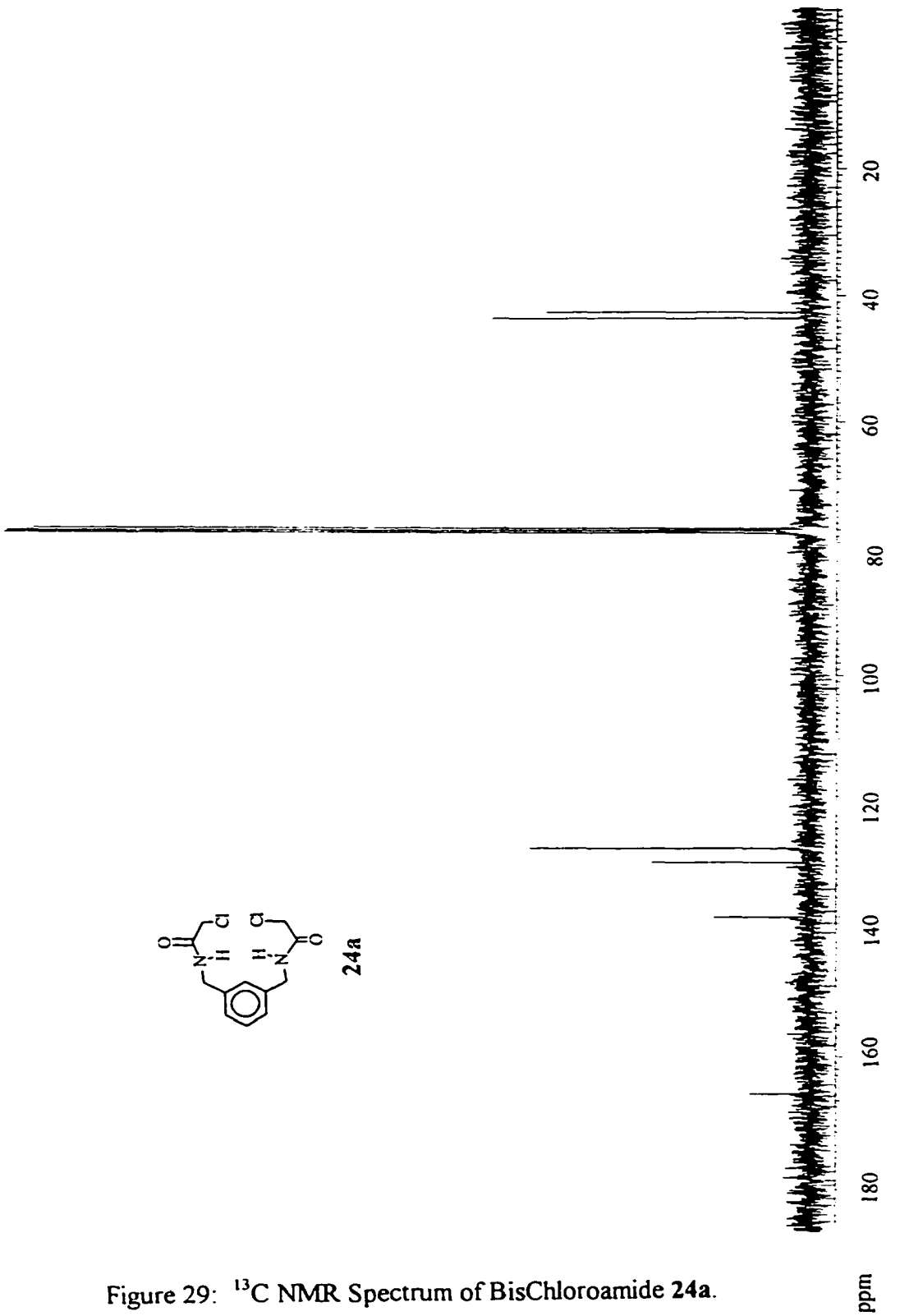

Figure 29: ^{13}C NMR Spectrum of BisChloroamide **24a**.

Synthesis of the diol **23** was less straightforward. Scheme 10 shows the route for initial trials of the synthesis. Once again, in order to examine the chemistry we started from the diacid **36** which was reduced using $LiAlH_4$ to the commercially available 1,3-benzenedimethanol **37** . The hydroxyl group of 4-chlorobutanol **33** was protected with dihydropyran **34** to yield the ω-chloro tetrahydropyranyl protected alcohol[60] **35** in 42% yield. Compound **37** reacted with **35** in dimethyl acetamide (DMA) using sodium hydride (NaH) as the base to generate the alkoxide of **37**. Using this method, the major product formed was the monosubstituted product **39**. The ^{13}C nmr for **39** is shown in Figure 30. The symmetry is lost in the aromatic region and there is one additional peak in the aliphatic region at 70.1 ppm that corresponds to the benzyl $\underline{C}H_2OH$. Deprotection of the impure mixture of **38** and **39** led to small amounts of the diol **23** that was difficult to purify and the major product, the monosubstituted diol **40** which was not the desired target.

An alternate route to compound **23** was devised where the commercially available α,α′-dibromo-*m*-xylene was dissolved with heating in 1,4-butanediol (Scheme 11). The excess butanediol was removed under vacuum. A rotoevaporator was connected to the vacuum pump and a heating mantle was used to heat the reaction mixture. Column chromatography on silica gel finally gave the diol **23** in 61% yield but the purification was cumbersome and time consuming. The ^{13}C nmr is shown in Figure 31. The molecule is symmetrical so there are five signals in the aliphatic region of the spectrum and there should be four aromatic signals. However, two of the nmr signals overlap at 126.9 ppm. The methylene of the primary alcohol is at 62.2 ppm and the benzyl methylene is at 72.7 ppm.

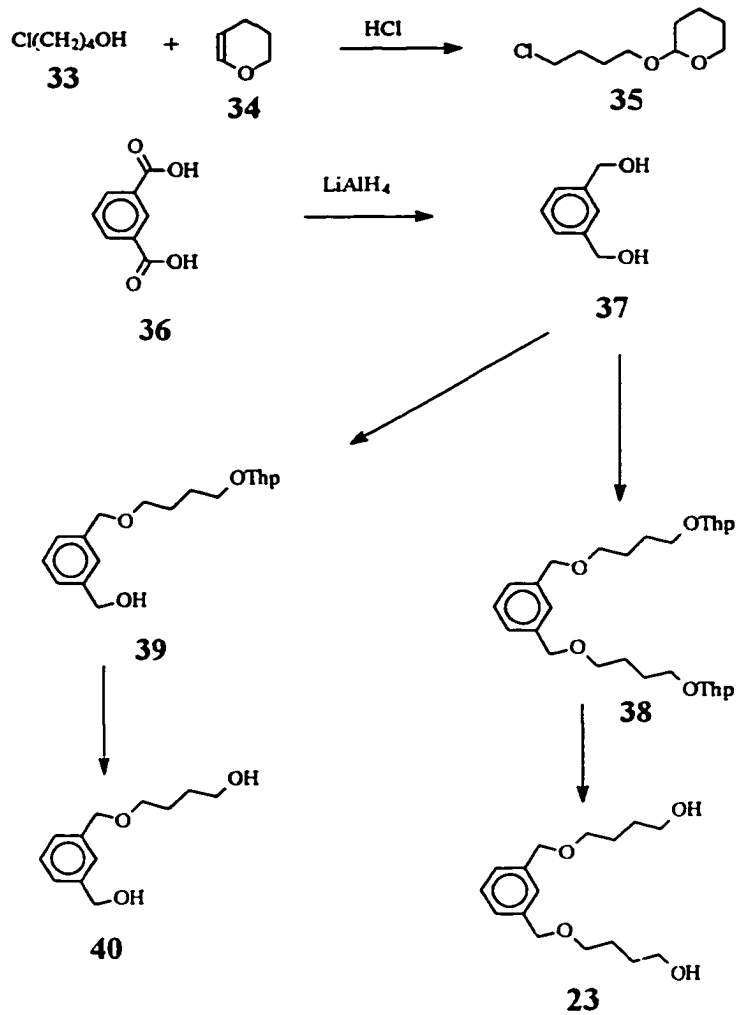

Scheme 10: Initial Attempts at the Synthesis of Diol **2**

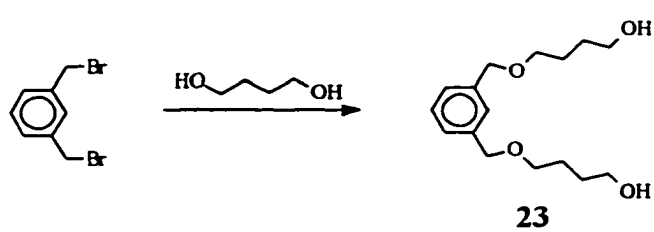

Scheme 11: Synthesis of Diol **23**

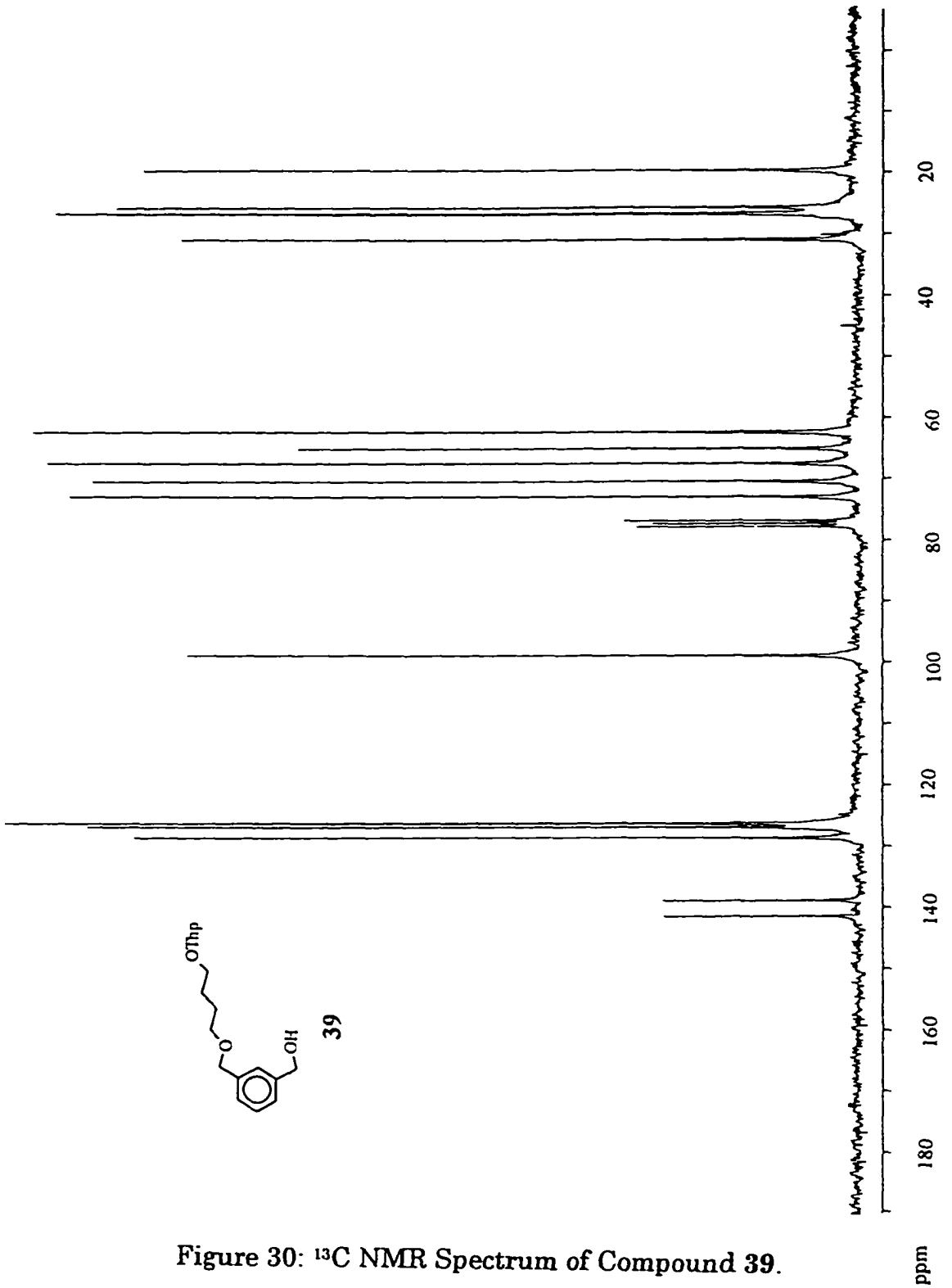

Figure 30: ^{13}C NMR Spectrum of Compound **39**.

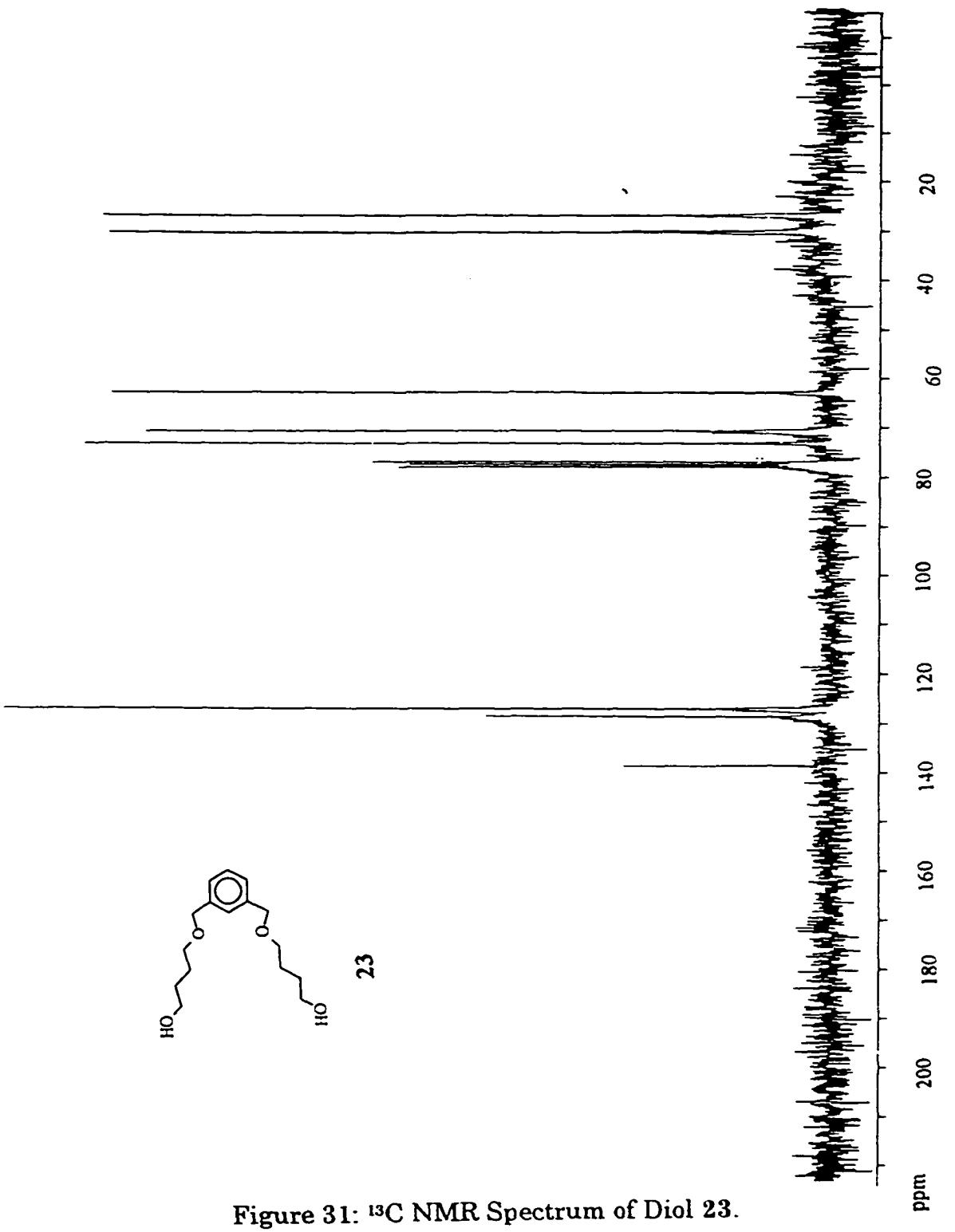

Figure 31: ^{13}C NMR Spectrum of Diol **23**.

Many trials of the cyclization (Scheme 8, p.58) were performed varying solvent (DMA, DMF, 10% DMSO in THF) and equivalents of base. When the ratio 1:1:2, **23**:**24a**:NaH was used, only starting material was isolated. The pK_a for a secondary amide is similar to that for a primary alcohol[55] and in this case it seems likely that the amide is being deprotonated preferentially over the alcohol. When an excess of base was used several species were obtained, none of which was the desired product. One of the products may result from the reduction of the amide as the carbonyl signal in the ^{13}C nmr disappeared.

In an attempt to overcome this problem, the secondary amide was changed to a tertiary amide by methyl group substitution for the hydrogen on the nitrogen. To obtain the N-methyl bischloroamide **24b**, isophthaloyl chloride **30** was reacted with methyl amine to produce the secondary amide **41** in 61% yield (Scheme 12). The ^{13}C nmr is simple with one peak at 26.8 ppm from the methyl carbon, four aromatic peaks at 125.1, 128.9, 129.6 and 134.8 ppm to represent the four different types of aromatic carbon atoms, and a carbonyl peak at 167.2 ppm. The aromatic region of the ^{1}H nmr demonstrates the meta coupling of C-2 H with C-4 and C-6 H's and C-2 H is a triplet. Protons on C-4 and C-6 are present as a doublet of doublets due to coupling to the ortho proton, C-5 H, and to the meta proton C-2 H. Proton C-5 H is of course present as a triplet.

Reduction of the amide **41** was carried out using $LiAlH_4$. The resulting diamine **42** was not purified but was used immediately in the next step. Using the same Schotten-Baumann conditions as outlined by Bradshaw[52] the N-methyl amine **42** was reacted with

chloroacetyl chloride in the presence of K_2CO_3. The N-methyl bischloroamide **24b** was obtained in 75% yield.

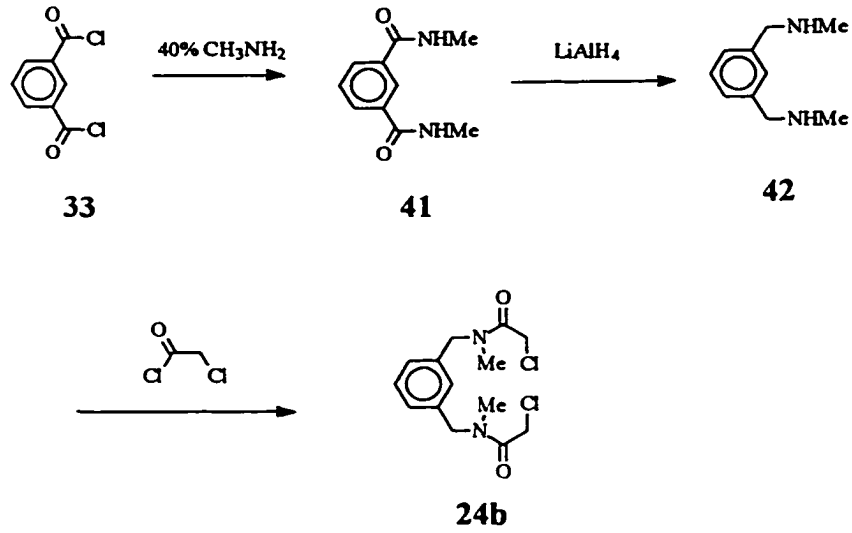

33 **41** **42** **24b**

Scheme12: Synthesis of Bischloroamide **24b**

There is a high barrier to rotation about the tertiary amide bond, so the amide may adopt either a cis or a trans geometry. This barrier is sufficiently high that at room temperature both conformational states are populated and at room temperature are not in equilibrium. Since there are two tertiary amides present in the molecule then there are three possible conformations, cis-cis, cis-trans, and trans-trans (Figure 32).

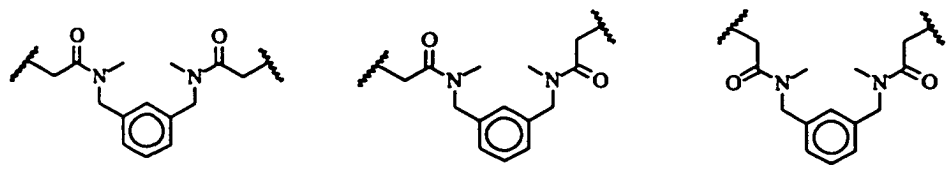

cis-cis cis-trans trans-trans

Figure 32: Conformations of Tertiary Amides

The ^{13}C and ^{1}H nmr's are shown in Figure 33 and Figure 34 respectively. In the aliphatic region there are three separate peaks in the ^{13}C nmr spectrum at 34.2, 35.1 and 35.2 ppm for the methyl groups, three peaks for the methylene next to Cl at 41.0, 41.2 and 41.3 ppm and two peaks for the benzyl methylenes at 51.0 and 53.4 ppm. The aromatic region follows a similar trend. For most of the carbons there are three peaks but for C-2 there are only two peaks. There are two carbonyl peaks at 166.6 and 166.8 ppm. The assignments of the ^{13}C nmr peaks are supported by a DEPT experiment. The carbonyl and quaternary signals disappear while the methyl signals are positive and the methylene signals are negative. The ^{1}H nmr also provides evidence for the different conformers. There are three singlets representing the methyl protons at 2.88, 2.93 and 2.96 ppm, two singlets for the methylene next to Cl at 4.04 and 4.08 ppm and the aromatic region appears too complicated for assignment.

The cyclization reaction between **24b** and **23** was not successful using DMA or DMF as the solvent. Others[62] have shown that the carbon α to the carbonyl deprotonates to generate a reactive carbanion in these solvents. Formation of the resulting anion could lead to any number of products including polymerization. Cyclization was effected using an excess of NaH as the base in 10% DMSO in THF (Scheme 13). The macrocycle was purified by centrifugal chromatography and was obtained in 7% yield. Five different products were isolated, one of them being the macrocycle **25a**. The ^{13}C nmr spectrum of the macrocycle **25a** showed more than one peak for each carbon. In fact, for several carbons there were three peaks, yet this compound was one spot on TLC in four different

solvent systems. The multiple peaks were a result of the high barrier to rotation in the tertiary amide and represented the cis-cis, cis-trans, and trans-trans conformations (Figure 32).Multiple peaks were observed in the ^{13}C nmr spectrum at room temperature in which $CDCl_3$ was the solvent (Figure 35), and at room temperature in DMSO (Figure 36). At 80°C the barrier is overcome and we see an average (Figure 37). With this modest success in the model system the target with linkers X and Y was attempted.

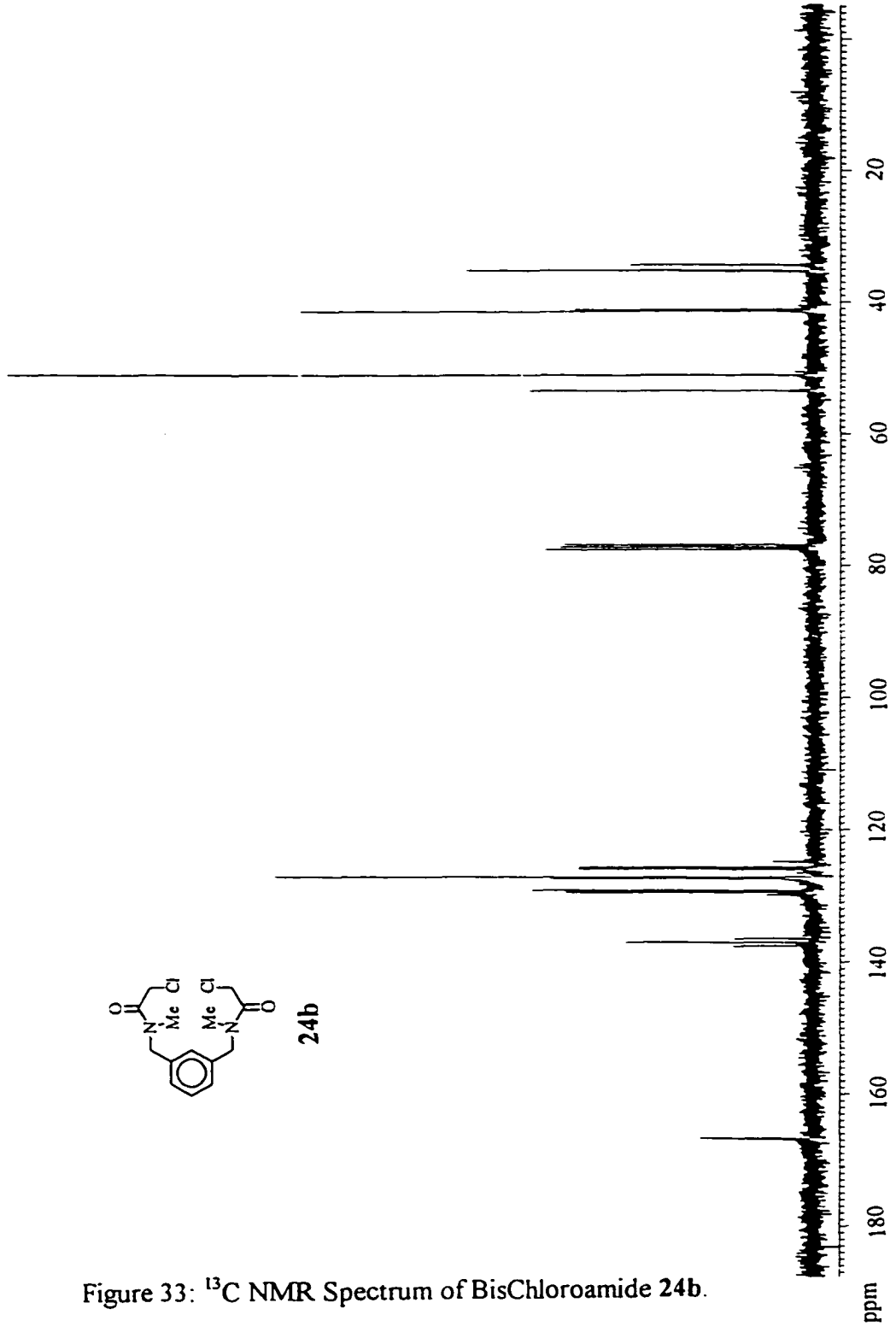

Figure 33: ^{13}C NMR Spectrum of BisChloroamide **24b**.

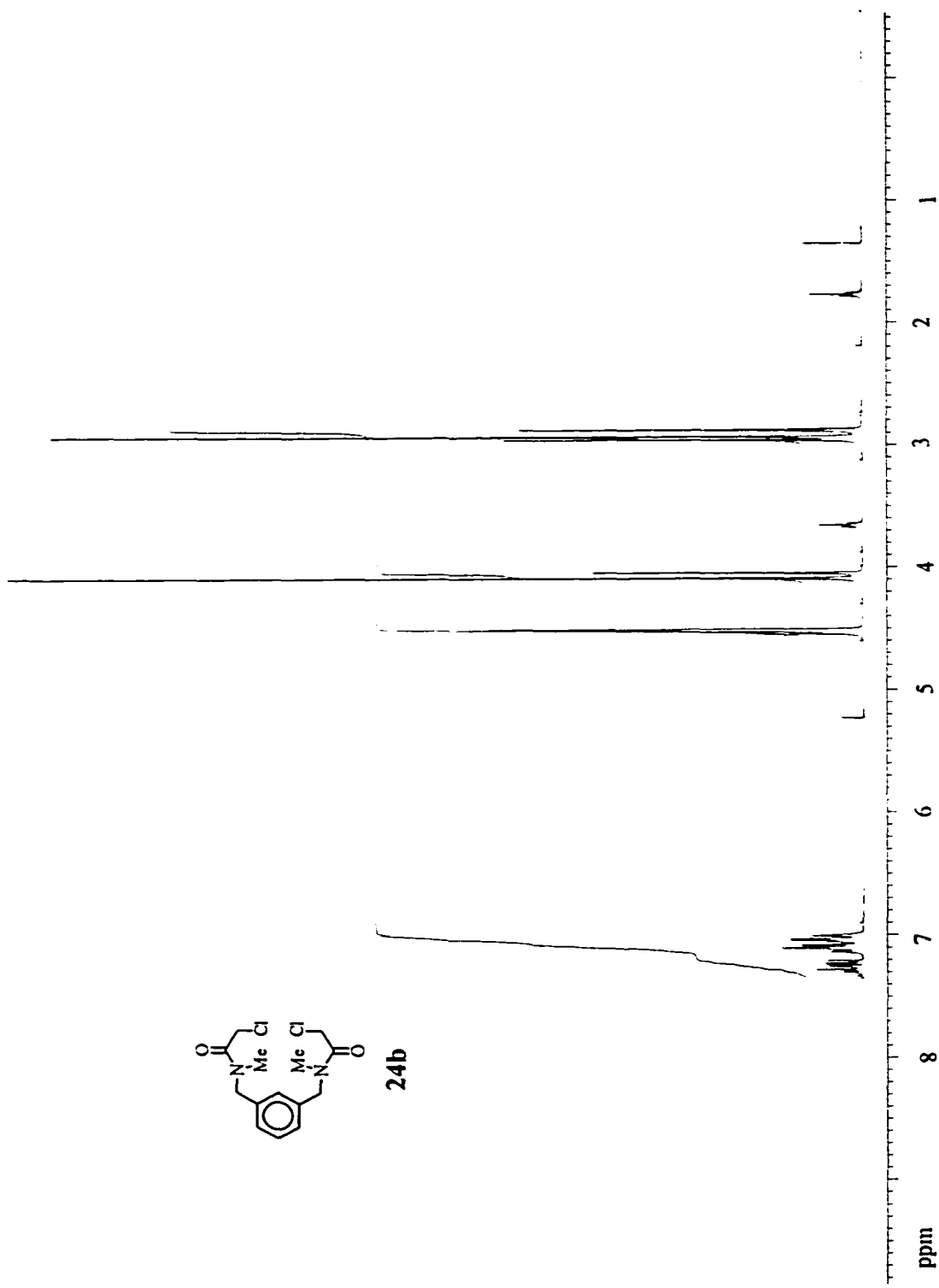

Figure 34: ^{1}H NMR of BisChloroamide **24b**.

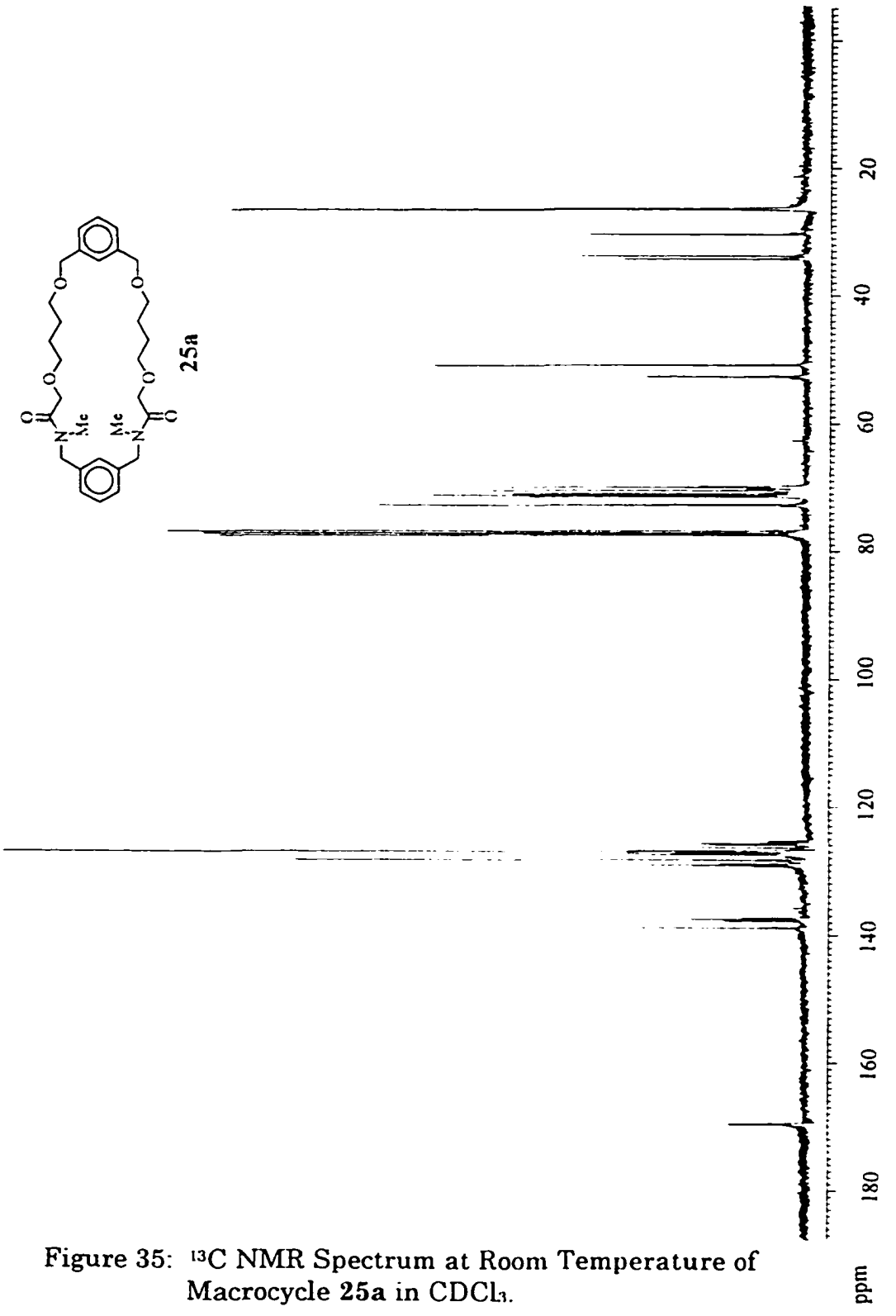

Figure 35: ^{13}C NMR Spectrum at Room Temperature of Macrocycle **25a** in $CDCl_3$.

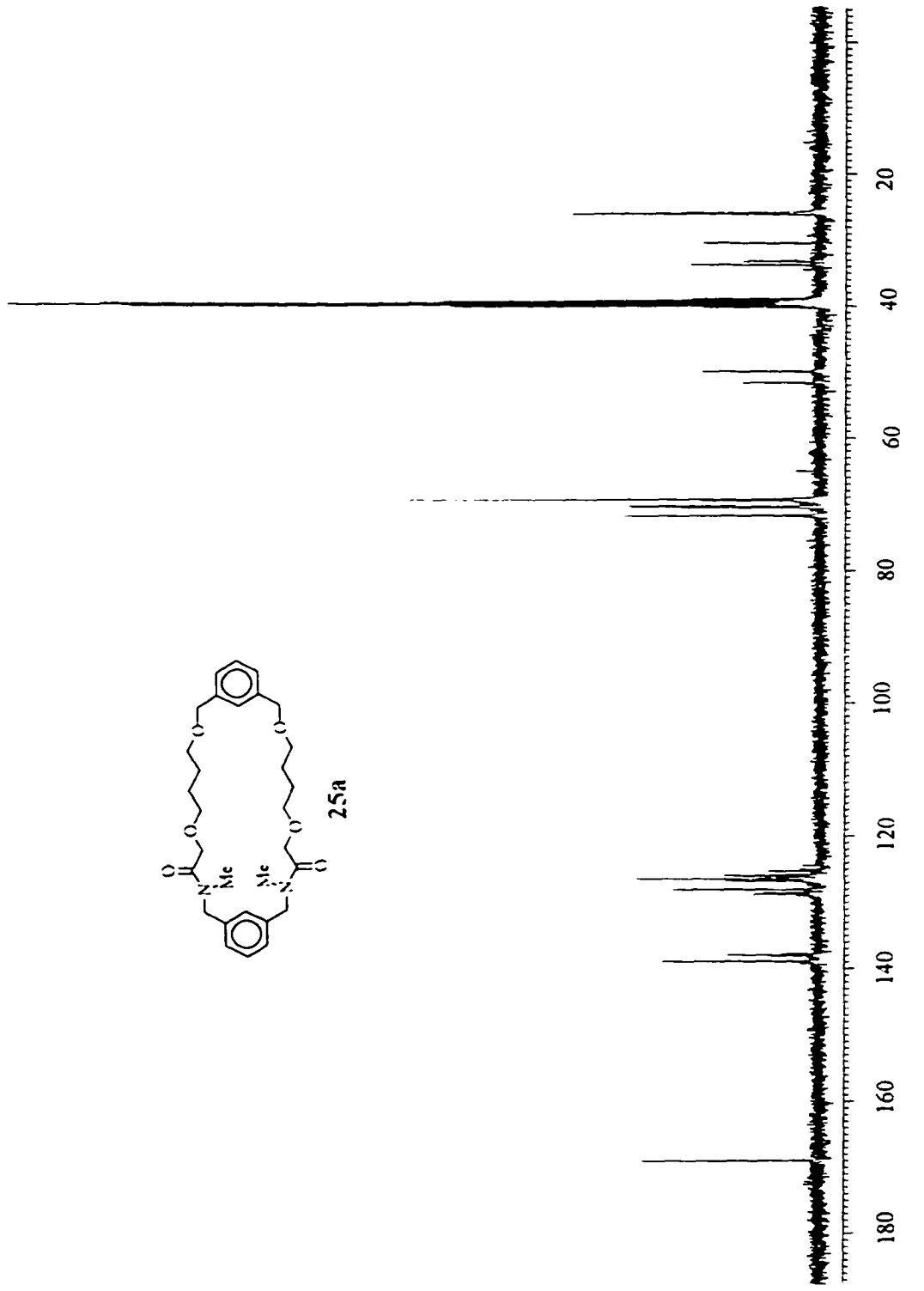

Figure 36: ^{13}C NMR Spectrum at Room Temperature of Macrocycle **25a** in DMSO.

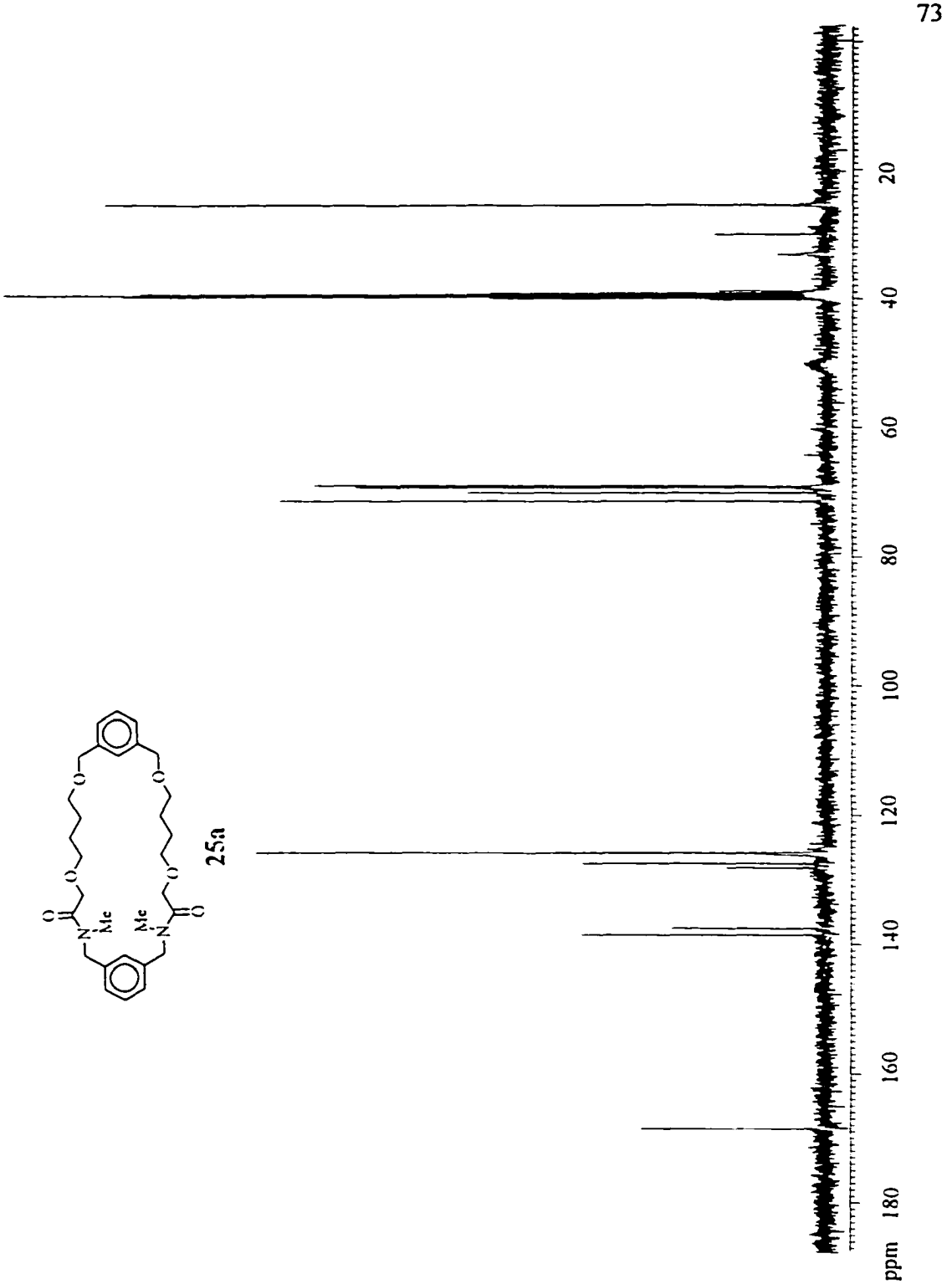

Figure 37: ^{13}C NMR Spectrum at 80 °C of Macrocycle **25a** in DMSO.

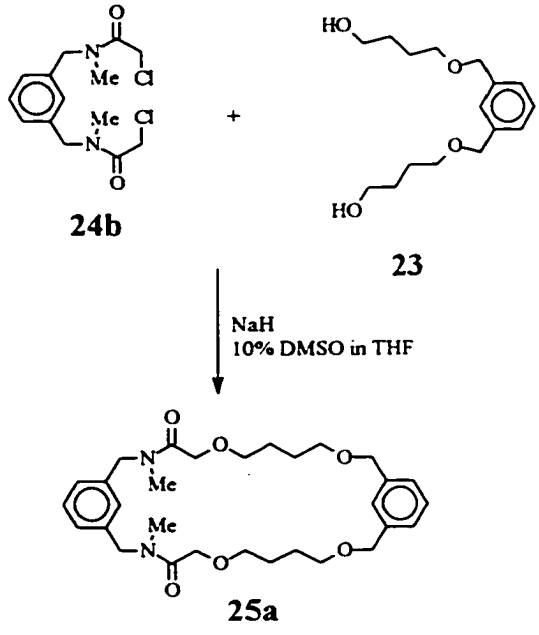

Scheme13: Synthesis of Macrocycle **25a**

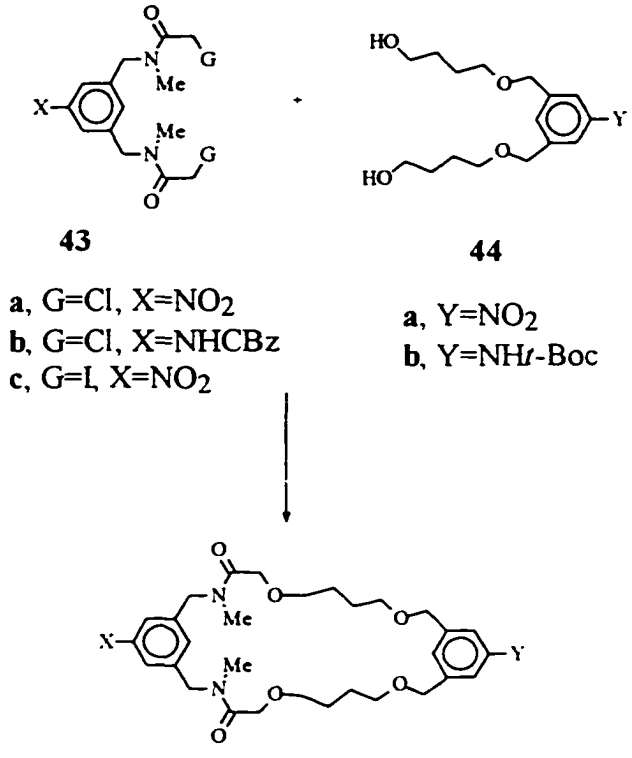

Scheme 14: Synthetic Pathway for Macrocycle **25**

Successful isolation of the model macrocycle **25a** prompted the synthesis of the wall unit with the linker sites **25b** or **25c**. As shown in Scheme 14, target **25b** should be obtained from the reaction of **43a** or **43c** and the diol **44b**. Target **25c** would involve the reaction of **43b** with **44a**. The bischloroamide **43a** was prepared as shown in Scheme 15 which is similar to the synthesis of the model compound **24b**.

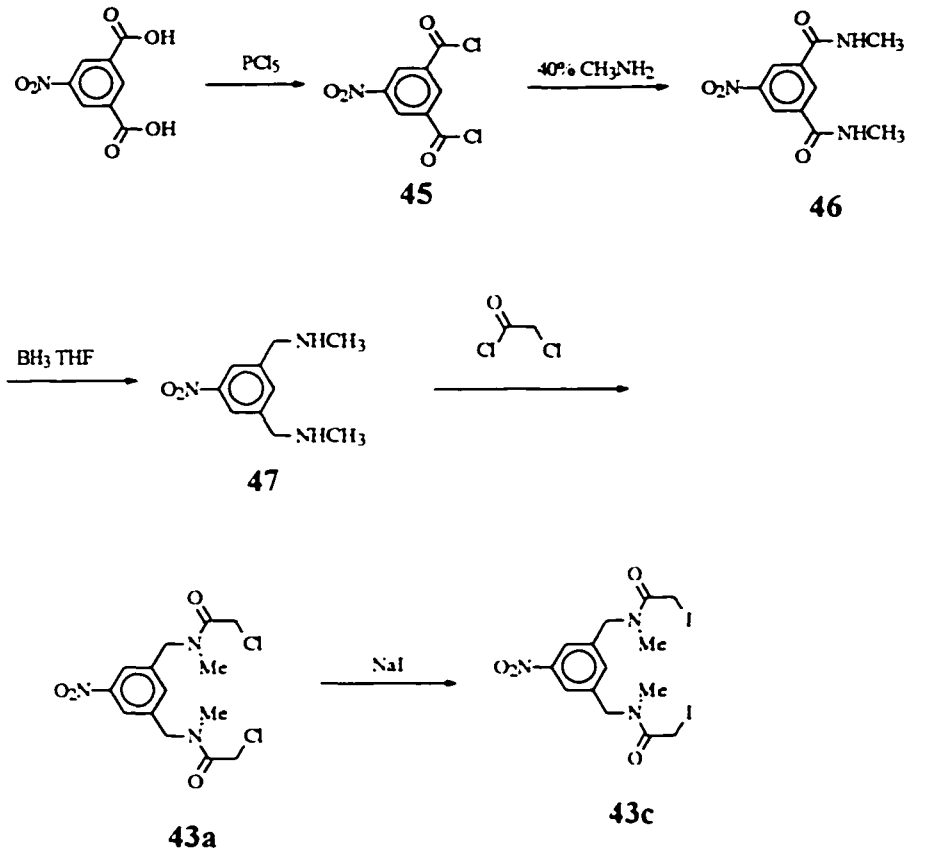

Scheme 15: Synthesis of Bischloroamide **43a** and Bisiodoamide **43c**.

5-Nitroisophthalic acid was melted with phosphorous pentachloride to yield 5-nitroisophthaloyl chloride **45** in quantitative yield. The acid chloride was not purified but was reacted immediately with methyl amine to give the diamide **46**. Attempts to reduce **46** with $LiAlH_4$ to the diamine **47** were not successful as the nitro group was partially reduced as well. The reduction was successful using borane with a crude yield of 85%. The ^{13}C nmr of the diamine shows the benzyl methylene signal at 54.9 ppm. If not used immediately, the diamine **47** was stored as the oxalate salt. To

liberate the free amine, the oxalate was dissolved in water and CH_2Cl_2 and made basic with KOH. The organic layer was extracted and the solvent was allowed to evaporate to yield the amine **47**. Reaction with chloroacetyl chloride gave the 5-nitro bischloroamide **43a** as a white solid in 58% yield. As expected, the ^{13}C nmr reveals the presence of the conformational isomers arising from the hindered rotation about the tertiary amide bond. The methylene peaks due to the α carbon are found at 40.8, 41.0 and 41.1 ppm and the carbonyl is found at 167 ppm. The chlorines in **43a** were replaced by iodines in **43c** to prepare a compound with a better leaving group by reacting with NaI in acetone to give the bisiodoamide **43c**. The ^{13}C nmr spectrum of **43c** (Figure 38) also shows the peaks due to the rotational isomers. An interesting feature of this spectrum is that by replacing Cl with I, we observe an upfield shift of the α carbon to -3.2 ppm. The carbonyl signal is downfield by 4.5 ppm relative to that for **43a**, which is found at 171.5 ppm

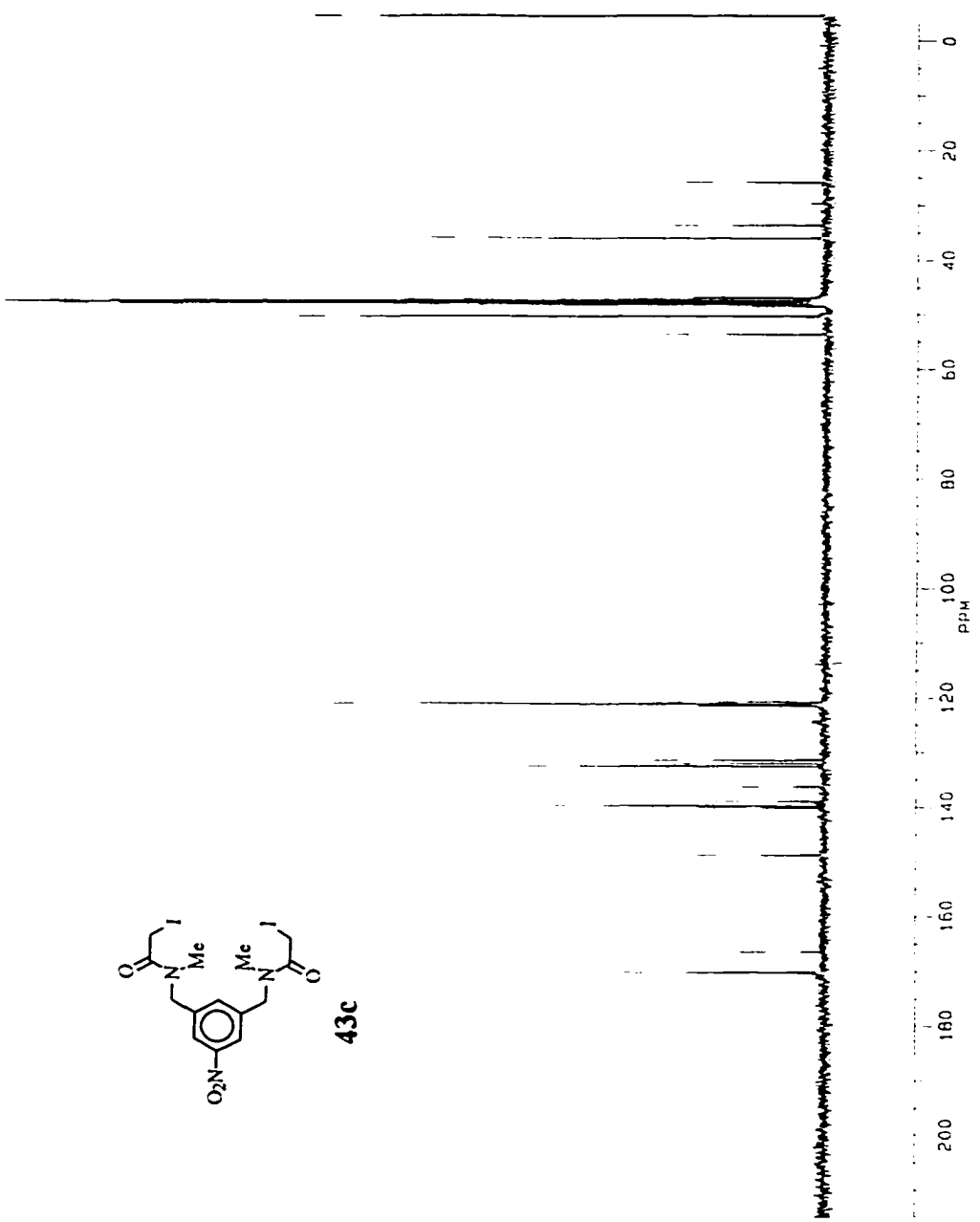

Figure 38: ^{13}C NMR Spectrum of Bisiodoamide **43c**.

An alternate route that involved one less step was devised for the synthesis of the diamine **47**[61] (Scheme 16). The diol **48** was converted to the dibromide **49** by heating with a 48% HBr aqueous solution and benzene. As the dibromide formed, it dissolved in the organic layer. The organic layer was extracted with water and then evaporated. The solid dibromide compound **49** remained, which was easily recrystallized from cyclohexene. The ^{13}C nmr showed the benzyl signal at 30.6 ppm. The ^{1}H nmr signal due to the benzyl protons was at 4.50 ppm. The bromide was displaced with methyl amine[61] to yield **47**. The spectra were identical for compound **47** obtained by either method.

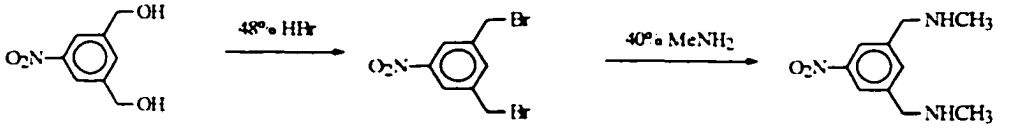

48 **49** **47**

Scheme 16: Alternate Route to **47**[61]

The diol **44a** was prepared as shown in Scheme 17. Compound **49** was heated with a large excess of 1,4-butanediol to afford **44a**. Purification was extremely tedious. Removal of the bulk of the butanediol involved 5-6 hours on the rotoevaporator connected to the vacuum pump. This was followed by a silica gel precolumn using Et_2O as the eluent to remove more of the residual butanediol. Finally centrifugal chromatography on silica gel using 1:1 Et_2O:hexanes as the eluent gave pure diol **44a**. The integration of the ^{1}H nmr shows that all the 1,4-butanediol has

been removed. Figure 39 is an expansion from 1-5 ppm and clearly shows the singlet due to the benzyl methylenes at 4.55 ppm, the triplet due to the methylene of the primary alcohol at 3.62 ppm and the triplet due to the methylene at the ether linkage at 3.53 ppm (assignments may be interchanged). The ratio of the integration for these peaks was 1:1:1. If there were octanediol present then the integration would be more for the primary alcohol at 3.62 ppm.

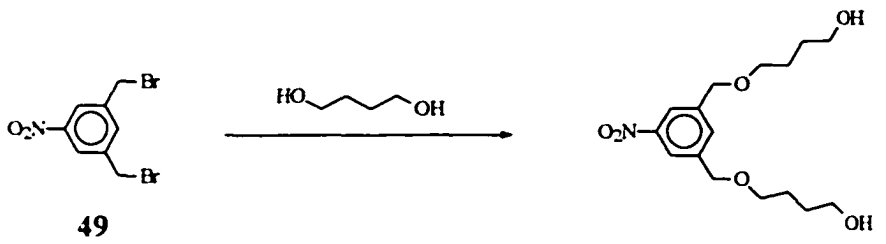

49 **44a**

Scheme 17: Synthesis of Diol **44a**

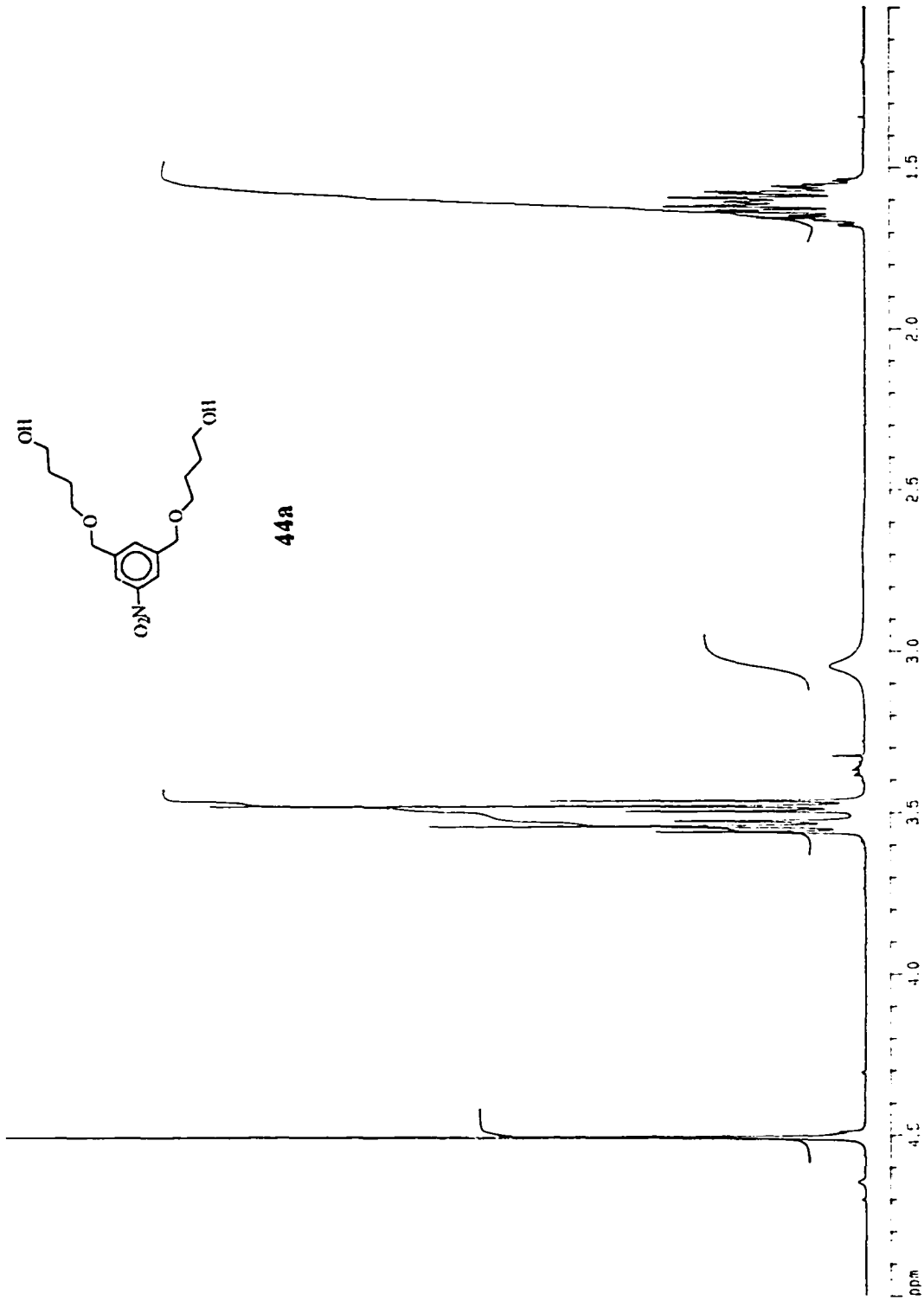

Figure 39: ^{1}H NMR of **44a**.

Now, both **43a** (or **43c**) and **44a** have nitro group linkers. To avoid the problem of creating a symmetric molecule, then one of them must be reduced and protected before cyclization. The reduction of the nitro groups of both **43a** and **44a** were investigated. Compound **44a** was reduced quantitatively with hydrazine in 2-methoxyethanol to afford the amine **50** (Scheme 18). The ^{13}C nmr shifts of the aromatic signals are shifted upfield at 113.6, 117.1, 139.4 and 146.6 ppm compared to the chemical shifts for the aromatic carbons of the nitro compound **44a**. Compound **50** was reacted without purification with di-*tert*-butyl dicarbonate to yield the *t*-Boc protected amine **44b**. The ^{13}C nmr reveals a peak representative of the quaternary carbon of the t-butyl group at 80.4 ppm and the carbamate carbonyl at 152.8 ppm.

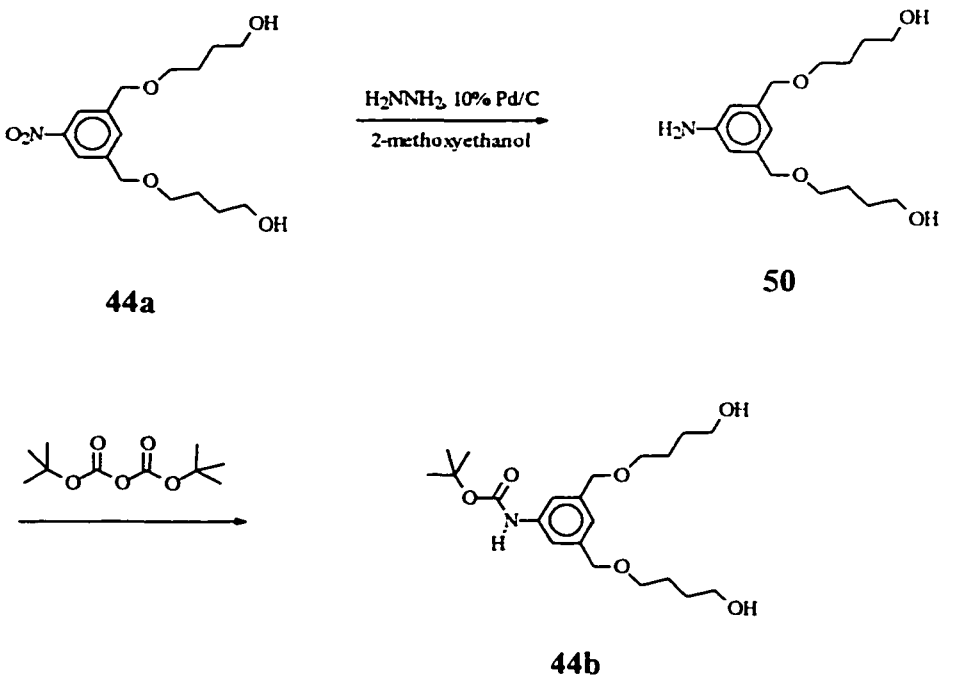

Scheme 18: Synthesis of *t*-Boc Protected Amine **44b**

Alternatively, the nitro group on compound **43a** was reduced quantitatively to compound **51** using H_2 and Adam's catalyst in acidic 95% ethanol (Scheme 19). Hydrazine could not be used here because it is nucleophilic and the hydrazine would displace the chloride. Also, if the solvent is not acidic, then the resulting amine displaces chloride in a nucleophilic substitution reaction as it forms. The ^1H nmr revealed the upfield shift of the aromatic signals due to the functional group change from a nitro group in compound **43a** to an amino group in compound **51**. The chemical shift of the aromatic signals in both the ^1H and ^{13}C nmr spectra are dependent on the pH of the solution. The amine hydrochloride **51** was reacted with benzyl chloroformate in the presence of a base to afford the Cbz protected compound **43b** in 34% yield. The signal for the Cbz benzyl carbon appears in the ^{13}C nmr at 67.6 ppm. There are three peaks assigned to the carbamate carbonyl at 141.1, 141.5 and 155.7 ppm that are a result of the tertiary amide conformational isomers. The ^{13}C nmr is shown in Figure 40.

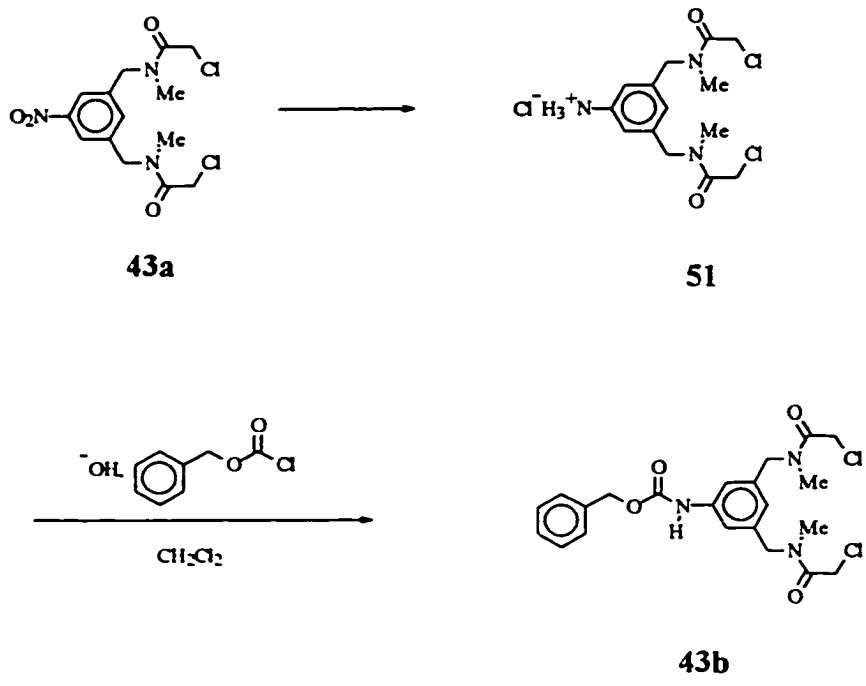

43a **51** **43b**

Scheme 19: Synthesis of **43b**

At this stage, either compounds **43a** (or **43c**) and **44b**, or compounds **43b** and **44a** would have to undergo reaction to yield the macrocyclic targets **25b** or **25c** respectively. The first route chosen was the reaction of **43a** with **44b**. Several attempts were made using 10% DMSO in THF or THF as the solvent and varying the equivalents of NaH added, but the macrocycle **25b** was not detected. There were many different products visible by TLC but none of the isolated products proved to be **25b**. One of the compounds isolated was the starting diol **44b**. The bischloroamide **43a** was not recovered. We thought a better leaving group may encourage the substitution reaction so **43c** was reacted with **44b** but still the desired target was not obtained. In a similar fashion, **43b** was reacted with **44a** but target **25c** was not

obtained. In the presence of the strong base, the α carbon may be deprotonated[60] to yield a carbanion which is a chloro enolate. One possibility is that the anion formed then reduces the aromatic nitro group. A second possibility is that the anion generated may do a nucleophilic attack on the aromatic ring. These pathways do not lead to the nucleophilic substitution of chloride at the α carbon.

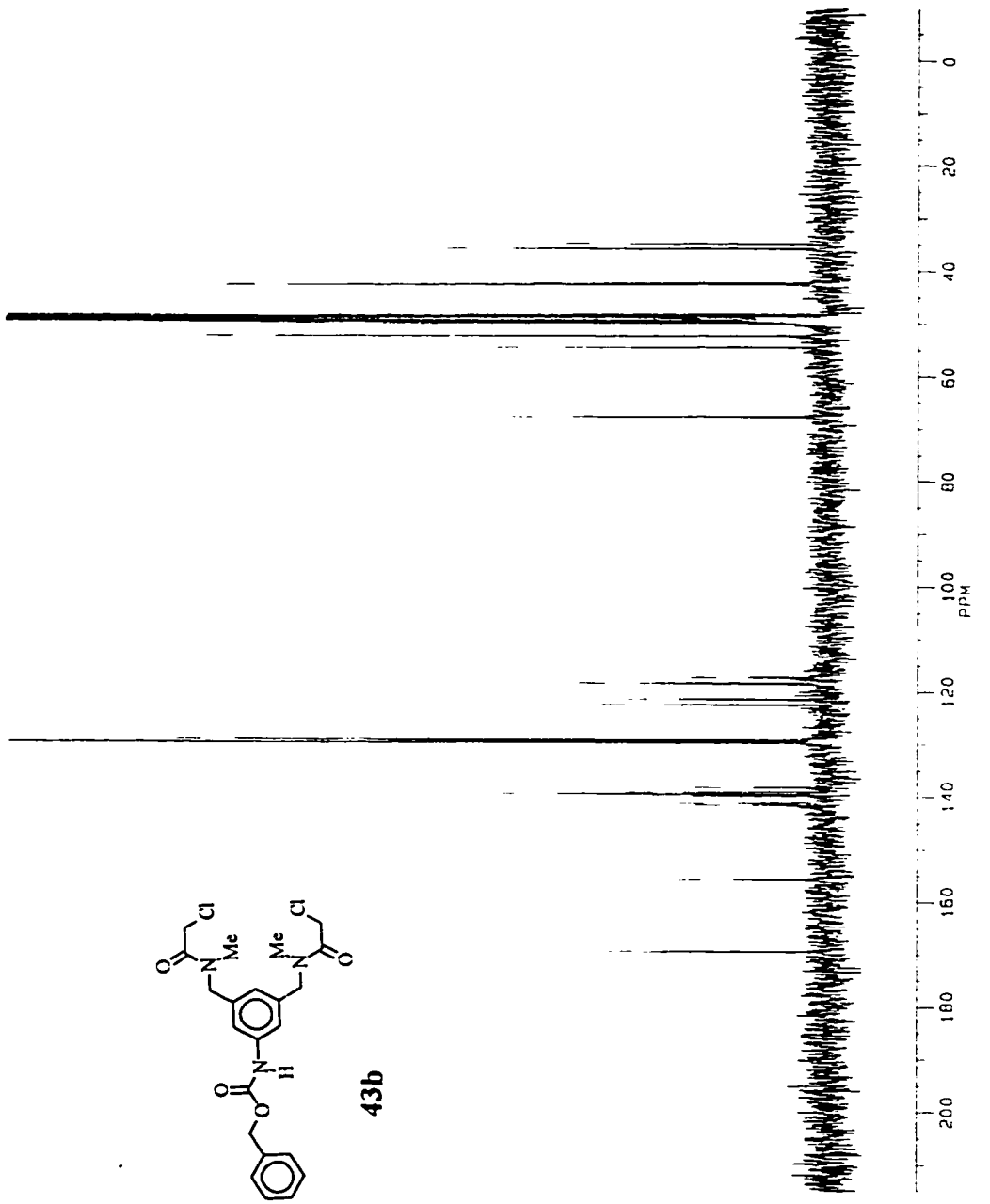

Figure 40: ^{13}C NMR Spectrum of Cbz Protected Compound **43b**.

3.2 Discussion Leading to the Synthesis of Macrocycle 27.

The synthesis of the diol **44a** was cumbersome making it difficult to obtain enough pure **44b** to fully investigate the chemistry, so an alternative diol **26** was synthesized. Compound **26** was obtained from the reaction of isophthaloyl chloride with 3-aminopropanol using triethyl amine as the base (Scheme 20).

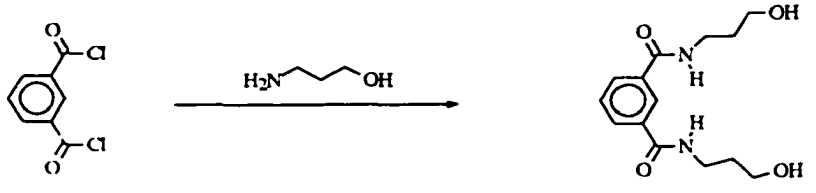

26

Scheme 20: Preparation of **26**

Compound **26** was isolated as a white solid in 76% yield by chromatography. The purification is far more facile than the purification for **23**. The ^{13}C nmr displayed the peak due to the amide carbonyl at 169.5 ppm and the signal associated with the methylene of a primary alcohol characteristically at 60.6 ppm. The analogous compound **52** was prepared with 5-nitroisophthaloyl chloride **45** under the same conditions required for the synthesis of **26** (Scheme 21). Compound **52** was reduced using hydrazine to **53** which was protected without purification to afford **54**.

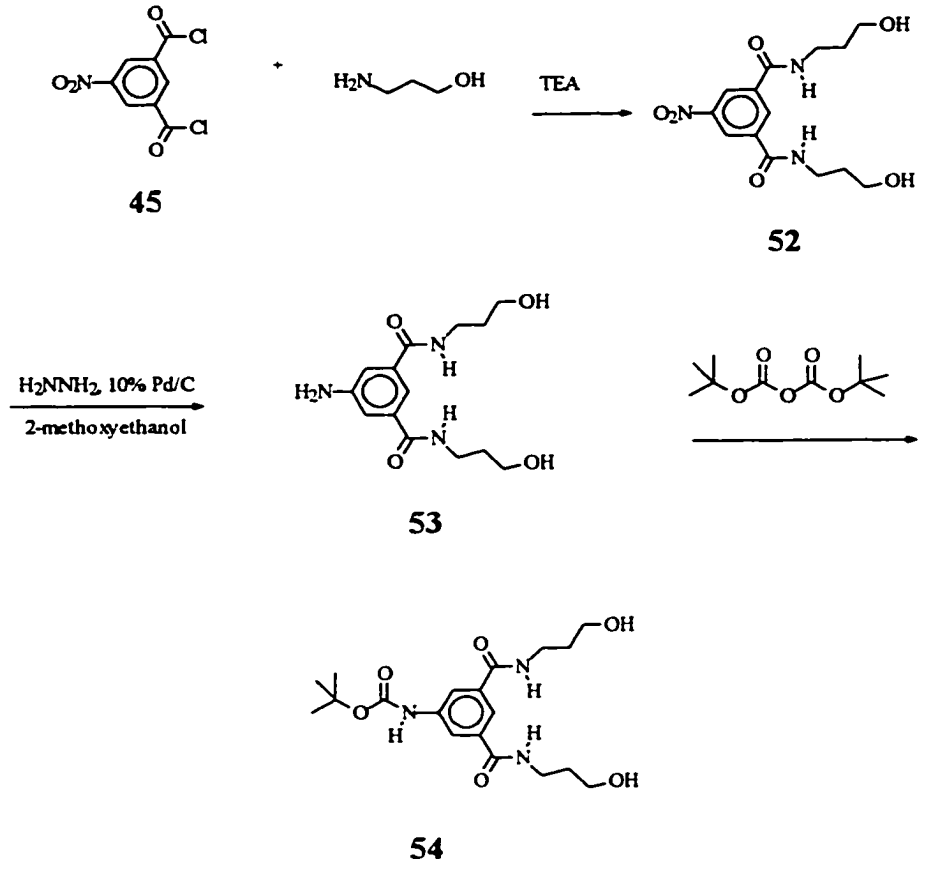

45 52 53 54

Scheme 21: Preparation of **54**

Compound **54** was purified by centrifugal chromatography and was the third, but major, product to elute. The fourth product that eluted was characterized as **54a** and is believed to arise from the hydroxylamine **55**, which was prepared via the incomplete reduction of the nitro group on compound **52** (Scheme 22). The ^{13}C and ^{1}H nmr of the two compounds are very similar and it was only from the differences in mass spectra that they could be identified. The mass spectra for the two compounds

demonstrated that **54a** was 16 mass units higher than **54**. The same was true for several of the fragment ions.

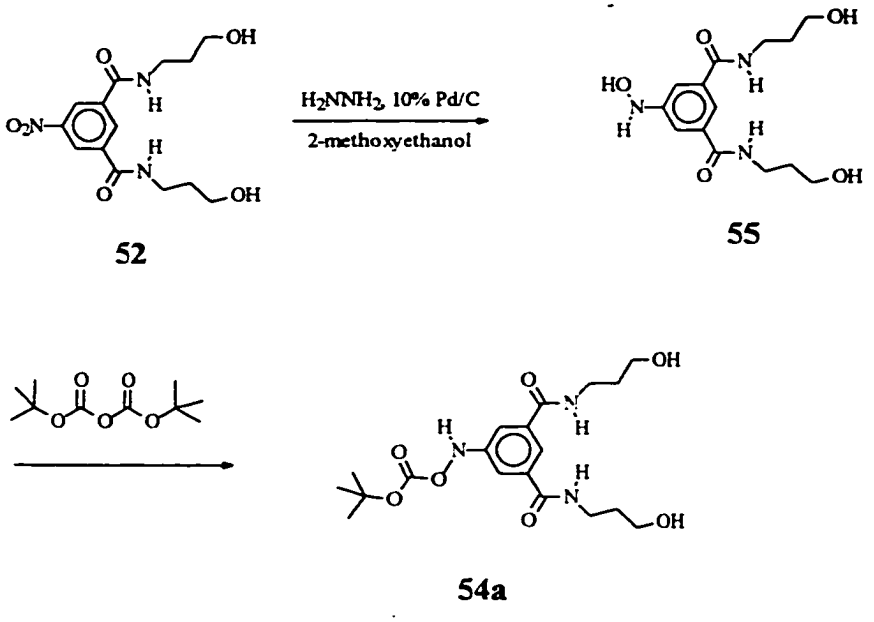

52 **55**

54a

Scheme 22: Pathway for the Formation of **54a**

The ^{13}C nmr's are shown for comparison in Figure 41 for both **54** and **54a** and the values of the chemical shifts are summarized in Table 2. The shifts of the propanol moiety are the same in both compounds. The difference is more pronounced at the quaternary carbon of the *t*-butyl group which is shifted by 2.3 ppm downfield in **54a**. Also, the signals resulting from the aromatic carbons are shifted downfield. The aromatic carbon, C-5, to which the nitrogen is bonded is shifted from 141.3 ppm in **54** to 144.4 ppm in **54a**. The substituent in **54a** is more deshielding and thus causes the downfield shift. The other aromatic carbons are also affected, though to a lesser extent. The carbamate carbonyl is shifted downfield in **54a** by 0.4 ppm.

The ^{1}H nmr's are shown for comparison in Figure 42 and the chemical shifts are summarized in Table 3. Consistent with the ^{13}C nmr, the signals associated with the aromatic protons are shifted downfield from 7.70 and 7.87 ppm in **57** to 7.86 and 8.03 ppm in **54a**.

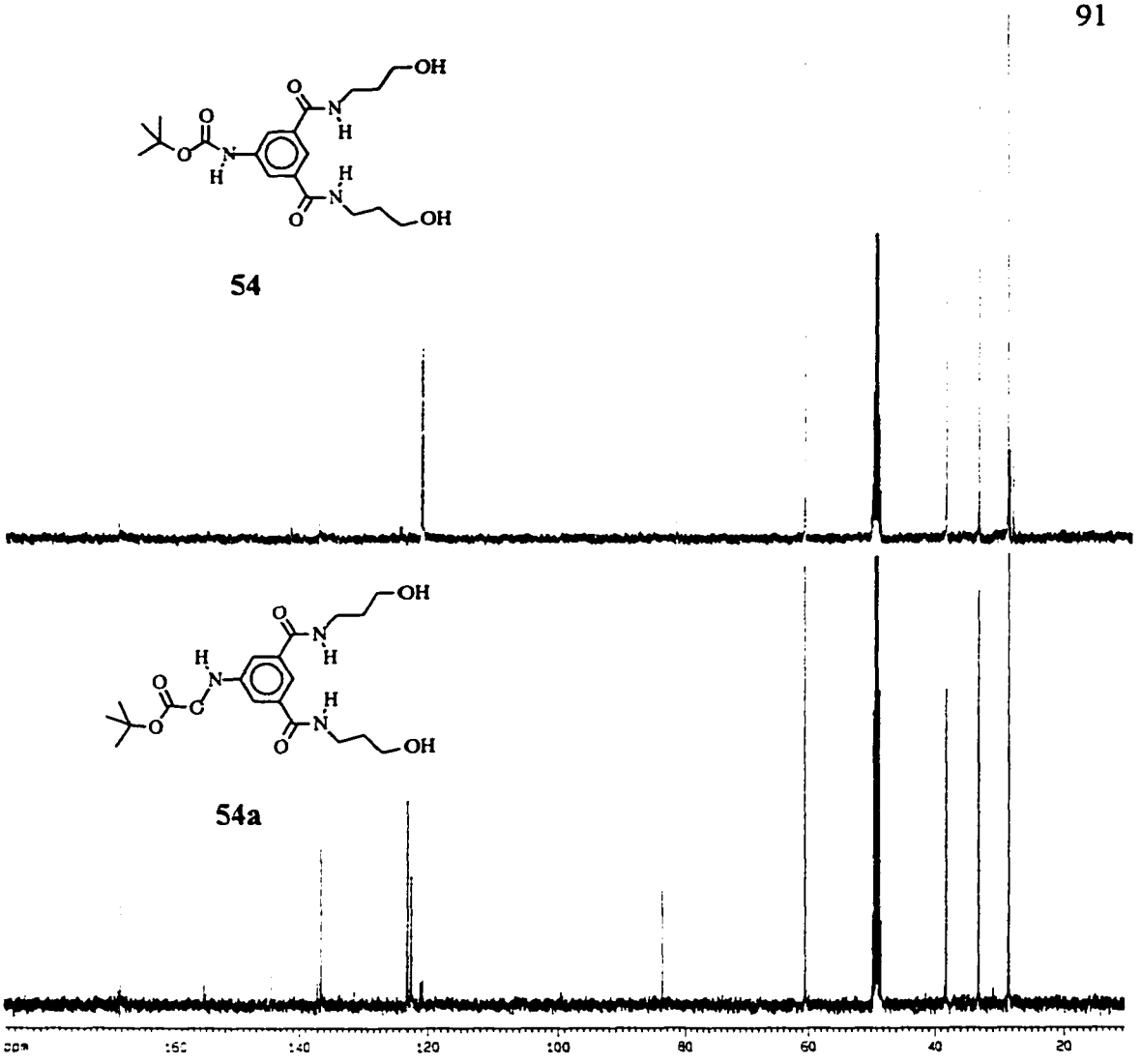

Figure 41: ^{13}C NMR Spectra of **54** and **54a**.

Table 2: Comparison of the ^{13}C nmr data for Compounds **54** and **54a**.

	54	**54a**
-CH_3	28.6	28.5
$CH_2CH_2CH_2$	33.1	33.1
NCH_2	38.1	38.2
CH_2OH	60.5	60.5
4°C	81.4	83.7
Ar	120.7, 121.0, 136.8, 141.3	122.4, 122.9, 136.4, 144.4
C=O $_{Carbamate}$	154.9	155.3
C=O $_{Amide}$	169.5	169.2

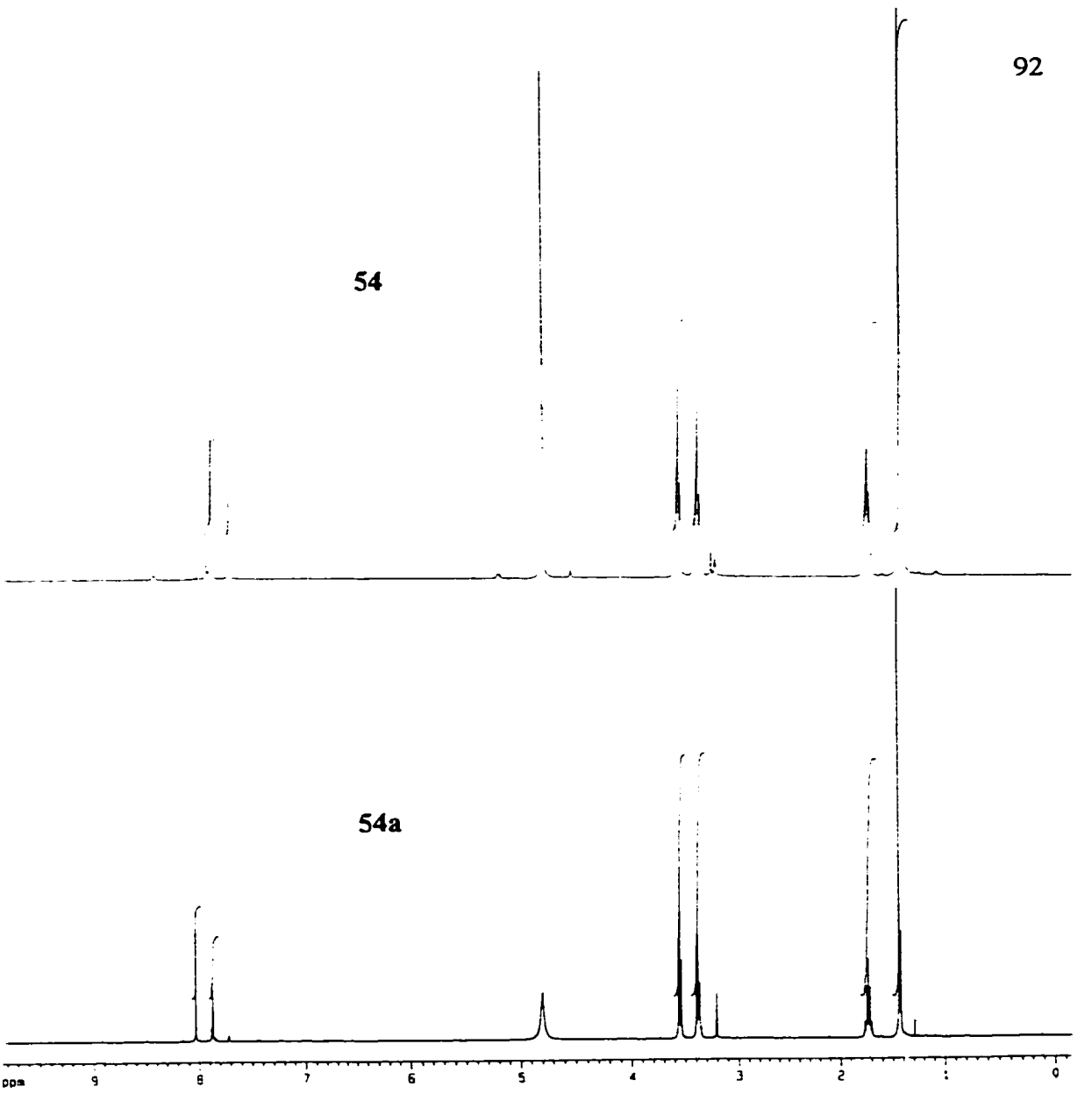

Figure 42: ^{1}H NMR Spectra of **54** and **54a**.

Table 3: Comparison of the ^{1}H nmr data for Compounds **54** and **54a**.

	54	**54a**
$-CH_3$	1.04 s	1.44 s
$CH_2CH_2CH_2$	1.72 qu	1.73 qu
NCH_2	3.36 t	3.38 t
CH_2OH	3.54 t	3.55 t
Ar	7.70 t, 7.87 d	7.86 t, 8.03 d

Reaction of the diol **54** with the bischloroamide **43a** to produce **27** (Figure 43) using NaH to generate the alkoxide and 10% DMSO in THF as the solvent proved futile. The solvent was varied to include DMA, DMF and THF but still no product resulted. Only the diol **57** was recovered. There was none of the bischloroamide **43a** remaining.

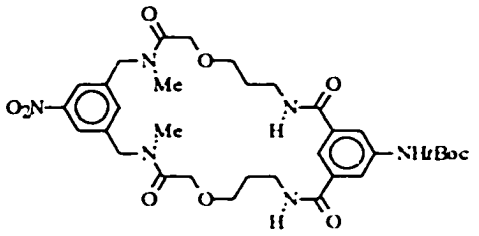

Figure 43: Macrocycle **27**

It was concluded that the conditions required to generate the alkoxide as well as the solvent needed to support such a reaction were not favourable for product formation.

To summarize, the N-H proton of a secondary amide is too acidic for the conditions necessary for the reaction to occur. Although cyclization was effected using the tertiary amide **24b** and the solvent system, 10% DMSO in THF, the same tertiary amide with the nitro group on the phenyl ring does not produce product. This problem is inherent with the aromatic nitro group. In the cases studied by Bradshaw[52,53] the methods employed thiols or secondary amines as the nucleophile. These groups are more nucleophilic and less extreme conditions are necessary for reaction. For example, the

thiol, RSH, can act as a nucleophile and it is not necessary to deprotonate. A weak base may be used to "mop up" any acid generated by the reaction. Instead of converting the diol **26** to the dithiol **58**, which did not work after several attempts, the dibromide **56** was prepared from isophthaloyl chloride and 3-bromopropylamine hydrobromide (Scheme 23). This compound was converted to the bisthiouronium salt **57** using thiourea under basic conditions which was not isolated but was immediately converted to the dithiol **58** with the addition of acid. This model compound was prepared[57] as an initial step towards macrocycle **28**, but polymerization resulted via oxidation of the thiols when purification was attempted; and in macrocyclization reactions, it is critical that starting materials are pure.

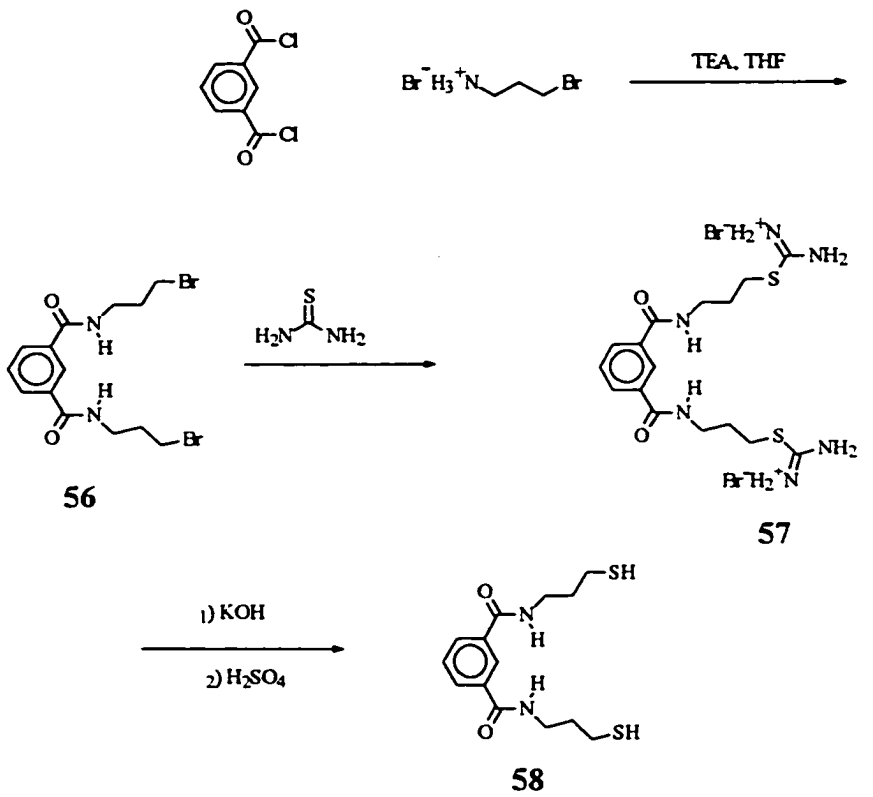

56 57 58

Scheme 23: Synthesis of **58**.

3.3 Synthesis of the Tetraester Macrocycles

A retrosynthetic analysis of the tetraester macrocycles is shown in Scheme 24. The Scheme illustrates that the macrocycle could be obtained either in one step, via a 2 + 2 coupling of reactants, or via a stepwise approach. If the reaction is completed in one step then substituents X and Y will be the same. If the reaction is done sequentially, by reacting two equivalents of 1,8-octanediol with one equivalent of diacid chloride and the resulting diol reacted with one equivalent of a different diacid chloride, then substituents X and Y could be different. Both of these pathways were investigated.

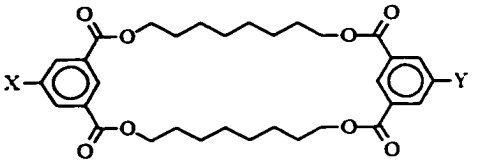

29

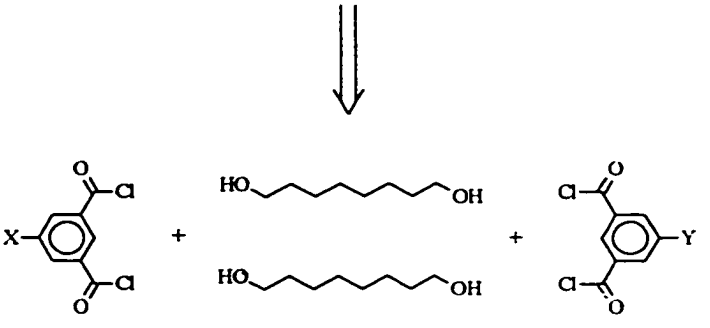

Scheme 24: Retrosynthetic Analysis of Tetraester Macrocycles

The first attempt at a tetraester macrocycle was the model system where X=Y=H. We decided to use the stepwise route as that would be eventually the route necessary to differentiate between the two linkers X and Y, and this would provide insight into the required chemistry.

Isophthaloyl dichloride was reacted with two equivalents of 1,8-octanediol (Scheme 25). Triethylamine hydrochloride precipitated and was discarded. The mother liquor, upon standing, yielded a second precipitate which proved to be the 2+2 product, macrocycle **29**, in 1.5% yield. These results were encouraging because not only did they indicate that the formation of compound **29** was favourable, but that it was also a solid compound. A third precipitate was isolated and appeared to be the smaller macrocycle **59**, a result of the 1 + 1 product, contaminated with a small amount of **29**.

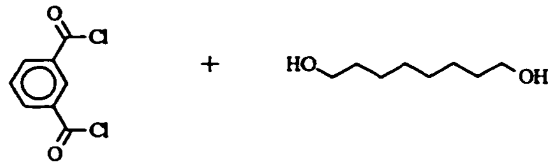

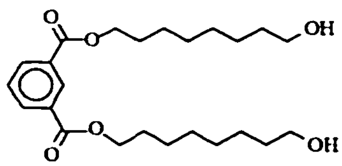

60

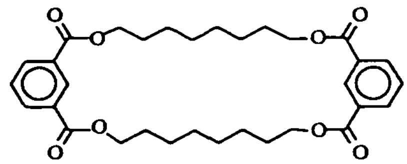

29

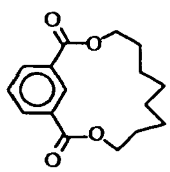

59

Scheme 25: Synthesis of **60**

The diol **60** was the major product isolated in 42% yield. The compounds were characterized by ^{13}C and ^{1}H nmr. The ^{13}C nmr of the diol is shown in Figure 44. There are 6 peaks clustered between 25.6 and 32.6 ppm and these shifts are characteristic of alkyl methylenes. The peak at 62.7 ppm is indicative of the primary alcohol and the peak at 65.5 is due to the carbon next to the ester oxygen. There are only four different aromatic signals in the spectrum (128.5, 130.6, 130.8 and 133.7 ppm), because of the plane of symmetry in the molecule. The ester carbonyl is also characteristic at 165.9 ppm.

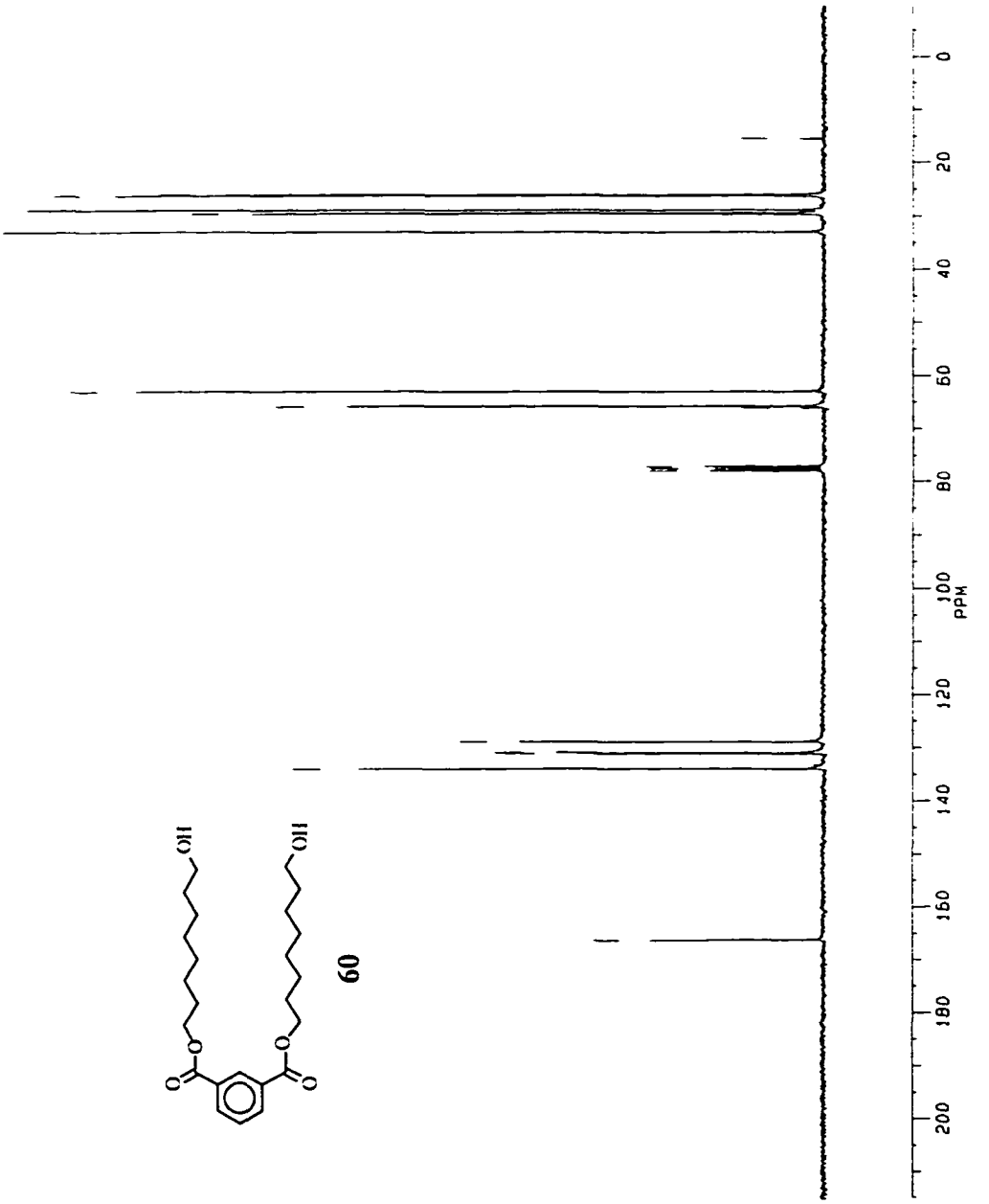

Figure 44: ^{13}C NMR Spectrum of Diol **60**.

The ^{13}C nmr of the macrocycle **29** appears to be much simpler. Still there are four peaks due to the aromatic carbons, which shifted slightly, probably due to ring formation. With the additional plane of symmetry the aliphatic region of the spectrum simplifies a great deal to give a 3 line shift pattern with peaks at 26.0, 28.6 and 29.1 ppm.

Given these encouraging results, 5-nitroisophthalic acid was reacted with one equivalent of 1,8-octanediol under high dilution conditions using tetrahydrofuran as the solvent and triethylamine as the base to neutralize the hydrochloric acid (Scheme 26).

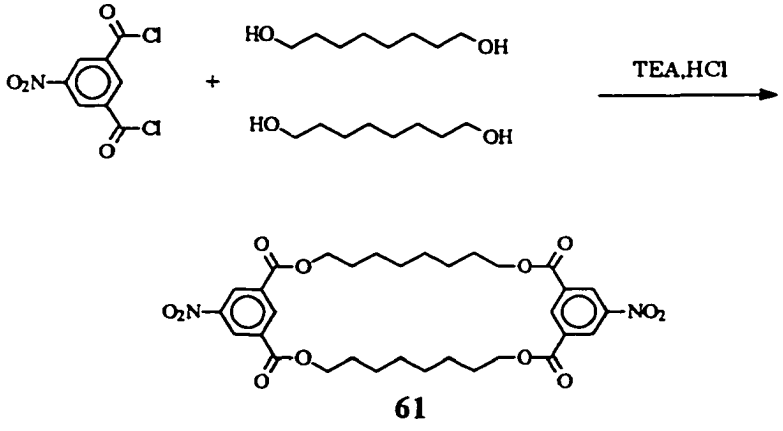

61

Scheme 26: Synthesis of Dinitro Macrocycle **61**

The triethylamine hydrochloride was filtered and discarded. The residue was dissolved in CH_2Cl_2 and precipitated by addition of 95% ethanol. The solid was collected in 96% yield and by ^1H and ^{13}C nmr the sample resembled pure macrocycle **61**. The mass spectrum (Figure 46) revealed the sample was a mixture of the 1+1, 2+2, 3+3 and 4+4 macrocyclic products (Figure 45). It is interesting that the nmr spectra appear to be the same for all four compounds. The mixture also had a sharp melting point at 81-82°C. The most

marked difference in the ^{13}C nmr spectrum compared to that of **29** is in the shift of the aromatic carbons. Due to the electron withdrawing substituent , $-NO_2$, the peaks are shifted downfield, especially the peak due to carbon 5 to which the nitro group is bonded. The peaks assigned to the aromatic carbons are found at 128.0, 132.7, 135.8 and 148.4 ppm. Overall, the ^{13}C nmr was very similar to the spectrum of the model compound **29**.

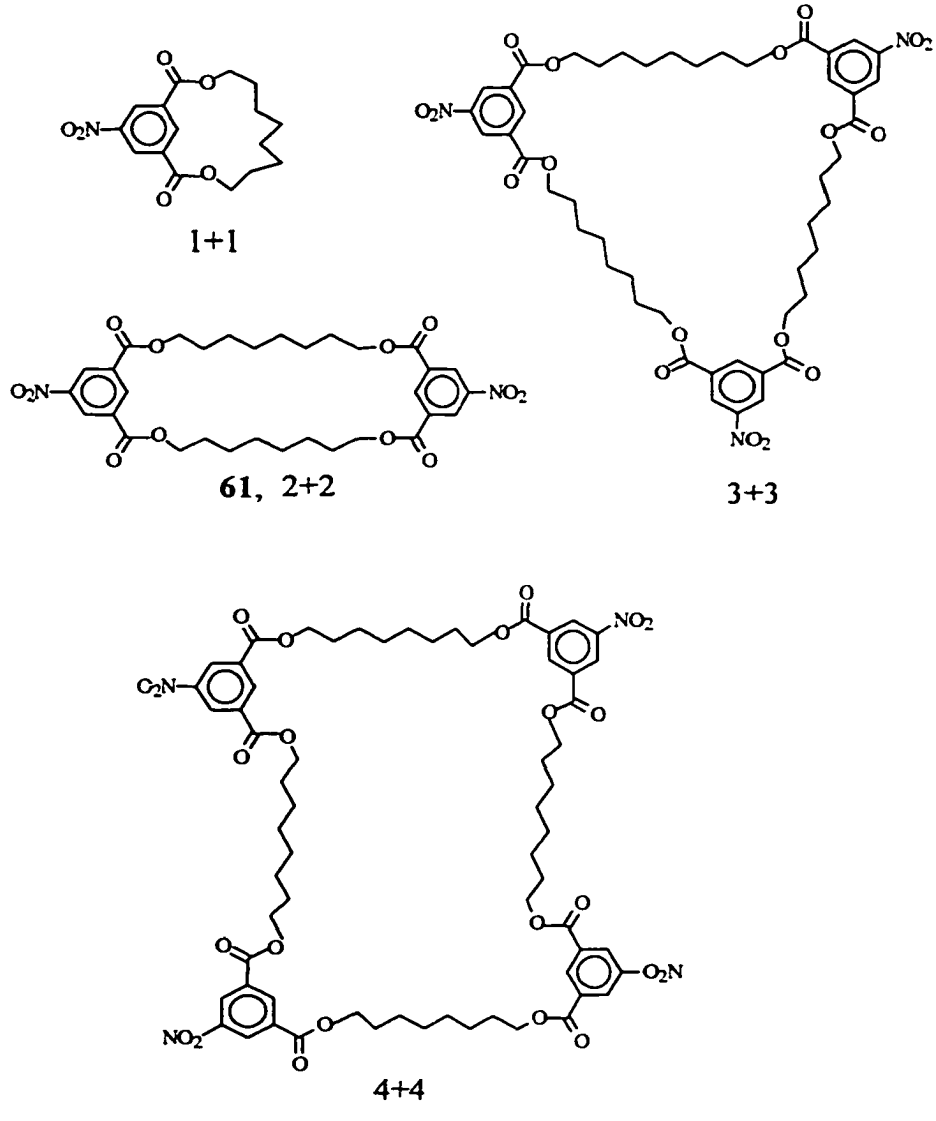

Figure 45: Mixture of Macrocyclic Products

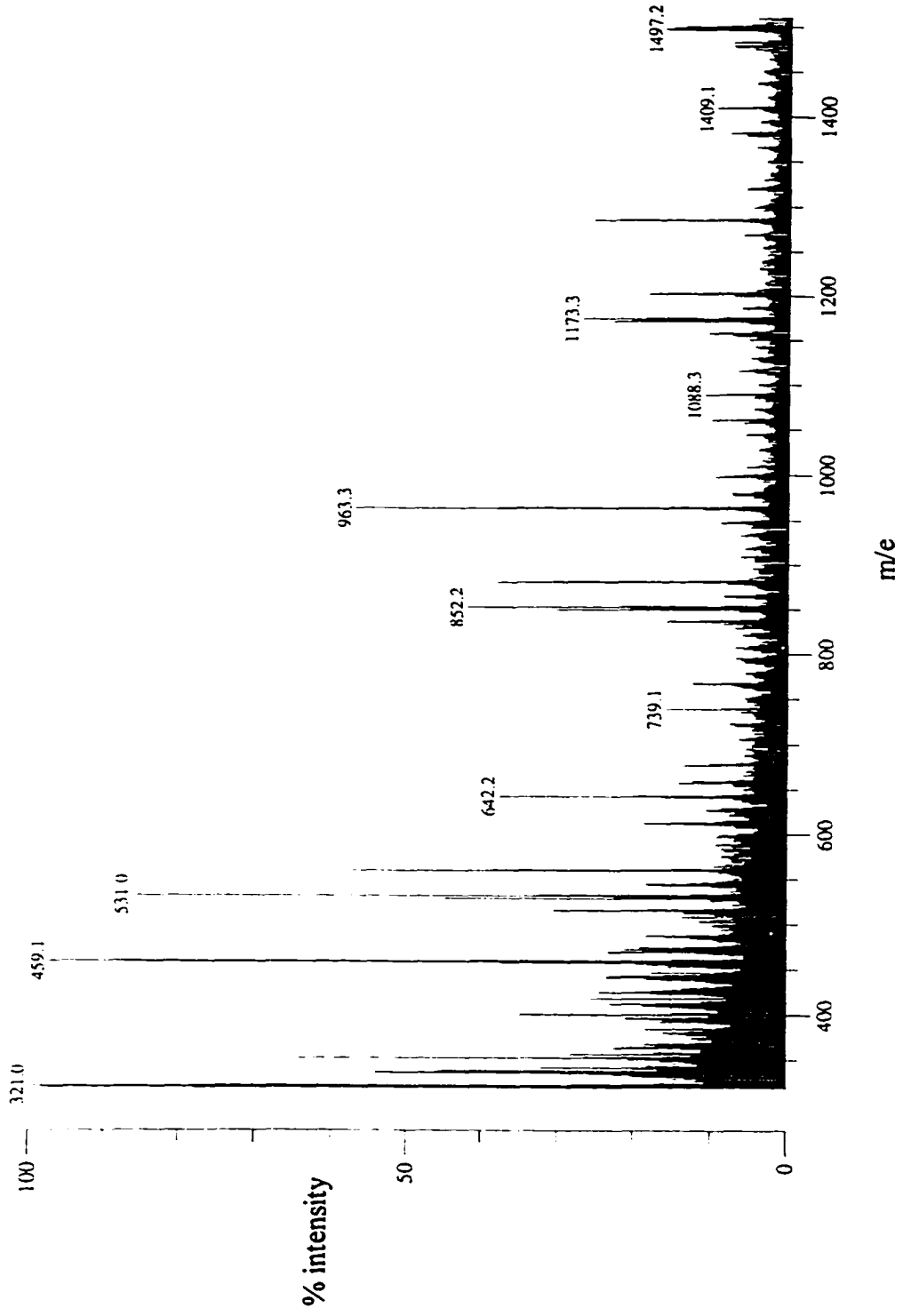

Figure 46: Mass Spectrum of Macrocyclic Mixture **61**

An alternate route in which the macrocycle is assembled in a stepwise fashion was employed (Scheme 27). This stepwise route involves the monoprotection of 1,8-octanediol with dihydropyran. The monoprotection was carried out conventionally and the purification of **62** was routine. It was critical to remove all traces of 1,8-octanediol at this stage because at any of the later purification steps all attempts at removing 1,8-octanediol impurities proved futile. The ^{13}C nmr spectrum exhibited the characteristic methine signal at 98.8 ppm and a primary alcohol at 62.8 ppm. The sample was assumed to be pure if there was only one spot on TLC (R_f=0.12 using 2:1, hexanes: Et_2O). The R_f of the diprotected 1,8-octanediol was 0.45 and 1,8-octanediol did not elute in the same solvent system. Also, the ratio of the ^1H nmr integration of the methine signal at 4.52 ppm to the three -OC$\underline{H}_2$ signals between 3.28 and 3.86 ppm was 1:6. With pure monoprotected 1,8-octanediol in hand, two equivalents of the alcohol **62** were reacted with the diacid chloride under the usual conditions (triethyl amine, tetrahydrofuran) to yield the diester compound **63**. The ^{13}C nmr revealed the loss of the peak attributed to the methylene which bears the primary alcohol but exhibits the peak due to the methylene carbon adjacent to an ester at 67.5 ppm. The four aromatic signals are found at 127.9, 132.7, 135.7 and 148.4 ppm. The nitro group on compound **63** was reduced to the amino **64** in quantitative yield using 25 psi of H_2 and a catalytic amount of Adam's catalyst in 95% ethanol. It was evident from the upfield chemical shift of the aromatic signals that a refunctionalization from an electron withdrawing nitro group to an electron donating amino group occurred. The peaks resulting from the aromatic carbons are found at 119.6, 120.6, 131.8 and 146.6 ppm. The

chemical shift of the aromatic protons depends on the pH, consistent with the aniline functional group.

The amine was protected with a *t*-butyloxycarbonyl (*t*-Boc) group by dissolving **64** and di-*tert*-butyl dicarbonate in CH_2Cl_2 and allowing the reaction to continue for 3 days. The reaction was monitored by TLC observing the disappearance of the fluorescent spot due to the amine at R_f=0.53 using Et_2O as the eluent. The carbamate compound **65** was isolated in 88% yield. Again, the aromatic signals are the most affected by the change in functional group. They shift to 123.4, 125.0, 131.7 and 139.0 and the carbamate carbonyl appears at 152.4 ppm.

The tetrahydropyranyl group was removed under acidic conditions to yield the diol **66** in 70% yield. Centrifugal chromatography using diethyl ether as the eluent afforded a white solid. The ^{13}C nmr reveals the loss of the tetrahydropyranyl group. Probably the most obvious peak loss is that due to the methine carbon which was usually at 98.8 ppm. Reaction of the diol **66** with the diacid chloride **45** under high dilution conditions using triethyl amine in THF produced macrocycle **67** in 16%. The triethylamine hydrochloride was filtered and discarded and the THF evaporated. Centrifugal chromatography using diethyl ether as the eluent produced a white solid. The ^{13}C nmr of the macrocycle **67** is more complicated than for the model **29** because of the loss of symmetry. Figure 47 and Table 4 summarize the chemical shift values for the aliphatic region and demonstrate the similarities between the two macrocycles **29** and **67** and the sample containing the mixture of macrocycles **61**.

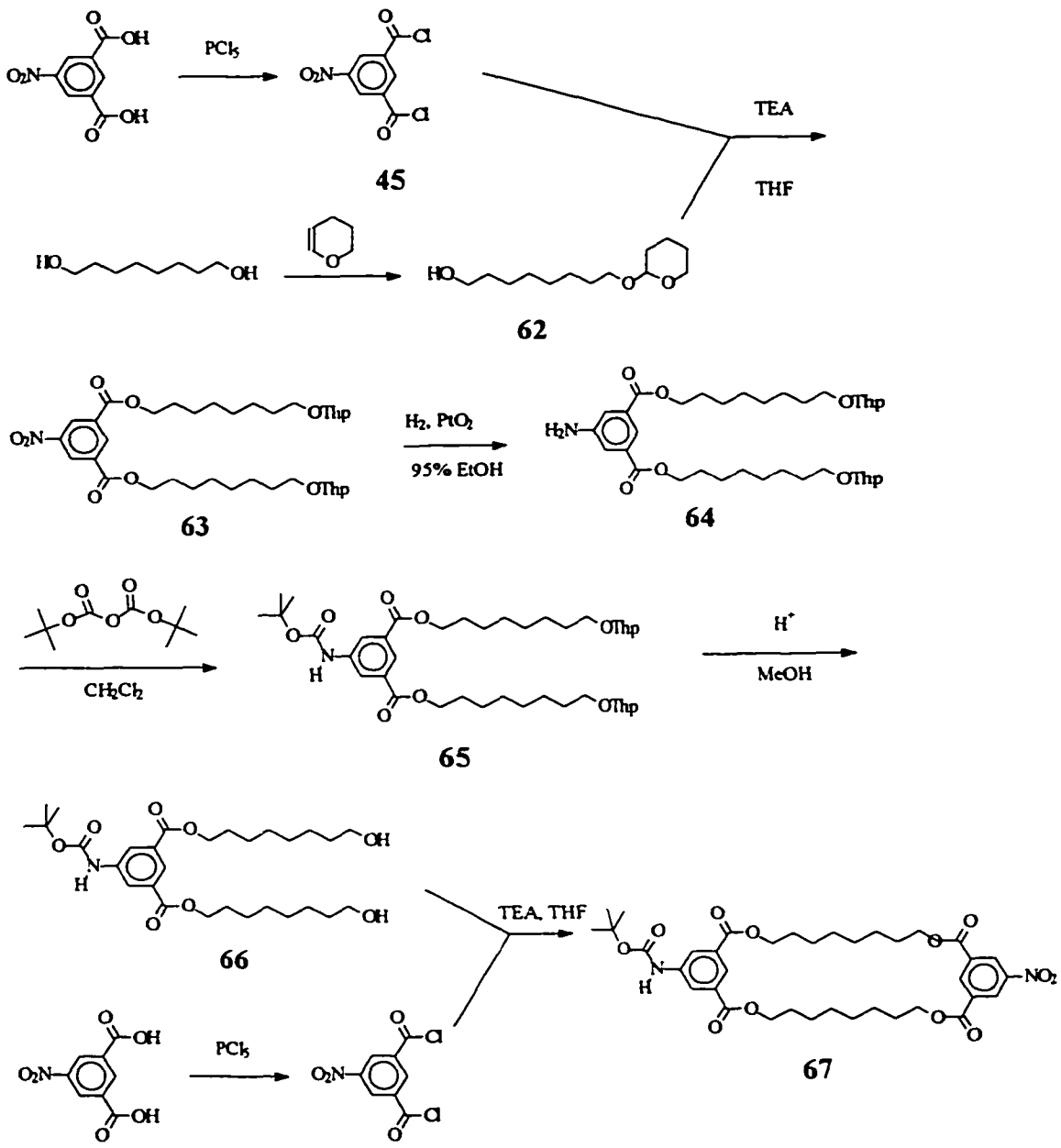

Scheme 27: Stepwise Synthesis of the Asymmetric Macrocycle **67**

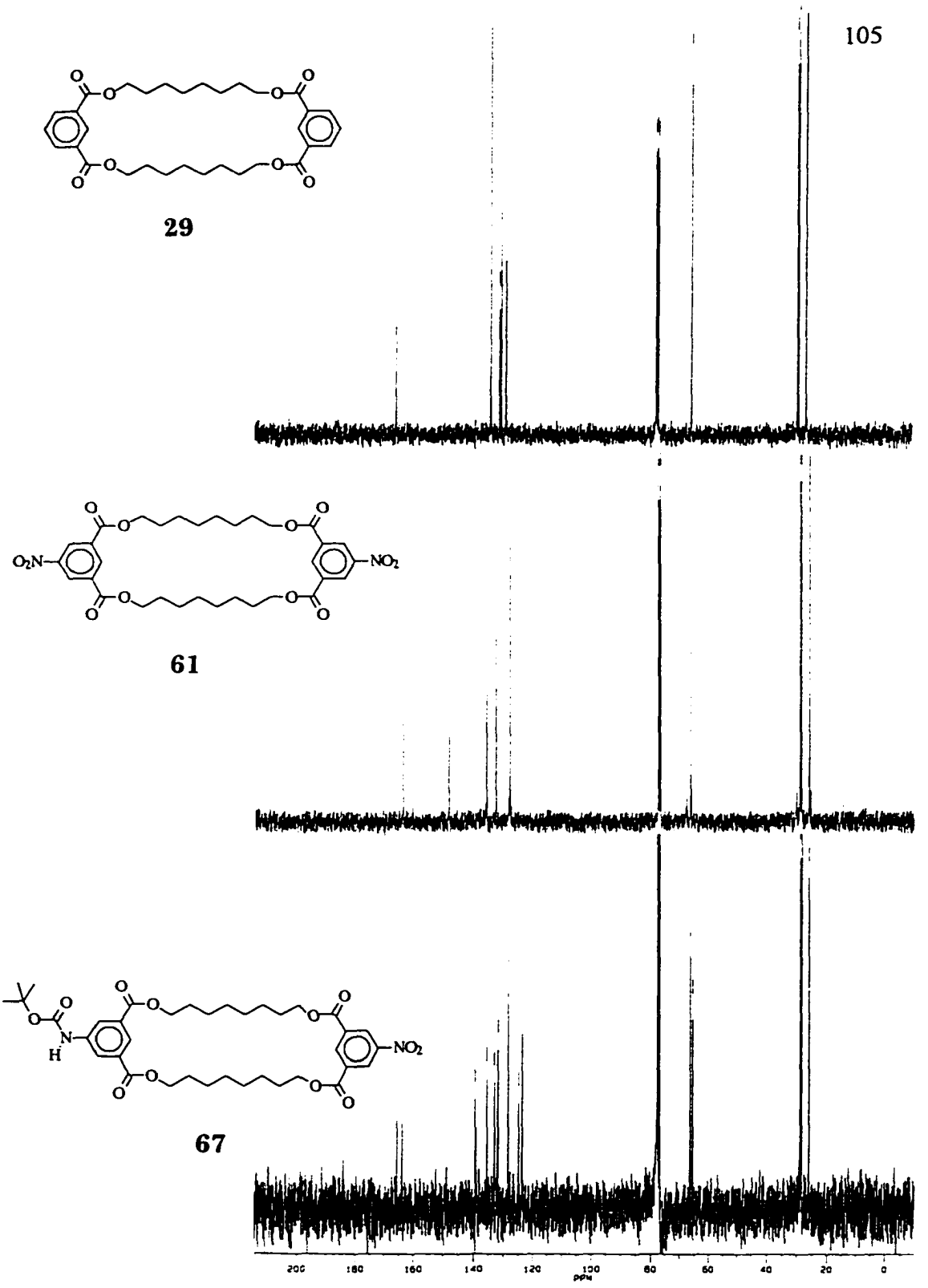

Figure 47: ^{13}C NMR Spectra of Macrocycles **29**, **67**, and a mixture **61**.

Table 4: ^{13}C nmr Chemical Shifts for Tetraester Macrocycles **29**, **67** and **61**.

Compound	$OCH_2CH_2\underline{C}H_2$	$OCH_2CH_2CH_2\underline{C}H_2$	$OCH_2\underline{C}H_2$	$O\underline{C}H_2$
12	26.0	28.6	29.1	65.3
61	25.8	28.5	29.1	66.4
67	25.8	28.3, 28.4	28.5, 28.9	65.4, 66.3

CHAPTER 4

CONCLUSIONS AND FUTURE WORK

4.1 Summary

In chapter 2, section 3.1, synthetic efficiency was introduced as a method of deciding whether a macrocyle was a viable candidate for the new modular set of wall units. To briefly summarize, a list of the advantages and disadvantages for the isolated target macrocycles is shown in Table 5. All the targets have substituted benzene moieties at each end and incorporate either amide or ester functionality along the edges. Macrocycle **25a** was estimated by molecular mechanics to be approximately 14 Å long and was shown using dynamics simulations to be fairly rigid upon heating. This would aid in the investigation of the rigidity requirements of an ion transporter. There are three conformations for this molecule and maybe only one of the three would be the active species. Due to the harsh reaction conditions necessary to deprotonate the alcohol, the target **25** with linkers was not synthesized and is therefore not an option.

The tetraester macrocycle **29** was shown to have a length of approximately 16 Å. From the previous set of active wall units we assume it has a complementary balance of hydrophilic/hydrophobic subunits. The sample containing macrocycle **61**, where both linkers are $-NO_2$, was shown to be a mixture of the 1+1, 2+2, 3+3 and 4+4 macrocycles.

The final and most successful target presented, **67**, was synthesized with linkers X and Y being different. So, even though a relatively low yield was obtained

for the cyclization, the ends are differentiated which will ultimately aid in the synthesis of the transporter.

Macrocycle 67 and the analogous wall unit in the previous generation of building blocks, 8_2, are compared and assessed for efficiency.

Table 5: Advantages and Disadvantages for Isolated Target Macrocycles.

	Advantages	Disadvantages
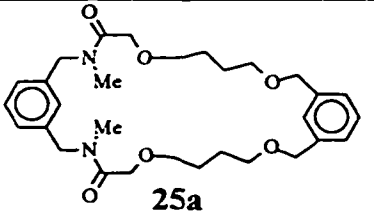 **25a**	- length ~14 Å - very rigid - incorporates different functionality	- conformational isomers, oil - low yield - could not prepare target with linkers
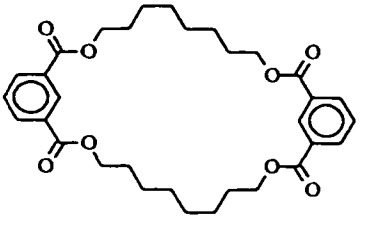 **29**	- length ~16 Å - hydrophilic/hydrophobic mix	- no H bonding capabilities
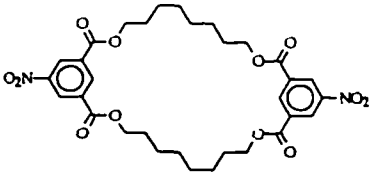 **61**		- linkers are the same - not pure, mixture of compounds
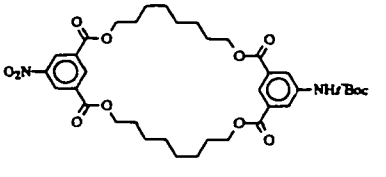 **67**	- linkers are different	- relatively low yield

4.2 Synthetic Efficiency

In order to judge synthetic efficiency a specific target must be considered. For example the synthesis for tetraester macrocycle **67** was extended hypothetically to include the macrocycle **68** shown in Scheme 28. The dashed line represents the synthetic step that has not been done, but is required to bring the macrocycle to a point where it may be fairly compared to the monosubstituted 8_2 shown in Scheme 29. Figure 48 shows the Hendrikson synthetic efficiency graph which corresponds to the synthesis in Scheme 28. This graph was prepared using Hendrikson's estimation of 80% yield at each step, so on the diagram, each centimeter is equivalent to one synthetic step and is therefore equal to 80% yield. At the planning stage of a synthetic strategy it is difficult to predict yield, so an average value of 80% is used. Recall from chapter 2 that the starting materials are each assigned a number, *i*. Scheme 28 has 5 starting materials which are labeled from i=1 to 5 in Figure 48. Each synthon is also assigned a rank, *l*, which indicates the number of steps they are away from the target, which has a rank of l=0. The ranks are given for each starting material and intermediate in Scheme 28. Synthons 1 and 2 correspond to 1,8-octanediol which is monoprotected with dihydropyran. The statistical yield of a monoprotection step is 50%, so in Figure 48 it is equivalent to three steps (3 x 80% steps=51%). Two equivalents of monoprotected 1,8-octanediol react with one equivalent of the 5-nitroisophthaloyl chloride **45** (i=3) so the diol is represented as synthon 1 and 2 in the plan graph. As discussed in chapter 2, the sum of the horizontal lines is equal to the number of synthetic steps, but since the 1,8-octanediol was

protected in the same reaction mixture, then the steps are only counted for one of them. Even though the protection is done in the same "pot", since two equivalents are required they are divided into two lines to simplify the weight calculations. The plan graph in Figure 48 shows that the synthesis of macrocycle **68** is an 11 step synthesis if theoretical yields of 80% are assumed. The plan graphs provide a good opportunity to examine the nature of the synthetic paths. Figure 48 shows that only 3 of the 11 steps belong to the critical path. That is only 3 steps are skeleton forming steps. They are the addition of the monoprotected diol to the diacid chloride to afford the diester **63** at rank l=5, the addition of t-Boc to yield the carbamate **65** at rank l=3, and finally the macrocyclization reaction of the diol **66** with 5-nitroisophthaloyl chloride **45** to macrocycle **67** at rank l=1. Protection of 1,8-octanediol takes another three steps and deprotection of the alcohols from l=3 to l=2 takes one step. A total of four steps are used to refunctionalize. 5-Nitroisophthalic acid is converted to the acid chloride **45** at l=7 to l=6 and l=3 to l=2 and the nitro group is reduced from l=5 to l=4 and l=1 to l=0 In an ideal synthesis there would be no extra steps, rather the skeleton could be built from starting materials that were already functionalized and protections would not be necessary. Table 1 (chapter 2, page 34) provides the calculated yields , y, inverse yields, x, and sum of inverse yields, S, for reactions of 80% yield. These numbers are used to calculate the theoretical (80%) weight values in Table 6. Table 6 summarizes for each starting material, i, the number of heavy atoms (C, N, O, S, Cl), n, a rank at which it joins the synthetic sequence, l, the relative weight of each starting material, nx, the relative contribution to the total weight manipulated, nS_l, and the

moles of reagent required, ΔS. The sum of these parameters provide the information used to evaluate the efficiency. For example n_o is the total number of heavy atoms in the starting materials and may be approximated as the number of heavy atoms in the target. The sum of the relative weights of the starting materials is equal to the total weight of starting materials used, W, and the total weight manipulated throughout the course of the synthesis, TW, is the sum of nS_l. The moles of reagent used is roughly estimated to be in a 1:1 ratio with the moles of starting material. To calculate this a rank l' is introduced so the amount of reagent is only counted once. The rank l' is the last rank at which a starting material is independent of the main line. For example, in Figure 48, the line beginning with starting material i=1 at rank, l=9, and ending at the target at rank, l=0, is the main line and has l'=0. But starting material 2 joins the main line at l=6, so l'=6. This ensures that the amounts of reagents are taken into account from l=9 to l=6. Having no prior knowledge of the yields, a prediction may be made using Hendrikson's 80% yield values. The plan graphs themselves are useful in providing the synthetic chemist with a simple visual layout of the nature of the Scheme. The weight summary values given in the tables are useful for comparing two or more synthetic pathways to a given target molecule or in the case of a property directed synthesis, it is possible to compare two similar structures since the exact chemical make-up of the molecules is not critical provided they have similar structural and functional complexity.

First, we need to examine how close the 80% estimation is compared to the real yields. The values in Table 6 accompany the plan graph in Figure 48. To

compare with the actual yields for macrocycle **68**, Table 7 summarizes the yields, inverse yields, and sum of the inverse yields. These values are all obtained from experiment except the first value which was assumed to be 80% In fact, the yield may be much higher because it is the reduction of the nitro group. In all of the cases these reductions proceed in very high yields, most of them quantitative. Table 8 gives the weight summaries for the actual synthesis whose plan graph is shown in Figure 49 and the actual yields are labeled on the plan graph. Note the monoprotection of starting materials 1 and 2 which was previously displayed as three steps is now shown as one step. This is possible because the yield is known. The theoretical case estimates the weight to be 286 while the actual weight is four times higher at 1184. The total weight manipulated throughout the course of the synthesis is theoretically 1107 while the actual weight manipulated was three times higher at 3411 and the amount of reagents used is estimated to be 57 while the actual yields estimate the amount of reagents needed as 125, two times as much. The discrepancy arises with the yield of the macrocyclization reaction. The low yield of 16% is equivalent to eight steps of 80% yield. If a low yielding step such as a monoprotection or a macrocyclization, which is known to be low yielding, is unavoidable, it is better to have it at the beginning of the synthetic pathway requiring less of other starting materials and reagents than enter the pathway at a later rank. Also, the total weight manipulated during the synthesis would be less.

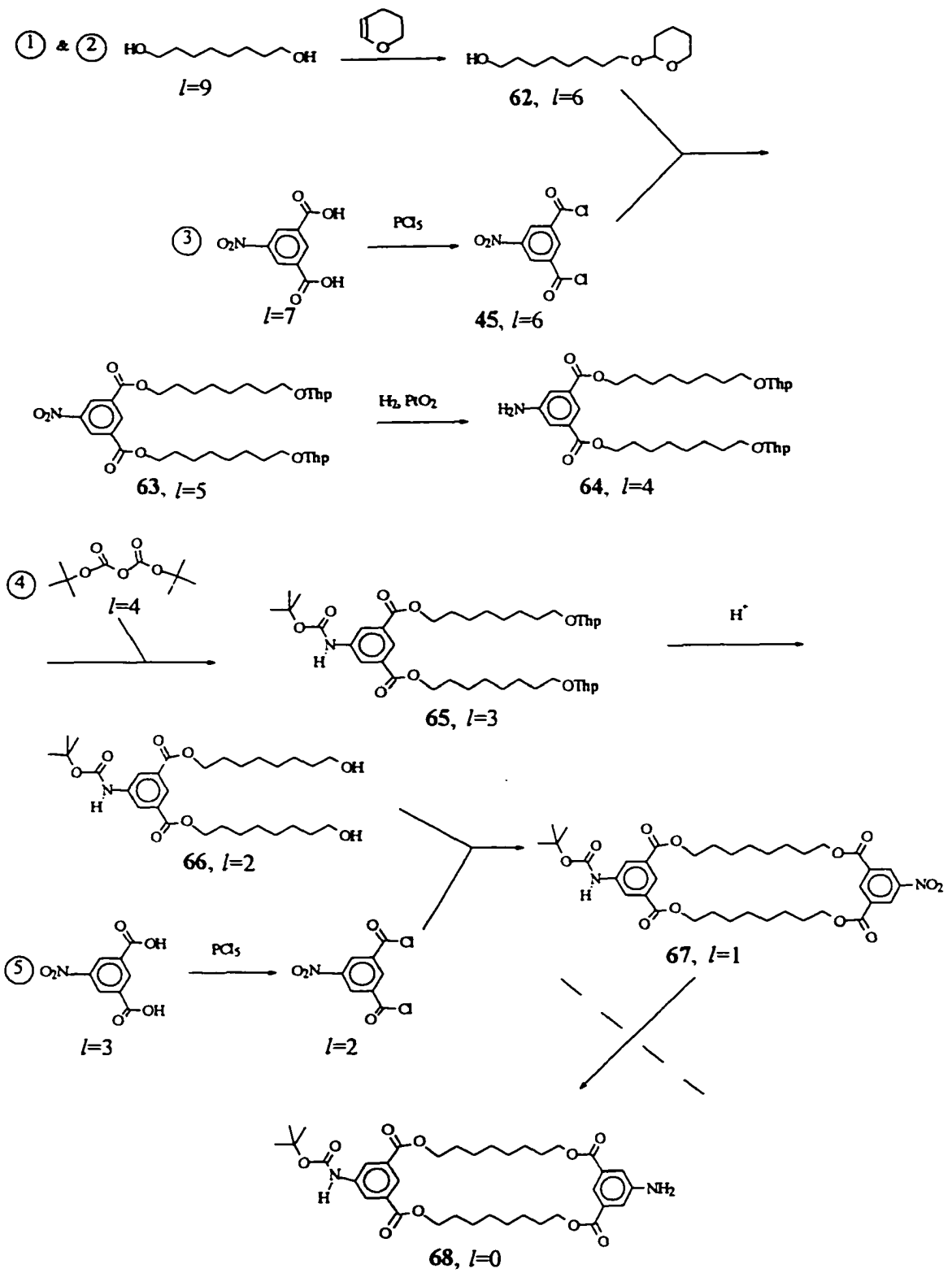

Scheme28: Synthesis of Macrocycle68

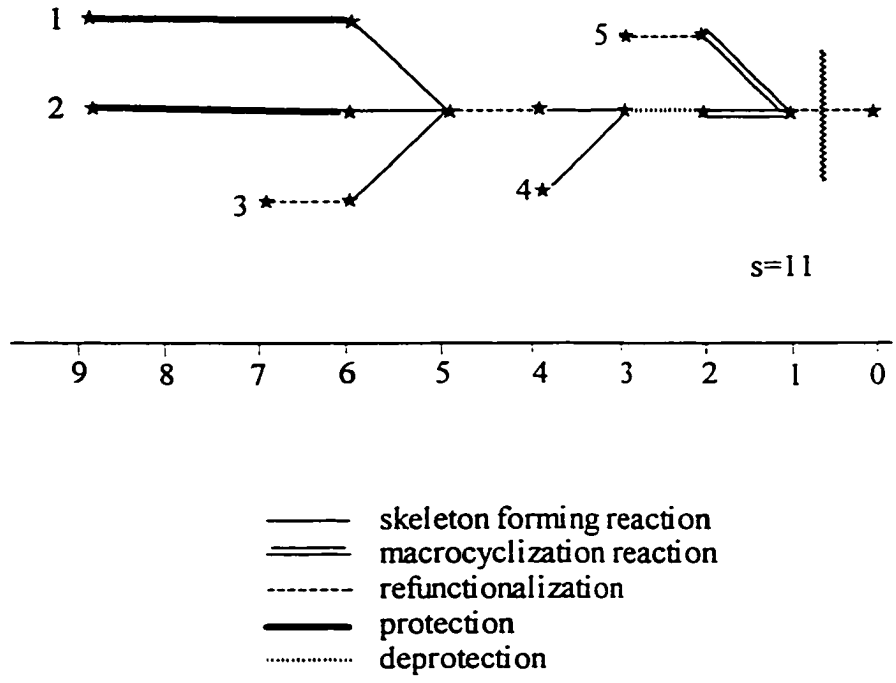

Figure 48: Plan Graph of Macrocycle 68 assuming 80% yield at each step.

Table 6: Weight Summaries for Macrocycle **68** Assuming 80% Yield at Each Step

i	n	l	x	nx	S_l	nS_l	l'	$S_{l'}$	ΔS
1	10	9	7.45	74.50	32.24	322.4	0	0	32.24
2	10	9	7.45	74.50	32.24	322.4	6	14.07	18.17
3	15	7	4.77	71.55	18.83	282.5	6	14.07	4.74
4	15	4	2.44	36.60	7.21	108. 2	4	7.21	0
5	15	3	1.95	29.25	4.76	71.4	2	2.81	1.95
Σ	**65**	32	24.06	**286.4**	95.28	**1107**	18	38.16	**57.1**
	n_o			W		TW			R

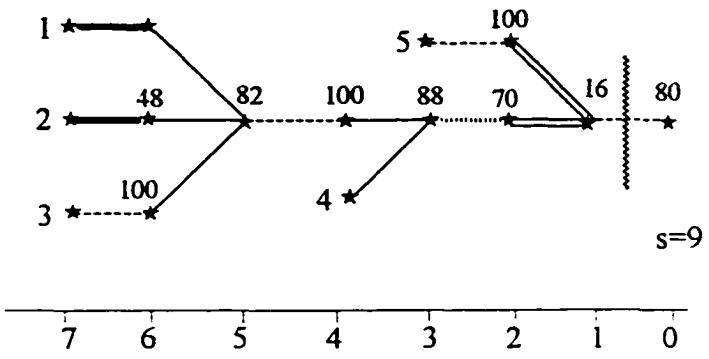

Figure 49: Plan Graph of Macrocycle **68** using real yields.

Table 7: Actual Yield for Macrocycle **68**

l	y	x	S_l
1	0.80	1.25	1.25
2	0.128	7.81	9.06
3	0.0896	11.16	20.22
4	0.0788	12.68	32.09
5	0.0788	12.68	45.58
6	0.0647	15.47	61.05
7	0.0310	32.22	93.27

Table 8: Weight Summaries for Macrocycle **68** using Real Yields.

i	n	l	x	nx	S_l	nS_l	l'	$S_{l'}$	ΔS
1	10	7	32.22	322.2	93.27	932.7	6	61.05	32.22
2	10	7	32.22	232.2	93.27	932.7	6	61.05	32.22
3	15	6(eq)	15.47	232.1	61.05	915.8	0	0	61.05
4	15	4	12.68	190.2	32.09	493.5	4	32.09	0
5	15	2(eq)	7.81	117.2	9.06	135.9	2	9.06	0
Σ	**65**			**1184**		**3411**			**125**
	n_o			W		TW			R

4.2.1 Comparison of the Monoprotected Macrocycle 68 With The Monosubstituted 8_2

The synthesis of 8_2 is shown in Scheme 29[45]. Two equivalents of maleic anhydride are reacted with 1,8-octanediol to produce the diacid **69**. Condensation with a second equivalent of 1,8-octanediol leads to macrocycle 8_2. In the preparation of a transport molecule, 8_2 must be monosubstituted. Scheme 29 shows that macrocycle 8_2 undergoes a Michael addition with 3-thiopropanol to produce the monosubstituted ring **70**. The hydroxyl is then refunctionalized with the better leaving group, mesyl. This compound may now be compared to the monoprotected macrocycle **68**. The plan graph shows a 4 step process where every step is a skeleton building step. The yields are labeled on the plan graph in Figure 50 and the yield data is summarized in Table 9. The weight values calculated from the yields in Table 9 are shown in Table 10. Since the target is a different molecule than **68**, a correction factor of $n_{68}/n_{71}=65/44=1.48$ is used and the corrected weights are given in the last line of Table 10. The weight of starting material used is slightly lower in the synthesis of **68** (1184-vs-1284). This may be explained by the fact that the synthesis of compound **68** has overall higher yields of the individual steps than the synthesis of monosubstituted 8_2. But, more total weight was manipulated (approximately 1.4 times) to obtain the target macrocycle **68**. This is directly related to the number of steps involved in the synthesis and the number of steps for **68** (s=9) is more than twice the number of steps for monosubstituted 8_2 (s=4).

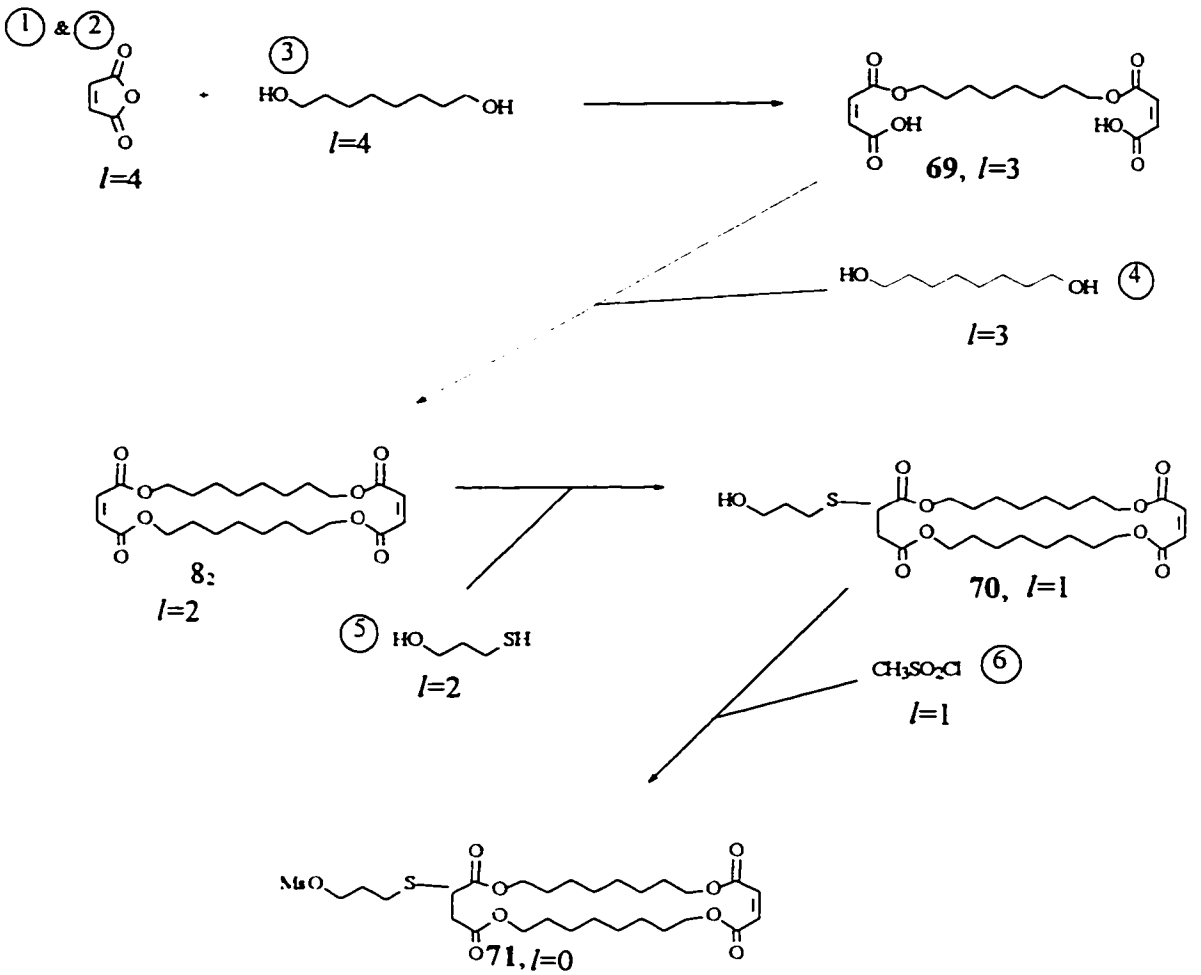

Scheme 29: Synthesis of Monosubstituted 8_2[45]

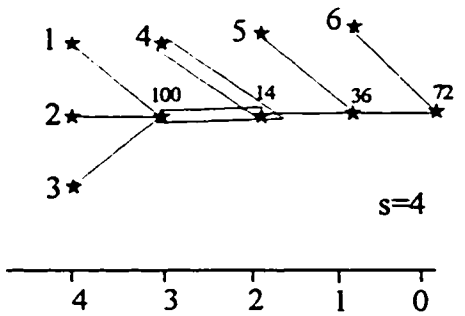

Figure 50: Plan Graph of Monosubstituted 8_2 .

Table 9: Yields, Inverse Yields and Sum of Inverse Yields for Monosubstituted 8_2, **71**

l	y	x	S
1	0.72	1.39	1.39
2	0.228	3.47	4.86
3	0.040	24.80	29.66
4	0.040	24.80	54.46

Table 10: Weight Summaries for Monosubstituted 8_2 , **71** Using Real Yields.

i	n	l	x	nx	S_l	nS_l	l'	$S_{l'}$	ΔS
1	7	4	24.8	173.6	54.46	381.2	0	0	54.46
2	7	4	24.8	173.6	54.46	381.2	4	54.46	0
3	10	4	24.8	248	54.46	54.46	4	54.46	0
4	10	3	24.8	248	29.66	296.6	3	29.66	0
5	5	2	3.47	17.35	4.86	24.3	2	4.86	0
6	5	1	1.39	6.95	1.39	6.95	1	1.39	0
Σ	44			867.5		1635			54.46
	n_o			W		TW			R
x1.48	65			1284		2420			80.6

As previously mentioned in chapter 2, time is dependent on the number of steps in a pathway and the amount of material being manipulated. Hendrikson proposes the equation, $T=s(TW/s)^{0.3}$, to calculate the time required for the synthesis. For compound **68**, the relative time is estimated to be $T=9(3411/9)^{0.3}=53$ compared to monosubstituted 8_2 where the time is estimated to be $T=4(2420/4)^{0.3}=27$. So, a synthesis of monosubstituted 8_2 appears to be a superior wall unit candidate based upon synthetic efficiency.

4.2.2 Comparison of the Pore Former Derived from 68 with the Pore Former Derived from 8_2.

The fate of the macrocycle is to be eventually incorporated into a transport molecule. The pathway is shown for the transformation of macrocycle **68** into a potential transporter. Two equivalents of compound **68** would react with the diacid chloride to afford the bis macrocyclic compound **72**. Removal of the *t*-Boc groups should result in the preparation of a potential transporter, the diamine compound **73**.

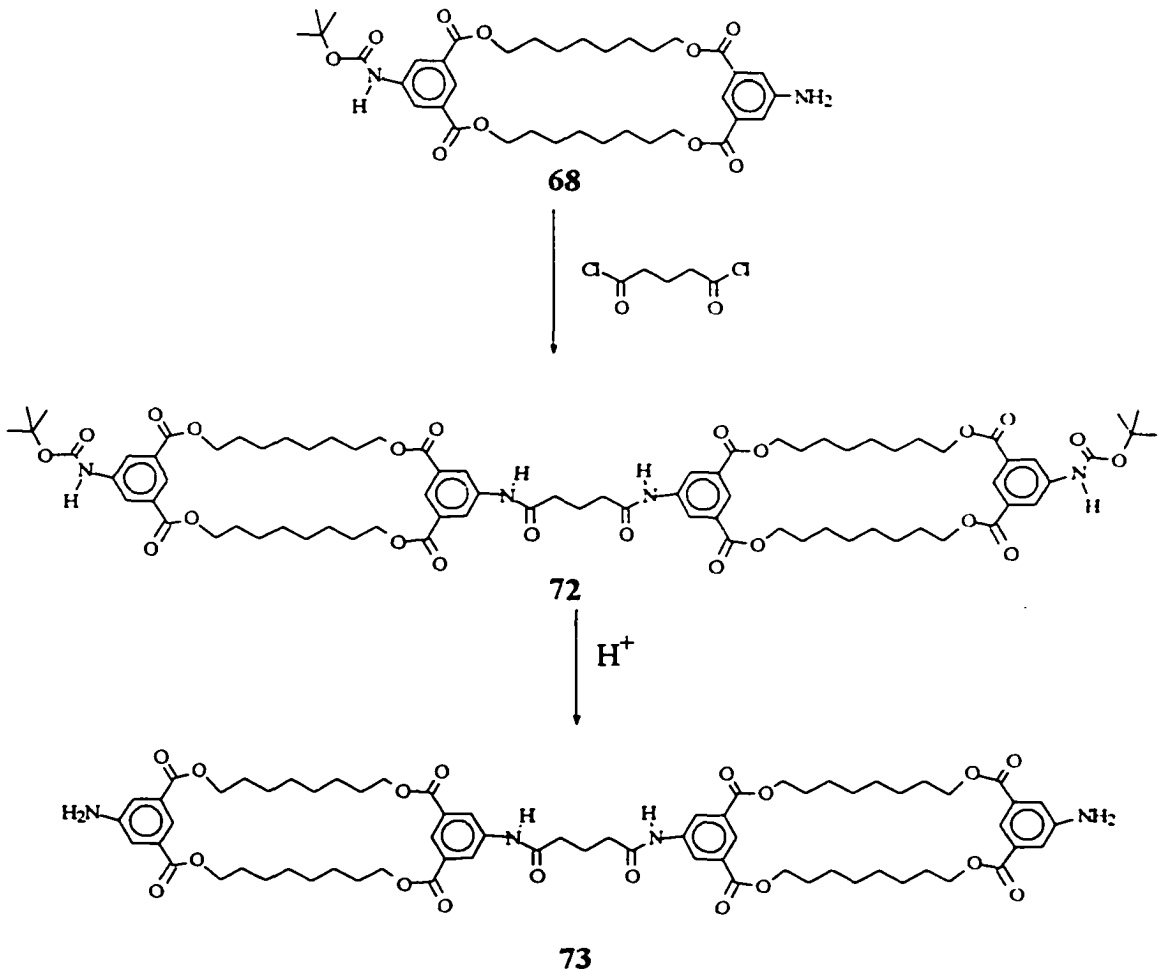

Scheme 30: Synthesis of PoreFormer 73

The plan graph for macrocycle **68** was extended to include formation of the potential transporter and is shown in Figure 51. Both branches of the plan graph would be done in the same reaction vessel so the steps were only counted once. The synthesis should be complete in 11 steps. The yields are summarized in Table 11 and the weight summaries are in Table 12.

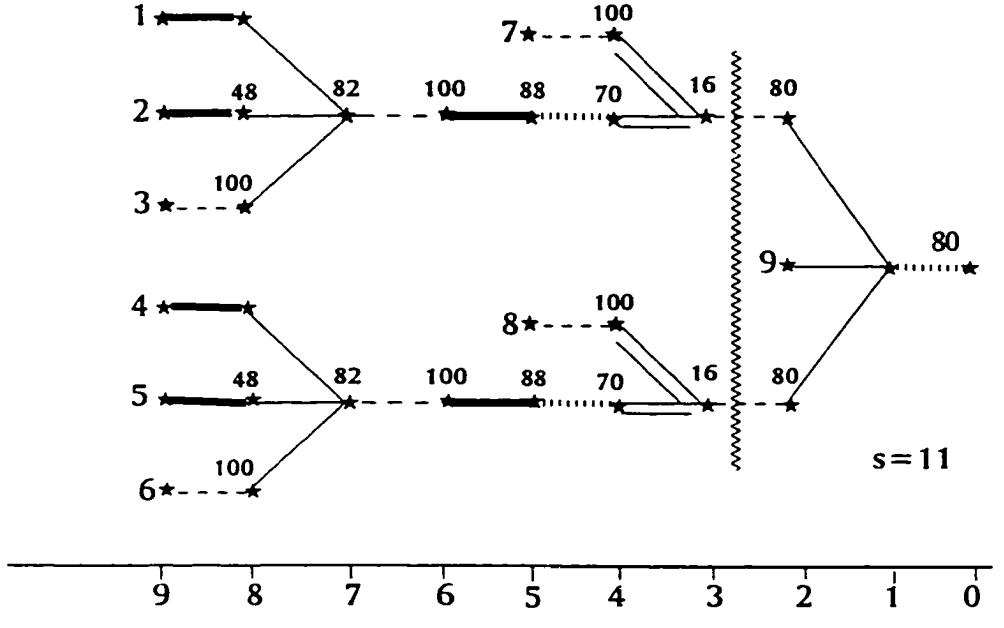

Figure 51: Plan Graph of Pore Former 73 using real yields.

Table 11: Yields for Pore Former 73

l	y	x	S
1	0.80	1.25	1.25
2	0.64	1.56	2.81
3	0.51	1.95	4.76
4	0.082	12.2	16.96
5	0.057	17.4	34.4
6	0.050	19.8	54.2
7	0.050	19.9	74.0
8	0.041	24.2	98.2
9	0.020	50.3	148.5

Table 12: Weight Summaries for Pore Former **73**

i	n	l	x	nx	S	nS	l'	$S_{l'}$	ΔS
1	10	9	50.3	503	148.5	1485	0	0	148.5
2	10	9	50.3	503	148.5	1485	8	98.2	50.3
3	15	9	24.2	363	122.4	1836	8	98.2	24.2
4	10	9	50.3	503	148.5	1485	2	2.81	145.7
5	10	9	50.3	503	148.5	1485	8	98.2	50.3
6	15	9	24.2	363	122.4	1836	8	98.2	24.2
7	15	5	12.2	183	29.2	437	4	17	12.2
8	15	5	12.2	183	29.2	437	4	17	12.2
9	9	2	1.56	14	2.81	25	2	2.81	0
	n_o			W		TW			R
	109			**3118**		**10511**			**468**

The synthesis for the pore former derived from 8_2 was also extended. The pathway is completed in Scheme 31 and depicted in the plan graph in Figure 52. Macrocycle 8_2 undergoes a Michael addition with 2 equivalents of thioacetic acid to give the disubstituted 8_2. Reaction with the monosubstituted 8_2.affords the bis macrocycle **74**, which undergoes a second Michael addition to place a head group at the other end of the molecule to yield the target, **75**. Table 13 is a summary of the yield data for **75** and the weight data is contained in Table 14.

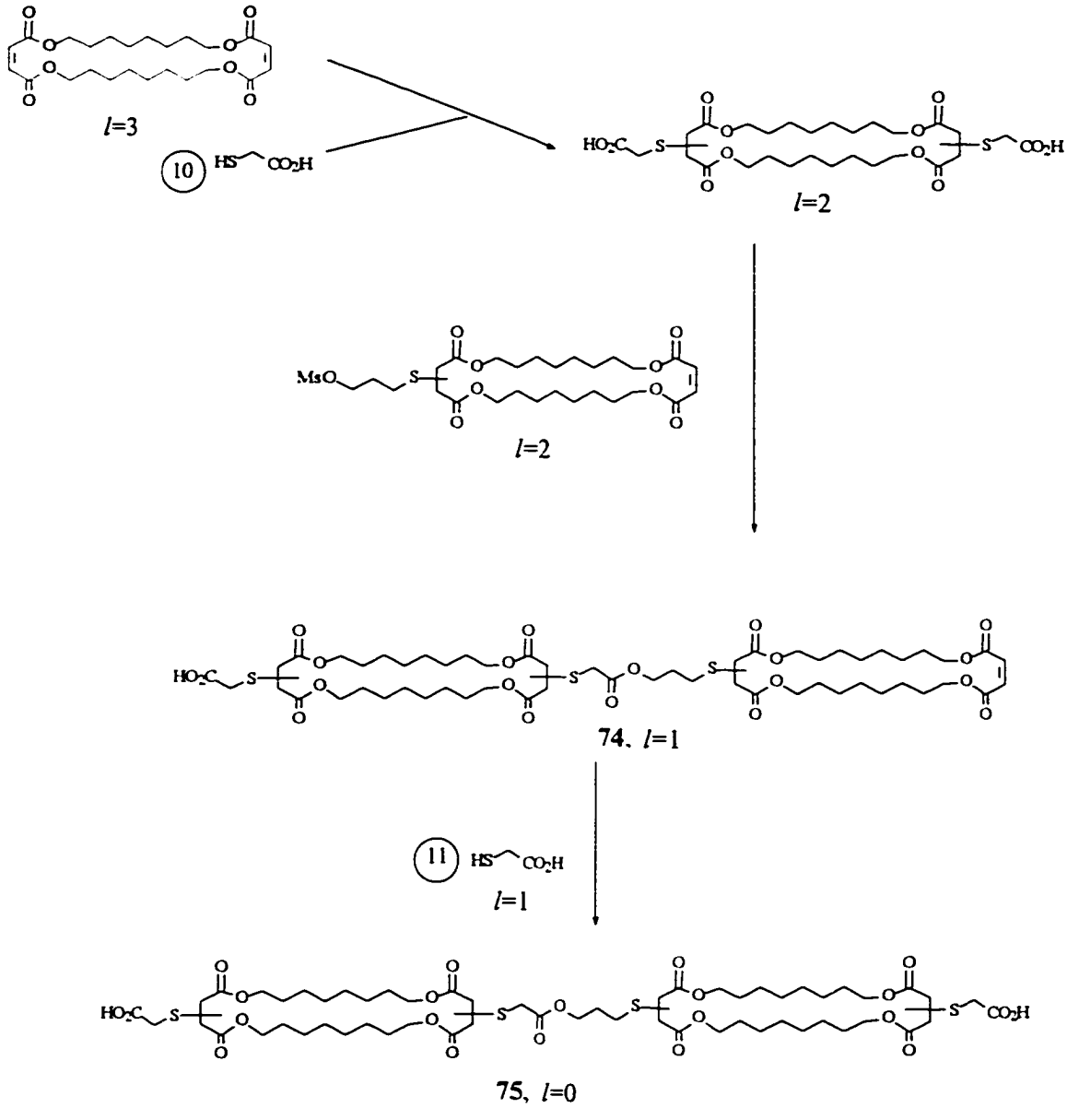

Scheme 31: Synthesis of Pore Former 75

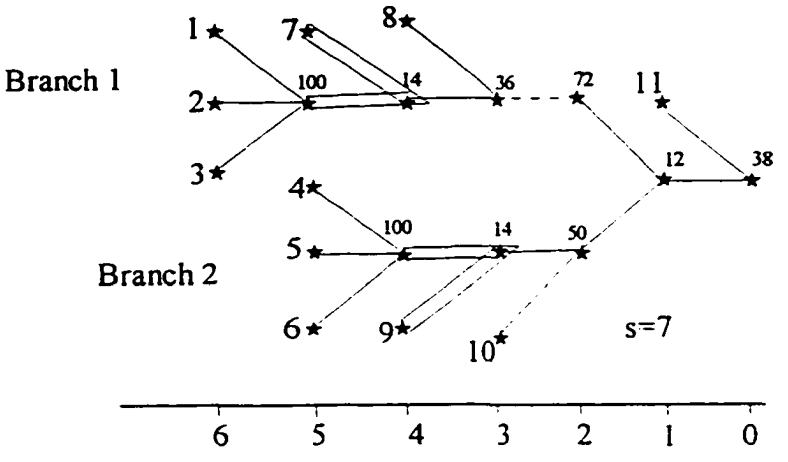

Figure 52: Plan Graph of Pore Former 75.

Table 13: Yield Values for Pore Former 75.

Branch 1 of Plan Graph in Figure 52

l	y	x	S
1	0.38	2.63	2.63
2	0.046	21.9	24.5
3	0.033	30.5	55
4	0.012	84.6	140
5	0.0017	604	744
6	0.0017	604	1348

Branch 2 of Plan Graph in Figure 52

l	y	x	S
1	0.38	2.63	2.63
2	0.046	21.9	24.5
3	0.023	43.9	68
4	0.0032	313	381
5	0.0032	313	694

Table 14: Weight Summaries for Pore Former 75.

i	n	l	x	nx	S	nS	l'	$S_{l'}$	ΔS
1	7	6	604	4228	1348	9436	0	0	1348
2	7	6	604	4228	1348	9436	6	1348	0
3	10	6	604	6040	1348	13480	6	1348	0
4	7	5	313	2191	694	4858	2	24.5	670
5	7	5	313	2191	694	4858	5	694	0
6	10	5	313	3130	694	6940	5	694	0
7	10	5	604	6040	744	7440	5	744	0
8	5	4	85	425	140	700	4	140	0
9	10	4	313	3130	381	3810	4	381	0
10	5	3	44	220	68	340	3	68	0
11	5	1	2.6	13	2.6	13	1	2.6	0
	n_o			W		TW			R
	83			31836		61311			2018
x 1.3	**108**			**41387**		**79704**			**2623**

The results are in favor of the synthesis for the pore former derived from **67** over that derived from 8_2. The pore former **73** requires 13 times less starting material that is required for **75**. The total weight manipulated is 7.5 times less for **73** and the estimated amount of reagents required is about 5.5 times less for the synthesis of **73**. Examination of the plan graphs show that transporter **73** has one low yielding step at the beginning of the synthesis with the monoprotection step and then again near the end at *l*=3 for the cyclization. The remaining yields are fairly high. The plan graph for **75** reveals that most of the yields are low with the exception of the first synthetic step where the yield is quantitative. The relative times required for the syntheses are 86 and 115 for **73** and **75** respectively. At the stage of a macrocyclic wall unit the efficiencies are similar but beyond that, to the complexity of a pore former, **73** provides a much more efficient route

Regarding the nature of the synthetic path, the sequence for **75** is convergent but is not symmetrical. For that reason a Table of yield values had to be calculated for each branch. That the head groups both originate from thiolacetic acid is merely a consequence of the design. A different pore former could be prepared from **71** with the second head group addition derived from something other than thiolacetic acid. The synthesis of the pore former from the macrocycle **68** also has the potential for an unsymmetric linker and/or different head groups but would require the addition of two or more steps.

4.2.3 Conclusions on Synthetic Efficiency

The above discussion brings to mind several points to consider when devising a synthetic plan. They are:

1. Probably the most obvious is to devise a plan that has the fewest number of extra steps. Every protection, deprotection, and refunctionalization reduces the yield and leads to an increase in the amount of starting materials required per unit of target.

2. Use small molecular weight starting materials. The idea here being that the fewer heavy atoms in the starting material there are, the more that must be incorporated into the final product. This minimizes the weight of starting materials required for the synthesis and hence cuts down on the total weight manipulated which generally translates to lower cost.

3. If low yielding steps are predictable and unavoidable it is better to have them at the highest rank possible. This will cut down on carrying a lot of weight through many

steps. It also cuts down on the amount of starting materials required at subsequent steps. This saves time as well as money.

4.3 Future Work

The macrocycle **67** is now ready to be incorporated into the modular set, which consists of polar head groups, spacers, and macrocylic wall units. It can be readily incorporated into target pore formers using the existing components or new ones.

Clearly, the next step is the incorporation of macrocycle **67** into the pore former molecule **73**. As in the pathway described in the previous discussions of synthetic efficiency, this entails reducing the remaining nitro group and reacting with the appropriate diacid chloride. The aromatic nitro group on compound **67** could be reduced using hydrogen and Adams' catalyst to yield **68**. Then, reaction of two equivalents of **68** with glutaryl dichloride should lead to the bismacrocyclic compound **72**. Subsequent removal of the *t*-Boc protecting group under acidic conditions will lead to the potential pore former molecule **73**.

Broader future studies could include additional functionalization via the head groups contained in the modular set. The end groups used previously could be accommodated using the appropriate chemistry. For instance, the amine **73** could add in a ring opening addition to maleic anhydride, yielding carboxylate head groups.

Variations in the spacer groups can also be readily achieved. In addition to the spacer groups within the modular set, the linkers could include the amides of tartaric acid, maleic acid, and varying lengths of hydrocarbon chains.

4.4 Conclusions

The described synthesis of a new wall unit proved to be an efficient method for obtaining macrocyclic wall units. The use of 1,3,5-trisubstituted benzene did avoid the problems of multiple stereo- and regio-isomers found in the previous pathway. Additionally, this synthetic path allows for the ready differentiation of the two linkers. While the macrocycles discussed are not identical to those previously studied, they do preserve the desirable physical features of the previous targets. The increased efficiency and greater control of the construction of the wall unit makes the synthesis of a variety of asymmetric pore formers possible. As hypothesized, this will eventually lead to a new modular set for synthesis of new candidates for evaluation by structure-activity studies.

Comparisons of the synthetic efficiency of the new macrocyclic target with the current wall unit demonstrates that construction of pore formers is greatly enhanced using the newer molecules. While the synthetic efficiency analysis of the two macrocycles gives comparable results, it is in the building of the pore formers that the two approaches deviate. With 8_2, the yields of all steps from the macrocyclization on to the final pore former fall below 50%, with many below that. In comparison, the final steps in the preparation of macrocycle **68** should be high, decreasing the amount of starting materials and reagents required and decreasing the total weight manipulated, which relates to a decrease in time.

Another important point is that the new synthetic path produces only one isomer. Structure activity relationships would clearly be facilitated with a

single stereo- and regioisomer of the pore former. Imposing this constraint upon the previous synthetic pathway is not synthetically viable. This route provides a more effective approach to the systematic studies of structure-activity relationships.

CHAPTER 5 EXPERIMENTAL

5.1 Apparatus

Nuclear magnetic resonance spectra were recorded using a Bruker WM250 (250 MHz ^{1}H and 62.89 MHz ^{13}C), Bruker AMX360 (360 MHz ^{1}H and 90.57 MHz ^{13}C) or a Bruker AC300 (300 MHz ^{1}H and 75.47 MHz ^{13}C). Chemical shifts are reported as ppm (δ) and are relative to tetramethylsilane (TMS). In reporting the nature of the signals, s, singlet, d, doublet, t, triplet, q, quartet, qu, quintet, m, multiplet and br, broad are used. Electron impact (EI) and chemical ionization (CI) mass spectra were recorded on either a Finnegan 3300 GC-MS or a Kratos Concept mass spectrometer. Liquid secondary ion mass spectra (LSIMS) were recorded on the Kratos Concept double focusing magnetic instrument using either glycerol or meta-nitrobenzyl alcohol (mNBA) as the matrix. Infrared spectra were recorded using either a Bruker IFS25 FTIR or a Perkin-Elmer 1330 FTIR spectrometer. Samples were studied as KBr discs or nujol mulls. Melting points were determined using a Gallenkamp melting point apparatus. Thin layer chromatography was performed using KODAK Chromagram Silica Sheets with fluorescent indicator. Centrifugal chromatography was carried out using a Harrison Research Chromatotron, model 7924T. The plates were prepared with silica gel (Merck, TLC grade 7749) purchased from Aldrich containing gypsum binder and fluorescent indicator. Partition chromatography was performed using a High Speed Countercurrent Chromatograph purchased from P.C. Inc. fitted with a #10 preparative column having a

volume of 365 mL and an Eldex pump model B-100-S. The flow was passed through a UV detector (254 nm) and collected.

5.2 Procedures

(4-Chlorobutoxy)-3,4,5,6-tetrahydropyran[61] 35

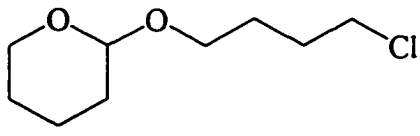

4-Chlorobutanol (24.3g, $2.25x10^{-1}$ mol) was stirred with dihydropyran (26.7 g, $3.18x10^{-1}$ mol) and HCl (1 drop) at 0-5°C for 20 min. The mixture was allowed to stir at room temperature for an additional 40 min. Sodium bicarbonate (5 g) was added to neutralize the solution and the mixture was stirred for 30 min. Undissolved $NaHCO_3$ was filtered and the resulting mixture distilled under vacuum. The product was distilled at 1.5 mm Hg at 85° and was recovered as a clear oil (17.95 g, $9.35x10^{-2}$ mol, 42%).

TLC (Kodak Chromagram, silica): R_f=0.68, 1:1, Et_2O:hexane.

^1H nmr (90 MHz), $CDCl_3$,δ: 1.48-1.95 (m, 10H, C-2,3,3',4' and 5' H), 3.34-3.87 (m, 6H, C-1, 4, and 6' H), 4.56 (br s, 1H, C-2' H)

^{13}C nmr (62.89 MHz), $CDCl_3$, δ: 19.0 (C-4'), 25.0 (C-5'), 26.6 (C-2), 29.2 (C-3), 30.1 (C-3'), 44.2 (C-4), 61.4 (C-1), 65.8 (C-6'), 98.0 (C-2').

ms (CI): 193 and 195 (M+1), 169, 157, 91and 93, 85 (100)

1,3-Benzene dimethanol [57] 37

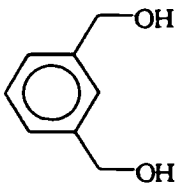

Lithium aluminum hydride (9 g), in a 1L 2-necked rbf fitted with a reflux condensor, was stirred in dry THF (400 mL) in an ice bath. Isophthalic acid **36** (7.22 g, 4.34×10^{-2} mol) was stirred in dry THF (100 mL) and added slowly to the $LiAlH_4$ solution. Not all of the isophthalic acid was dissolved before it was added. The reaction was refluxed for 48 h. under N_2.

Work-up required the dropwise addition of H_2O (2 mL) to the cooled reaction mixture (on ice). An HCl solution (4 M, 50 mL) was added dropwise through the top of the condenser until the $LiAlH_4$ was destroyed. Diethyl ether (400 mL) was added and the mixture was suction filtered. The filtrate was dried over $MgSO_4$ and then evaporated to yield a colorless oil. The oil was distilled using a Kugelrohr pressure/temp to produce a pure oil that formed white needles upon sitting (4.15 g, 3.01×10^{-2} mol, 69%, m.p. 47-48°C, Aldrich[57] m.p. 56-60). Needles may also be formed by seeding the distilled product followed by recrystallization from benzene.

^{1}H nmr (250 MHz), MeOH, δ: 4.59 (s, 4H, 2 x -CH_2-), 7.23-7.34 (m, 4H, aromatic H's)

^{13}C nmr (62.89 MHz), MeOH, δ: 65.1 (-$\underline{C}H_2$-), 126. 6 (C-2), 126.9 (C-4 and C-6), 129.4 (C-5), 142.7 (C-1 and C-3)

ms (CI): 138 (M^+), 121 (100), 119, 91

Preparation of 38

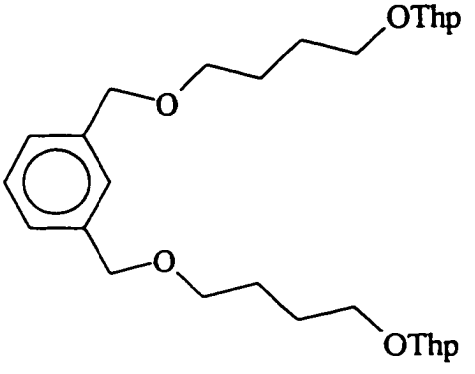

The diol **37** (4.12 g, $3.00x10^{-2}$ mol) was dissolved in dry DMA (50 mL) and NaH (1.03 g, 60% in oil, washed with petroleum ether and dried) was added. The chloro compound **35** (4 equivalents) was dissolved in DMA (50 mL) and added to the diol. The reaction was heated overnight at 60°C under N_2. The DMA was evaporated and the residue was extracted with diethyl ether and H_2O. The product was a mixture of **38** and **39**.

^{1}H nmr (90 MHz), $CDCl_3$, crude sample, δ: 1.30-1.80 (m, 20H, -$CH_2\underline{CH_2}CH_2$-'s), 3.20-3.50 (m, 12H, -O-$\underline{CH_2}CH_2$-), 3.55-3.90 (m, 4H, -O-$\underline{CH_2}$-Ar)), 4.40 (m, 1H, -O-$\underline{CH}$-O-), 7.20-7.35 (br, 4H, Ar H's)

1,3-bis (2-oxa-6-hydroxyhexyl) benzene 23

Method 1

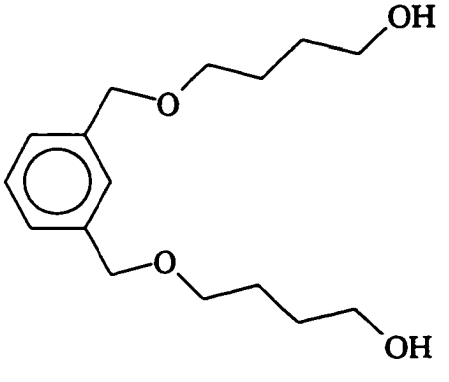

The impure compound **38** was dissolved in methanol (10 mL per g of **36**) and a few drops of conc. H_2SO_4 were added. The mixture was stirred at r.t. for 24 h. The residue was extracted with CH_2Cl_2 and washed with H_2O, NaCl (sat.) and H_2O in that order. The

product **23** was partially purified by countercurrent chromatography. The retention time of **23** was 90 min. using 25% isopropyl alcohol in H_2O as the mobile phase and 12% $CHCl_3$ in heptane as the stationary phase. The chromatograph was run at 800 RPM with a flow rate of 240 mLh^{-1}.

ms (CI): 283 (M+1), 219, 210, 193 (100), 190, 189, 176, 138, 122, 120

Method 2

α,α'-Dibromo-*m*-xylene (5.07 g, $1.92x10^{-2}$ mol) was dissolved with heating in 1,4-butanediol (150 mL). The round bottom flask was fitted with a reflux condenser and was heated overnight at 70°C. The excess 1,4-butanediol was evaporated on the vacuum pump while heating with a heating mantle. A silica gel column was used to pre-purify the product with diethyl ether as the eluent. Final purification was performed by centrifugal chromatography using silica gel as the stationary phase and diethyl ether as the eluent. The product **23** was obtained as a clear oil (3.29 g, $1.17x10^{-2}$ mol, 61% yield).

^1H nmr (250 MHz), $CDCl_3$, δ: 1.61 (m, 8H, $-CH_2-CH_2-CH_2-$), 3.22 (s, 2H, -OH), 3.45 (t, 4H, $O-CH_2$), 3.53 (t, 4H, $O-CH_2$), 4.46 (s, 4H, $Ar-CH_2-$), 7.22 (m, 4H, aromatic H's).

^{13}C nmr (90.57 MHz), $CDCl_3$, δ:26.3 (C-4'), 29.7 (C-5'), 62.2 (C-6'), 70.2 (C-3'), 72.7 (C-1'), 126.9 (C-2, C-4 and C-6), 128.4 (C-5), 138.3 (C-1 and C-3).

Method 2 is the more efficient of the two procedures.

General Procedure for the Preparation of Isophthalamides

A solution of the amine (large excess) was placed in a 500 mL beaker and stirred in an ice bath. The isophthaloyl dichloride was slowly added. After addition was complete, the mixture was allowed to stir for 2h. at r.t. The white solid, which was product, was filtered off, rinsed with cold H_2O and dried under vacuum.

Isophthalamide 31

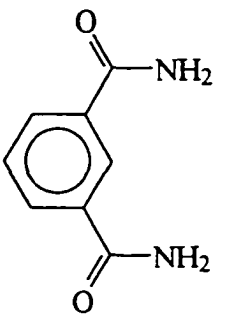

Refer to the general procedure for the preparation of isophthalamides p. 136. Isophthaloyl dichloride (30.69 g, 0.151 mol) was slowly added to ammonium hydroxide (100 mL). Isophthalamide was isolated as a white solid (24.50 g, 1.49×10^{-1} mol, 99%) mp 264°C.

^{1}H nmr (300 MHz), DMSO-d_6, δ: 7.47 (s, 2H, N-H), 7.52 (t, C-5 H, J=7.8 Hz), 7.99 (dd, 2H, C-4 and C-6 H's, $J_{2,4}$=7.8 Hz, $J_{4,5}$=1.5 Hz), 8.07 (s, 2H, N-H's), 8.39 (t, 1H, C-2 H, J=1.5 Hz).

^{13}C nmr (75.47 MHz), DMSO-d_6, δ: 126.8 (C-2), 128.3 (C-5), 130.1 (C-4 and C-6), 134.4 (C-1 and C-3), 167.6 (C=O).

General Procedure for the Reduction of Isophthalamides

The isophthalamide was added in small portions to lithium aluminum hydride in dry THF on ice. Once all the amide was added, the reaction was refluxed overnight. The reaction

was cooled and placed on ice. Excess $LiAlH_4$ was destroyed by the dropwise addition of H_2O and then NaOH. Diethyl ether (approximately 10 mL Et_2O/mmol amide) was added and the solution was filtered. The filtrate was collected and dried over $MgSO_4$ and the ether was allowed to evaporate.

Usually the residue was not purified further but used in the next step. The diamine could be stored as the oxalate salt by dissolving oxalic acid in acetone and dissolving the diamine in acetone. When mixed together, the salt precipitated and was collected

m-Xylylenediamine [59] 32

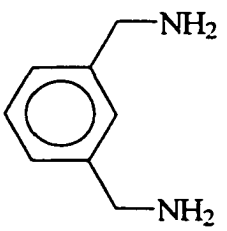

Isophthalamide **31** (7.76 g, 0.05 mol) was added in small portions to lithium aluminum hydride (7 g) in THF (400 mL) on ice. The reaction mixture goes from brown to yellow. Diethyl ether (300 mL) was added and the solution was filtered. The product (free amine) was isolated as a yellow oil. (3.92g, 0.03 mol, 60%)

^1H nmr (250 MHz), $CDCl_3$, δ: 1.62 (s, 4H, -$N\underline{H}_2$), 3.80 (s, 4H, -$C\underline{H}_2$-), 7.14-7.22 (m, 4H, aromatic H's)

^{13}C nmr (62.89 MHz), $CDCl_3$, δ: 46.2 (-$\underline{C}H_2$-), 125.3 (C-2), 125. 6 (C-5), 128.4 (C-4 and C-6), 143.3 (C-1 and C-3).

General Procedure for the Preparation of Bischloroamides[53,54]

The *m*-xylylenediamine was dissolved in $CHCl_3$. H_2O was added and the mixture was cooled to 0°C. Two solutions were added dropwise simultaneously. The first solution was

chloroacetyl chloride dissolved in $CHCl_3$. The second solution was K_2CO_3 dissolved in H_2O. The mixture was stirred at 0-5°C for 1 h., then at r.t. for another 2 h. The organic layer was separated and washed twice with H_2O, dried over $MgSO_4$ and allowed to evaporate.

N,N'-Di-chloroacetyl-*m*-xylylenediamine[59] 24a

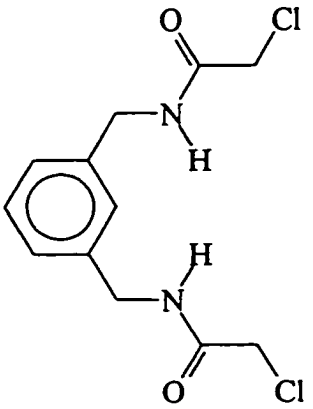

Refer to the general procedure for the preparation of bischloroamides p.137. The amounts of reagents are given below. *m*-Xylylenediamine (3.61 g, $2.65x10^{-2}$ mol) was stirred in $CHCl_3$ (50 mL) and H_2O (25 mL). Chloroacetyl chloride (7.63 g, $6.75x10^{-2}$ mmol) dissolved in $CHCl_3$ (50 mL) and K_2CO_3 (6.3 g) dissolved in H_2O (250 mL) were added. The solid was purified by trituration with EtOAc. (2.55 g, $8.85x10^{-3}$ mol, 18% yield from **31**, m.p.148°C, lit. m.p. 149-150°C).

^1H nmr (300 MHz), $CDCl_3$, δ:1.60 (s, 2H, 2x-NH), 4.09 (s, 4H, 2x-CH_2Cl), 4.47 (d, 4H, 2x-CH_2Ar, J=5.9 Hz), 6.89-7.35 (m, 4H, aromatic H's).

^{13}C nmr (62.89 MHz), $CDCl_3$, δ: 42.6 (-$\underline{C}H_2$-Ar), 43.6 (-$\underline{C}H_2$-Cl), 127.1 (C-5), 127.2 (C-4 and C-6), 129.4 (C-1 and C-3), 138.1 (C-2), 165.9 (C=O).

Exact mass calculated for $C_{12}H_{14}N_2O_2Cl_2$ m/e 288.0432, found m/e 288.0433 (intensity 35%).

N,N′-Dimethyl isophthalamide 41

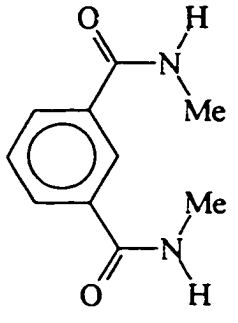

Refer to the general procedure for the preparation of isophthalamides p. 136. Isophthaloyl chloride (28.98 g, 1.43×10^{-1} mol) was added to methyl amine (100 mL, 40% in H_2O). N,N′-Dimethyl isophthalamide **41** was isolated (16.62 g, 8.70×10^{-2} mol, 61% , m.p. 196°C).

^{1}H nmr (360 MHz), $CDCl_3$, δ: 3.00 (d, 6H, Me H's), 6.36 (br, 2H, N-H), 7.48 (t, 1H, C-5 H, J=7.8 Hz), 7.87 (dd, 2H, C-4 and C-6 H's, $J_{2,4}$=1.6 Hz, $J_{4,5}$=7.8 Hz), 8.14 (t, 1H, C-2 H, J=1.6 Hz).

^{13}C nmr (90.57 MHz), $CDCl_3$, δ: 26.8 ($-CH_3$), 125.1 (C-2), 128.9 (C-5), 129.6 (C-4 and C-6), 134.8 (C-1 and C-3), 167.2 (C=O).

N,N′-Dimethyl-*m*-xylylenediamine 42

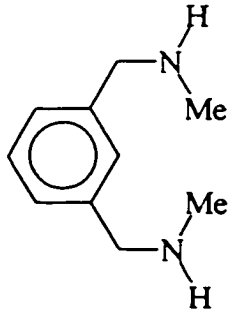

Refer to the general procedure for the reduction of isophthalamides p.136. N,N′-Dimethyl isophthalamide **41** (10 g, 0.052 mol) was added to a solution of $LiAlH_4$ (7 g) in THF (500 mL). The solution turned dark purple and then yellow. The crude product was isolated as a yellow oil (6.60 g, 0.040 mol, 77%). The ^{13}C nmr was consistent with the expected ^{13}C nmr so the crude product was used immediately in the next step without further purification.

^{13}C nmr (62.89 MHz), $CDCl_3$, δ: 35.7 ($-CH_3$), 55.7 ($Ar-CH_2-$), 126.5 (C-4 and C-6), 127.6 (C-2), 128.1 (C-5), 140.0 (C-1 and C-3).

N,N′-Dimethyl-N,N′-bis-chloroacetyl-*m*-xylylenediamine 24b

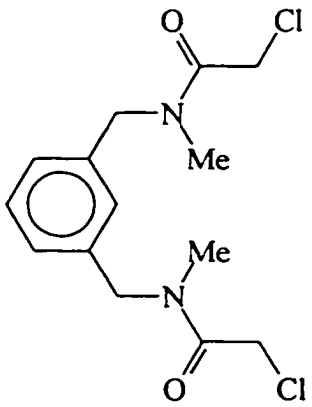

Refer to the general procedure for the preparation of bischloroamides p.137. The amounts of reagents are given below. N,N′-Dimethyl *m*-xylylenediamine **45** (6.60 g, $4.02x10^{-2}$ mol) was dissolved in $CHCl_3$ (100 mL). H_2O (50 mL) was added. Chloroacetyl chloride (11.3 g, 0.10 mol) dissolved in $CHCl_3$ (150 mL) and K_2CO_3 (10 g) dissolved in H_2O (250 mL) were added. The oil was purified by centrifugal chromatography using silica gel as the stationary phase and THF as the eluent. The product was obtained as a clear oil (9.56 g, $3.03x10^{-2}$ mol, 75%). The TLC revealed only one spot in four different solvent systems. Et_2O, (10:1) Et_2O:MeOH, THF and (1:1) Et_2O:THF R_f=0.60.

^1H nmr (360 MHz), $CDCl_3$, δ: 2.96, 2.93 and 2.88 (3 x s, 6H, Me H's), 4.08 and 4.04 (2 x s, 4H, CH_2Cl), 4.54-4.51 (m, 4H, $Ar-CH_2$), 7.30-7.00 (m, 4H, aromatic H's).

^{13}C nmr (90.57 MHz), $CDCl_3$, δ: 34.2, 35.1, 35.2 ($-CH_3$), 41.0, 41.2, 41.3 ($-CH_2Cl$), 51.0, 53.4 ($Ar-CH_2-$), 125.5, 125.8, 125.9 (C-4 and C-6), 127.0, 127.2, 127.3 (C-5), 129.1, 129.4 (C-2), 136.3, 136.9, 137.4 (C-1 and C-3), 166.6, 166.8 (C=O).

^{13}C nmr DEPT experiment (62.89 MHz), $CDCl_3$, δ: 166.6 and 166.8 (C=O), 136.3 ,136.9 and 137.4 (quaternary C on aromatic moiety) disappear, 41.0 41.2, 41.3, 51.0 and 53.4 are negative. All other peaks are positive (CH and CH_3).

Coupling of **24b** and **23** to yield the macrocycle **25a**.

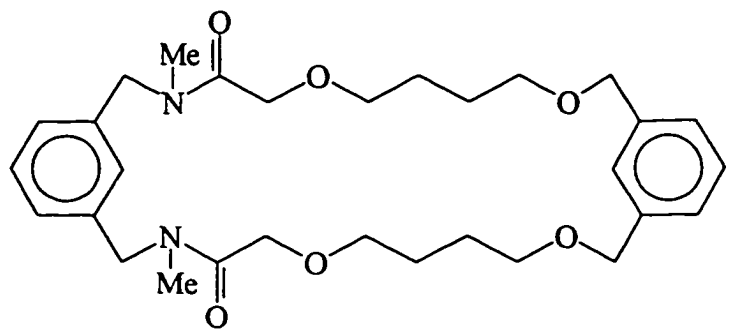

An excess of NaH (2 g, ~80% powder) was stirred in freshly distilled THF (200 mL) at r.t. The diol **23** (2.34 g, $8.3x10^{-3}$ mol) was added to the THF solution along with DMSO (2 mL, dried over CaH_2) and the mixture was refluxed for 1 h. The bischloroamide **24b** (2.63 g, 8.3 $x10^{-3}$ mol) was dissolved in THF (50 mL) and added to the refluxing mixture. The reaction was allowed to reflux overnight. The color changed from the NaH grey color to yellow. Work-up involved quenching the reaction with MeOH first and then H_2O. It was diluted with Et_2O (500 mL) and extracted three times with H_2O until the yellow color disappeared. The organic layer was dried over $MgSO_4$ and evaporated to yield a slightly yellow oil. The TLC of the crude product revealed four spots but centrifugal chromatography isolated five bands. The first band was recovered diol **23** (0.43 g, 18%). The second band was the macrocycle **25a** (0.22 g, 4.2×10^{-4} mol, 7%) and the other bands were presumed to be polymers varying in chain length. The centrifugal chromatography was performed using Et_2O as the eluent to

collect the first band then switching to THF to collect bands two and three. MeOH was used to remove bands four and five. TLC, (1:1) Et_2O:THF, R_f=0.68.

The ^{13}C nmr also revealed that there were three distinct conformers of the macrocycle present.

^1H nmr (360 MHz), DMSO-d_6, δ: 1.57-1.49 (m, 8H, -CH_2-CH_2-CH_2), 2.84-2.74 (m, 6H, Me H's), 3.42-3.30 (m, 8H, -O-CH_2), 4.13-4.07 (m, 4H, -O-CH_2-C=O), 4.50-4.42 (m, 8H, Ar-CH_2), 7.36-6.86 (m, 8H, aromatic H's).

^{13}C nmr (90.57 MHz), $CDCl_3$, δ: 26.2, 26.4, 30.2, 33.6, 34.1, 50.7, 52.5, 52.6, 69.6, 69.8, 70.3, 70.7, 71.0, 71.3, 72.6, 125.5, 125.8, 126.2, 126.7, 126.8, 126.9, 127.2, 127.3, 128.1, 128.7, 128.9, 137.3, 137.6, 138.7, 169.5, 169.6.

^{13}C nmr (90.57 MHz), DMSO-d_6, δ: 25.9, 26.0, 26.1, 30.4, 33.1, 33.7, 49.8, 51.6, 69.1, 69.2, 69.4, 70.2, 70.4, 71.6, 125.2, 125.7, 125.9, 126.3, 126.7, 128.0, 128.4, 128.7, 137.8, 138.0, 138.8, 168.9.

^{13}C nmr (90.57 MHz, 80°C), DMSO-d_6, δ: 25.3(C-5″), 25.5 (C-4″), 30.0 (-CH_3), 68.8 (Ar-CH_2-), 69.0 (C-6″), 69.2 (C-3″), 70.0 (C(O)CH_2-O-), 71.2 (C-1″), 125.6 (C-2′, C-4′ and C-6′), 125.7 (C-4 and C-6), 127.3 (C-5), 128.0 (C-2 and C-5′), 137.4 (C-1 and C-3), 138.4 (C-1′ and C-3′), 168.4 (C=O).

ms (CH_4, CI): 527 (M+1), 555 (M+29), 567 (M+41), 407 (100%).

EI: 526.4 ($M^{+\cdot}$), 407, 207 (100%) Looked for higher mass (1052) to eliminate the possibility of a catenane.

Exact mass (+LSIMS, mNBA) calculated for M+1 $C_{30}H_{43}N_2O_6$ was 527.3121, found 527.3117

N,N'-Dimethyl-5-nitro-isophthalamide 43a

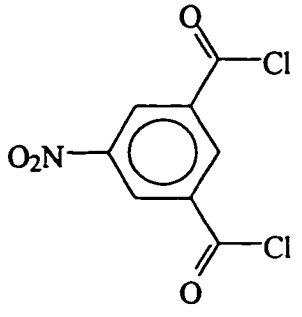

Phosphorous pentachloride (12 g, $5.77x10^{-2}$ mol) was stirred with 5-nitroisophthalic acid (6 g, $2.84x10^{-2}$ mol) in a 250 mL rbf fitted with a reflux condensor and a drying tube. The mixture was heated until the solids were melted The mixture solidified under vacuum and was used without further purification.

^{1}H nmr (360 MHz), $CDCl_3$, δ: 9.08 (t, 1H, C-2 H, J=1.7 Hz), 9.19 (d, 2H, C-4 and C-6 H's, J=1.7 Hz).

^{13}C nmr (90.57), $CDCl_3$, δ: 130.8 (C-4 and C-6), 135.9 (C-1 and C-3), 137.3 (C-2), 148.9 (C-5), 165.5 (C=O).

ms, CI: 247 ($M^{+\cdot}$), 248 (M+1), 276 (M+29), 288 (M+41), 212 and 214.

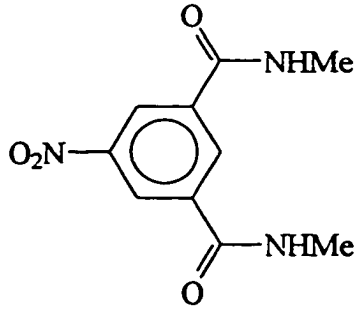

5-Nitroisophthaloyl dichloride **45** (6.66 g, $2.67x10^{-2}$ mol) was added to methyl amine (50 mL, 40% in H_2O) on ice. The general procedure for the preparation of isophthalamides p. 136 was followed. N,N'-Dimethyl-5-nitro isophthalamide **46** was isolated as a white solid (3.68 g, $1.55x10^{-2}$ mol, 73% yield, m.p. 236°C).

^{1}H nmr (360 MHz), CD_3OD, δ: 2.55 (s, 2H, 2X-N<u>H</u>), 2.96 (s, 2X-C<u>H</u>$_3$), 8.65 (t, 1H, C-2 H , J=1.6 Hz), 8.79 (d, 2H, C-4 H and C-6 H, J=1.6 Hz).

^{13}C nmr (90.57 MHz), CD_3OD, δ: 27.1 (-<u>C</u>H$_3$), 125.4 (C-4 and C-6), 132.8 (C-1 and C-3), 137.8 (C-2), 149.8 ((C-5), 167.4 (C=O).

ms, CI : 238 (M+1), 266 (M+29), 278 (M+41).

N,N'-Dimethyl-5-nitro-isophthalyl diamine 47

Method 1

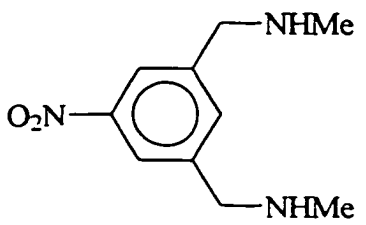

The reduction of the bis amide **46** was carried out by placing **45** (5.31 g, 2.24×10^{-2} mol) in a 250 mL 2 necked rbf and placing it on ice. The rbf was fitted with a reflux condenser and the reaction proceeded under N_2. Diborane (1M in THF, 60 mL, 0.06 mol) was added to the amide **46**. The reaction was then refluxed for 4 h. More diborane (60 mL) was added and the reaction continued to reflux for 2 days. The reaction mixture turned from yellow to white and remained quite thick throughout the procedure. The reaction was cooled to 0^0C and the excess diborane was destroyed by the dropwise addition of MeOH. The solvents were allowed to evaporate and the residue was dissolved in HCl (1 M) to destroy the boron complex. The reaction was refluxed for 4 h. The solvent was evaporated and the residue was dissolved in aq. NaOH and extracted with $CHCl_3$, dried over $MgSO_4$ and allowed to evaporate. A thick yellow oil resulted (3.97g, 1.90×10^{-2} mol, 85%)

Method 2[62]

The dibromide compound **49** (6.92g, $2.24x10^{-2}$ mol) was dissolved in THF. Methylamine (40% solution, 4 eq.) was added and the reaction was stirred for two days at r.t. The THF was removed. A basic solution (2N NaOH) was added and extracted twice with Et_2O and twice with CH_2Cl_2. The organic layers were combined, dried over $MgSO_4$ and evaporated. (2.95g, $1.41x10^{-2}$ mol, 63%)

^1H nmr (360 MHz), $CDCl_3$, δ: 2.30 (s, 6H, 2X-$C\underline{H}_3$), 3.72 (s, 4H, 2XAr-$C\underline{H}_2$-), 7.54 (m, 1H, C-2 H), 7.95 (m, 2H, C-4 H and C-6 H).

^{13}C nmr(90.57 MHz), $CDCl_3$, δ: 35.9 (-$\underline{C}H_3$), 54.9 (Ar-$\underline{C}H_2$-), 121.3 (C-4 and C-6), 133.7 (C-1 and C-3), 142.3 (C-2), 148.3 (C-5).

ms, CI: 210 (M+1), 218 (M+29), 250 (M+41), 180.

Preparation of the Bis chloroamide 43a

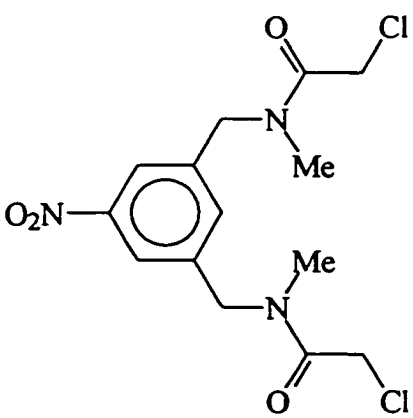

Refer to the general procedure for the preparation of bischloroamides p. 137. The amounts of reagents used are given below. N,N'-Dimethyl-5-nitro-isophthalyl diamine **47** (1.72g, $8.23x10^{-3}$ mol) was dissolved in $CHCl_3$ (10 mL). H_2O (5 mL) was added. Chloroacetyl chloride (2.42g, 2 mL, d=1.42g/mL, $2.56x10^{-2}$ mol) dissolved in $CHCl_3$ (20 mL) and K_2CO_3 (1.30g) was dissolved in H_2O (20 mL) were added.

The solvent evaporated to yield a white solid (1.74g, 4.81×10^{-3} mol, 58%) that was recrystallized from MeOH and Et_2O.

^1H nmr (360 MHz), $CDCl_3$, δ: 3.05 (s, 6H, 2x-CH_3), 4.13 (s, 4H, 2x-CH_2Cl), 4.62 (s ,4H, Ar-CH_2-), 7.24 (s, 1H, C-2 H), 7.95 (s, 2H, C-4 and C-6 H's).

^{13}C nmr (90.57 MHz), $CDCl_3$, δ: 35.7 (-Me), 41.1 (-CH_2-Cl), 50.8 (Ar-CH_2-), 121.6 (C-4 and C-6), 132.8 (C-2), 139.3 (C-1 and C-3), 148.7 (C-5), 167.0 (C=O). Only the major peaks are reported but there are several rotational isomers.

ms calculated for $C_{14}H_{17}N_3O_4Cl_2$ m/e 361.05961, found m/e 361.05862 (intensity 34%).

Preparation of bisiodo compound 43c

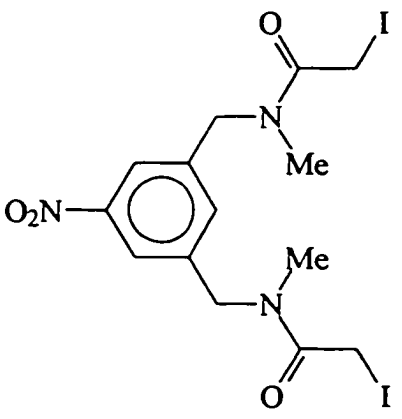

The bischloro compound **43a** (0.21g, 5.82×10^{-4} mol) was added to a mixture of NaI (7.86g, 5.24×10^{-2} mol) in acetone (50 mL) and refluxed for 2 h. The reaction mixture turned yellow during this process. The acetone was evaporated and then taken up in water and extracted with CH_2Cl_2. The organic layer was dried over $MgSO_4$ and was allowed to evaporate. A fluffy white solid resulted when placed on the vacuum pump. Also, the addition of MeOH will induce solidification. The yield is quantitative. m.p. 98°

^{13}C nmr (75.47 MHz), CD_3OD, δ: -3.2 (-CH_2I), 37.3 (-CH_3) 51.7 (Ar-CH_2-), 122.4 (C-4 and C-6), 133.9 (C-2), 141.1 (C-1 and C-3), 150.1 (C-5), 171.5 (C=O).

ms, CI, methane: 546 (M+1), 574 (M+29), 586 (M+41), 25[illegible].

5-Nitro-α,α′-dibromo-*m*-xylene[64] 49

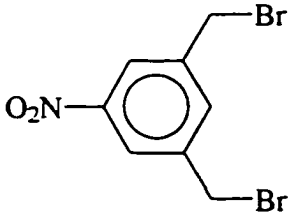

The 5-nitro-*m*-xylene-α,α′-diol (5 g, 2.73×10^{-2} mol) was dissolved with heating in a two phase system of HBr (48% solution, d=1.490, 30 mL, 2.65×10^{-1} mol) and benzene (100 mL). The reaction was refluxed for 16 h. at which time the organic layer was extracted. After washing three times with sat. $NaHCO_3$, the organic layer was dried over $MgSO_4$, filtered and the solvent was allowed to evaporate. A white solid remained which could be recrystallized (4.92 g, 1.59×10^{-2} mo , 58%, m.p. 77°C, lit.[64] m.p. 105-106.5°C) from cyclohexene.

^{1}H nmr (360 MHz), $CDCl_3$, δ: 4.50 (s, 4H), 7.73 (t, 1H, J=1.5 Hz), 8.17 (d, 2H, J=1.5 Hz).

^{13}C nmr (90.57 MHz), $CDCl_3$, δ: 30.6 (Ar-CH_2-), 123.6 (C-4 and C-6), 135.2 (C-2), 140.3 (C-1 and C-3), 148.5 (C-5).

ms (CI, CH_4): 308, 310 and 312 (M+1); 336, 338 and 340 (M+29); 348, 350 and 352 (M+41); 228 and 230 (loss of one Br).

1,3-bis(2-oxa-6-hydroxyhexyl)-5-nitro benzene 44a

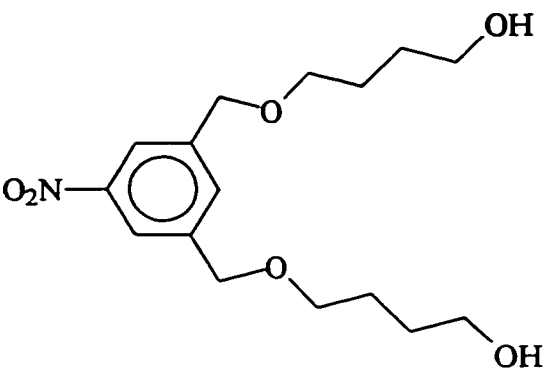

The dibromide **49** (2.12 g, $6.86x10^{-3}$ mol) was dissolved with heating in 1,4-butanediol (150 mL) and the reaction was allowed to continue overnight. Most of the butanediol was removed under vacuum with heating. A silica gel precolumn using Et_2O as eluent was used to remove more butanediol. Residual butanediol was removed by centrifugal chromatography using silica gel as the stationary phase and 1:1, ether:hexanes as the eluent. A clear oil resulted (1.65 g, $5.05x10^{-3}$ mol, 74%).

^1H nmr (360 MHz), $CDCl_3$, δ: 1.65 (m, 4H, $-CH_2C\underline{H}_2CH_2CH_2OH$), 1.67 (m, 4H, $-CH_2CH_2C\underline{H}_2CH_2OH$), 2.42 (s, 2H, -OH), 3.53 (t, 4H, $-C\underline{H}_2CH_2CH_2CH_2OH$, J=6.0 Hz), 3.62 (t, 4H,- $C\underline{H}_2OH$, J=3.0 Hz), 4.55 (s, 4H, Ar-CH_2-), 7.64 (t, 1H, C-2 H, J=0.7Hz), 8.06 (d, 2H, C-4 and C-6 H's, J=0.7 Hz).

^{13}C nmr (90.57 MHz), $CDCl_3$, δ: 26.2 (C-4'), 29.6 (C-5'), 62.4 (C-6'), 70.8 (C-3'), 71.5 (C-1'), 121.2 (C-4 and C-6), 131.9 (C-2), 140.7 (C-1 and C-3), 148.2 (C-5).

^{13}C nmr DEPT experiment (90.57 MHz), $CDCl_3$, δ: 148.3 (C-5) and 140.7 (C-1 and C-3 quaternary C's on aryl moiety) disappear, 26.2, 29.6, 62.4, 70.8 and 71.5 are negative indicating CH_2.

ms (CI, CH_4): 328 (M+1) (100%), 356 (M+29), 368 (M+41), 310, 73.

General Procedure for the Reduction of Aromatic Nitro groups by Hydrazine [65]

The reduction of the aromatic nitro group was carried out by dissolving the compound in 2-methoxyethanol (100 mL). Hydrazine (4 eq.) and a catalytic amount of 10% Pd/C was added and refluxed for 3 h. The solution was allowed to cool slightly. Celite was added and the warm mixture was filtered through a sintered glass filter funnel. The 2-methoxyethanol was allowed to evaporate and the amines were used without further purification.

5-Amino-1,3-bis(2-oxa-6-hydroxyhexyl) benzene 50

1,3-Bis(2-oxa-6-hydroxyhexyl)-5-nitro benzene **44a** (2.71 g, 8.29×10^{-3} mol) was dissolved in 2-methoxyethanol. The general procedure for the reduction of aromatic nitro groups by hydrazine p. 149 was followed.

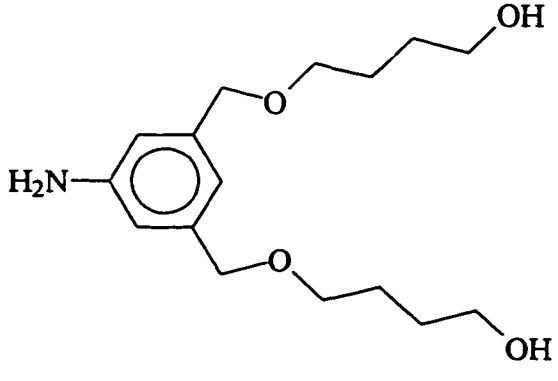

The 2-methoxyethanol was allowed to evaporate and a yellow oil resulted. The ^1H nmr (90 MHz) revealed an upfield shift of the aryl protons consistent with this chemical transformation. The reaction was quantitative.

^{13}C nmr (90.57 MHz), $CDCl_3$, δ: 26.4 (C-4′), 29.8 (C-5′), 62.3 (C-6′), 70.1 (C-3′), 72.8 (C-1′), 113.6 (C-4 and C-6), 117.1 (C-2), 139.4 (C-1 and C-3), 146.6 (C-5).

^{13}C nmr DEPT experiment (90.57 MHz), $CDCl_3$, δ: 26.4, 29.8, 62.3, 70.1 and 72.8 are negative, 113.6 and 117.1 are positive (aromatic CH's) and 139.4 and 146.6 have disappeared (quaternary aromatic C's).

ms (CH_4, CI): 298 (M+1), 208 (100%), 136, 120, 73.

Protection of 5-amino-1,3-bis(2-oxa-6-hydroxyhexyl) benzene 44b

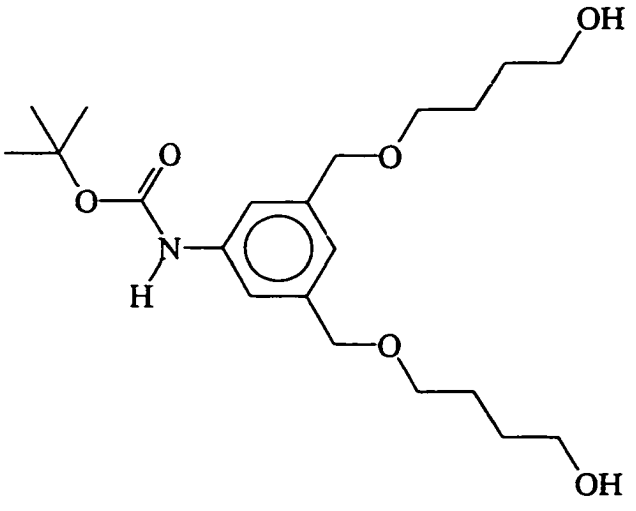

5-Amino-1,3-bis(2-oxa-6-hydroxyhexyl) benzene **50** was stirred at r.t. overnight with di-*t*-butyl dicarbonate (1.81g, 8.30×10^{-3} mol) in freshly distilled THF (10 mL). The product was purified by centrifugal chromatography using silica gel as the stationary phase and 10% MeOH in Et_2O as the eluent (2.97g, 7.48×10^{-3} mol, 90% yield from the nitro compound **44a**).

^{13}C nmr (90.57 MHz), $CDCl_3$, δ: 26.4 (C-4′), 28.2 (C-5′), 29.9 (3x-CH_3), 62.4 (C-6′), 70.2 (C-3′), 72.6 (C-1′), 80.4 (quaternary C of *t*-butyl group), 116.8 (C-4 and C-6), 121.1 (C-2), 138.6 (C-1 and C-3), 139.3 (C-5), 152.8 (C=O).

ms (CH_4, CI): 398 (M+1), 73 (100%).

General Procedure for the Preparation of the N,N′-Bis (substituted propyl) isophthalamides

The isophthaloyl dichloride (1 eq) was added slowly to a cold solution of the substituted propylamine (2 eq) in freshly distilled THF (approximately 10 mL per 2.5 mmol)

and triethylamine (2 eq). This reaction was quite vigorous. After the addition was complete, the reaction was allowed to warm to r.t. for about 1 h. and the triethylamine hydrochloride was filtered off. The THF was allowed to evaporate yielding a clear oil. Centrifugal chromatography using silica gel as the stationary phase and THF as the eluent provided the product as a white solid.

N,N'-Bis (3-hydroxypropyl) isophthalamide 26

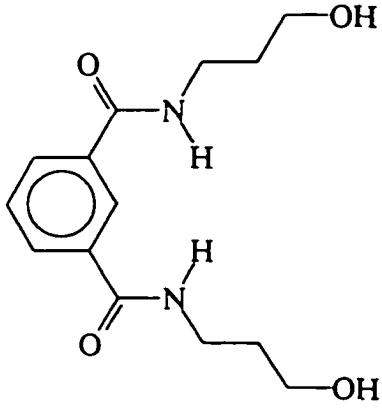

Isophthaloyl dichloride (0.94 g, 4.63×10^{-3} mol) was added to 3-aminopropanol (0.69 g, 9.26×10^{-3} mol, d=0.982, 0.71 mL) in THF (20 mL) and triethylamine (0.94 g, 9.26×10^{-3}mol) as described in the general procedure for the preparation of N,N'-Bis (substituted propyl) isophthalamides p. 150.(0.98g, 3.50×10^{-3} mo , 76%).

^{1}H nmr (360 MHz), CD_3OD, δ: 1.87 (tt, 4 H, J=6.5 Hz), 3.52 (t, 4 H, J=7.0 Hz), 3.68 (t, 4 H, J=6.3 Hz), 7.57 (t, 1 H), 7.98 (dd,2 H), 8.29 (d, 1 H).

^{13}C nmr (90.57 MHz), CD_3OD, δ: 33.2 ($-CH_2\underline{C}H_2CH_2-$), 38.2 ($N-CH_2-$), 60.6 ($CH_2OH$), 127.2 (C-2), 129.8 (C-5), 131.1 (C-4 and C-6), 136.2 (C-1 and C-3), 169.5 (C=O).

N,N'-Bis (3-hydroxypropyl)-5-nitro isophthalamide 52

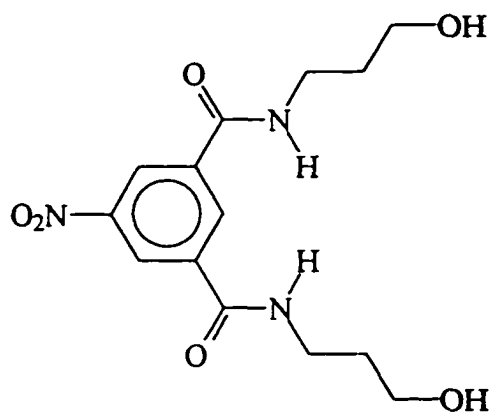

5-Nitro isophthaloyl dichloride **45** (5.18 g, $2.10x10^{-2}$ mol) was added slowly to a cold solution of 3-aminopropanol (6.29 g, $8.39x10^{-2}$ mol, 6.41 mL)and triethylamine (8.47 g, $8.39x10^{-2}$ mol) in THF (100 mL) as described in the general procedure for the preparation of N,N'-Bis (substituted propyl) isophthalamides p. .50. Chromatography was performed as described in the general procedure but further trials revealed that the mixture turned solid on standing and could be triturated with H_2O. A white solid resulted (5.05 g, $1.55x10^{-2}$ mol, 74%, m.p. 112°C).

^{1}H nmr (360 MHz), CD_3OD, δ: 1.75 (qu, 4H, $-CH_2\underline{CH_2}CH_2-$), 3.40 (t, 4H, NCH_2-, J=7.0 Hz), 3.56 (t, 4H, $-CH_2OH$, J=6.2 Hz), 8.50 (d, 1H, C-2 H, J=1.6 Hz), 8.63 (d, 2H, C-4 and C-6 H's, J=1.6 Hz).

^{13}C nmr (90.57 MHz), CD_3OD, δ: 32.8 ($-CH_2\underline{C}H_2CH_2-$), 38.3 ($NCH_2-$) , 60.4 ($-CH_2OH$), 125.3 (C-1 and C-3), 132.7 (C-2), 137.5 (C-4 and C-6), 149.3 (C-5), 166.6 (C=O).

^{13}C nmr DEPT experiment (90.57 MHz), CD_3OD, δ: 166.6 (C=O), 125.3 and 149.3 disappear (quaternary C on aryl moiety), 32.8, 38.3 and 60.4 are negative (CH_2's), and 132.7 and 137.5 are positive which indicate -CH-.

ms (CI, CH_4): 326 (M+1), 354 (M+29).

Ms calculated for $C_{14}H_{19}N_3O_6$ m/e 325.1274, found m/e 325.1272 (intensity 8.24%).

5-Amino-N,N'-Bis (3-hydroxypropyl) isophthalamide 53

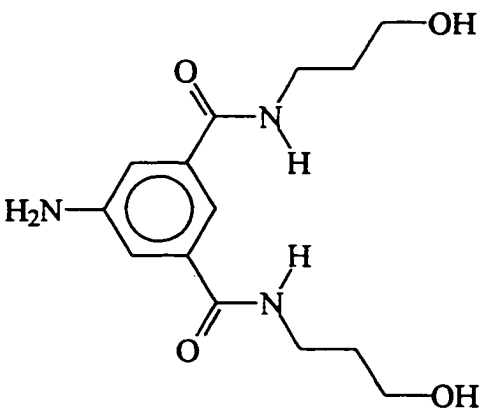

Refer to the general procedure for the reduction of aromatic nitro groups by hydrazine p. 149. The reaction was quantitative for the reduction of N,N'-Bis (3-hydroxypropyl)-5-nitro-isophthalamide **52** (1.28g, 3.94×10^{-3} mol). The product was used without purification but ^1H nmr reveals the expected upfield shift of the aryl protons.

ms (CI, CH_4): 296 (M+1), 324 (M+29).

Protection of amine 53.

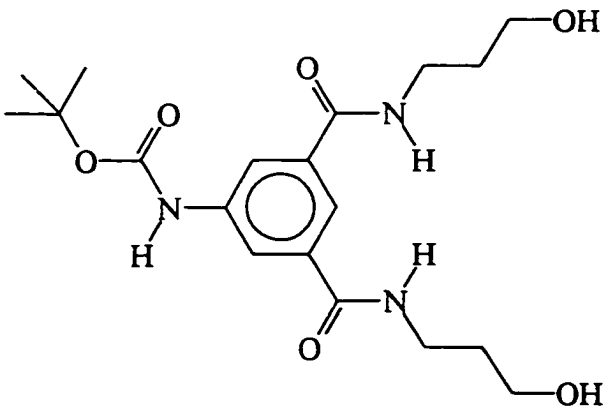

5-Amino-N,N'-bis (3-hydroxypropyl) isophthalamide **53**, a yellow oil, was stirred with di-tert-butyl di-carbonate (amount). Connected to the nitrogen bubbler, the reaction was monitored by the efflux of CO_2.

Centrifugal chromatography was performed using silica gel as the stationary phase and a 10% MeOH in Et_2O solution as eluent. Four bands were eluted and band 3 was the product **54** (0.35g, 8.86×10^{-4} mol, 82% from the nitro compound, 0.35g, 1.08×10^{-3}).

^{1}H nmr (360 MHz), CD_3OD, δ: 1.40 (s, 9H, 3x-CH_3), 1.72 (qu, 4H, -$CH_2CH_2CH_2$-), 3.36 (t, 4H, NCH_2-, J=6.9 Hz), 3.54 (t, 4H, -CH_2OH, J=6.3 Hz), 7.70 (t, 1H, C-2 H, J=1.5 Hz), 7.87 (d, 2H, C-4 and C-6 H's, J=1.5 Hz).

^{13}C nmr (90.57 MHz), CD_3OD, δ: 28.6 (-CH_3), 33.1 (-$CH_2CH_2CH_2$-), 38.1 (NCH_2-), 60.5 (-CH_2OH), 81.4 (quaternary *t*-butyl C), 120.7 (C-2), 121.0 (C-4 and C-6), 136.8 (C-1 and C-3), 141.3 (C-5), 154.9 (carbamate C=O), 169.5 (amide C=O).

ms (+LSIMS, mNBA): 396 (M+1), 340, 265 (100%)

ms calculated for $C_{19}H_{29}N_3O_6$ m/e 395.2056, found m/e 395.2071.

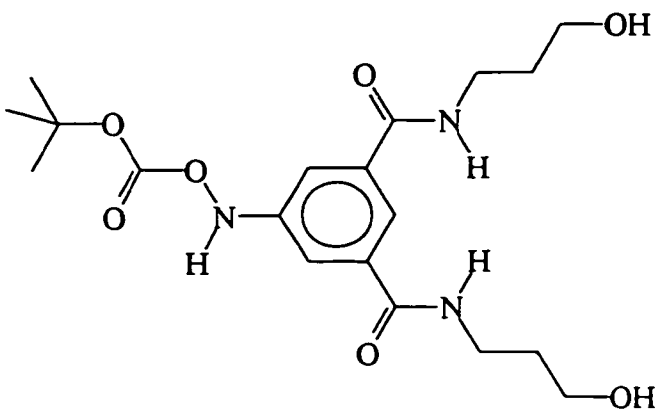

A minor product **54a** was isolated (band 4) which was a result of partially reducing the nitro compound **52**. (0 03g, 7.30 x 10^{-5} mol, 6.8%).

^{1}H nmr (360 MHz), CD_3OD, δ: 1.44 (s, 9H, 3x-CH_3), 1.73 (qu, 4H, -$CH_2CH_2CH_2$-), 3.38 (t, 4H, NCH_2-, J=6.9 Hz), 3.55 (t, 4H, -CH_2OH, J=6.3 Hz), 7.86 (t, 1H, C-2 H, J=1.5 Hz), 8.03 (d, 2H, C-4 and C-6 H's, J=1.5 Hz).

^{13}C nmr (90.57 MHz), CD_3OD, δ: 28.5 (-CH_3), 33.1 (-$CH_2CH_2CH_2$-), 38.2 (NCH_2-), 60.5 (-CH_2OH), 83.7 (quaternary *t*-butyl C), 122.4 (C-4 and C-6), 122.9 (C-2), 136.4 (C-1 and C-3), 144.4 (C-5), 155.3 (carbamate C=O), 169.2 (amide C=O).

ms (+LSIMS, mNBA): 412 (M+1), 340, 311 (100%), 281, 265, 236.

N,N′-Dibutyl-5-nitroisophthalamide[66]

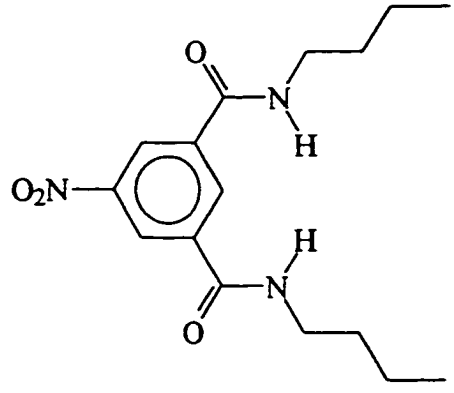

5-Nitroisophthaloyl dichloride **45** ($3.32x10^{-2}$ mol) was added to a solution of 1-aminobutane (4 eq., 9.7g, $1.33x10^{-1}$ mol) in CH_2Cl_2 (100 mL) as described in the general procedure for the preparation of N,N′-Bis (substituted propyl) isophthalamides p.150.

After work-up, a white solid remained (8.6g, $2.67x10^{-2}$ mol, 80%, lit[66]. m.p. 145-146°C)

^{1}H nmr (360 MHz), CD_3OD, δ: 0.86 (t, 6H, 2x-CH_3, J=7.3 Hz), 1.31 (m, 4H, 2x-$C\underline{H}_2CH_3$), 1.52 (m, 4H, 2x-$CH_2C\underline{H}_2CH_2$-), 3.30 (t, 4H, 2x-NCH_2-, J=7.2 Hz), 8.53 (t, 1H, C-2 H, J=1.5 Hz), 8.65 (d, 2H, C-4 and C-6 H's, J=1.5 Hz).

^{13}C nmr (90.57 MHz), CD_3OD, δ: 14.1 (-CH_3), 21.2 (-$\underline{C}H_2CH_3$), 32.5 (-$CH_2\underline{C}H_2CH_2$-), 41.0 (-NCH_2-), 125.4 (C-4 and C-6), 132.8 (C-2), 137.9 (C-1 and C-3), 149.7 (C-5), 166.7 (C=O).

5-Amino-N,N′-Dibutylisophthalamide

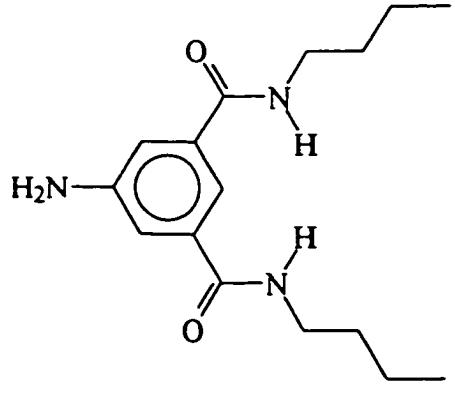

N,N′-Dibutyl-5-nitro isophthalamide (4.32g, $1.35x10^{-2}$ mol) was reduced with hydrazine in 2-methoxyethanol as described in the general procedure for the reduction of aromatic nitro groups by hydrazine p. 149. The residue was a thick yellow oil (3.53g,

$1.21x10^{-2}$ mol, 90%).

^{13}C nmr (90.57 MHz), CD_3OD, δ: 16.7 ($-CH_3$), 23.7 ($-\underline{C}H_2CH_3$), 35.1 ($-CH_2\underline{C}H_2CH_2-$), 43.3 ($-NCH_2-$), 118.4 (C-2), 121.0 (C-4 and C-6), 139.3 (C-1 and C-3), 156.2 (C-5), 172.3 (C=O).

^1H nmr (360 MHz), CD_3OD, δ: observed shift in the aromatic protons, 7.35 (d, 2H, C-4 and C-6 H's, J=1.6 Hz), 7.52 (t, 1H, C-2 H, J=1.6 Hz).

Protection of 5-Amino-N,N'-Dibutylisophthalamide

The amine (3.53g, $1.21x10^{-2}$ mol) was stirred with di-*t*-butyl dicarbonate (3g, $1.38x10^{-2}$ mol) in CH_2Cl_2 (50 mL) until no more CO_2 was evolved (about 10 min.). The CH_2Cl_2 was evaporated and the residue chromatographed using 2% MeOH in Et_2O as the eluent on the chromatotron. The nmr spectra of the first two bands collected were very similar. The first band was product identified by mass spectrometry.

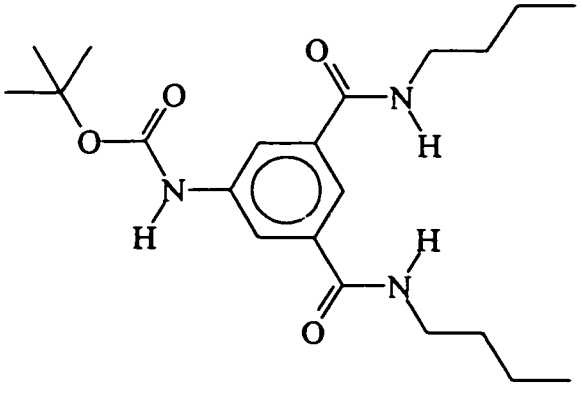

^{13}C nmr (90.57 MHz), CD_3OD, δ: 14.2 ($-CH_2\underline{C}H_3$), 21 2 ($-\underline{C}H_2CH_3$), 28.6 (*t*-butyl - CH_3's), 32.6 ($-CH_2\underline{C}H_2CH_2-$), 40.9 ($-NCH_2-$), 81.5 (quaternary C of *t*-butyl), 120.8 (C-2), 121.1 (C-4 and C-6), 137.1 (C-1 and C-3), 141.4 (C-5), 158.3 (carbamate C=O), 169.4 (amide C=O).

ms (LSIMS, mNBA): 392.2 (M+1), 336.1, 291.1.

m.p. 115°C

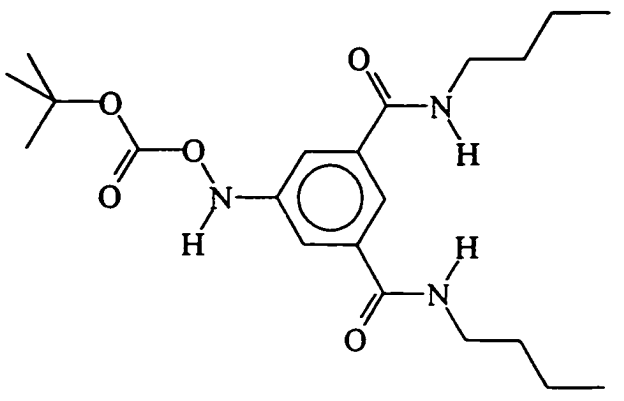

The second band was the minor product which was the result of protecting a partially reduced nitro group. ^{13}C nmr (90.57 MHz), CD_3OD, δ: 14.2 ($-CH_2\underline{C}H_3$), 21.2 ($-\underline{C}H_2CH_3$), 28.5 (*t*-butyl $-CH_3$'s), 32.6 ($-CH_2\underline{C}H_2CH_2-$), 40.9 ($-NCH_2-$), 83.7 (quaternary C of *t*-butyl), 122.5 (C-2), 123.0 (C-4 and C-6), 136.6 (C-1 and C-3), 144.5 (C-5), 155.4 (carbamate C=O), 169.1 (amide C=O).

ms (LSIMS, mNBA): 408.2 (M+1), 352.1, 307.1.

N,N'-Bis (3-bromopropyl) isophthalamide 56

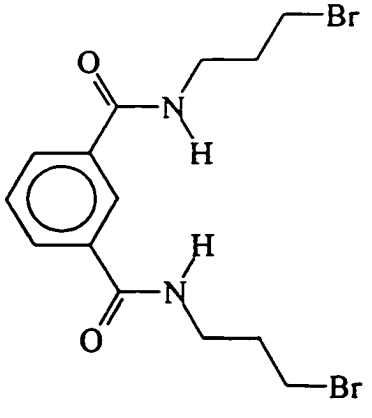

Isophthaloyl dichloride (5.18g, $2.56x10^{-2}$ mol) was slowly added to 3-bromopropylamine hydrobromide (11.2g, $5.13x10^{-2}$ mol) in water (200 mL) at r.t. The pH was maintained at 8 by the constant addition of aqueous KOH. The reaction was allowed to continue for 2 h. A white solid was collected by suction filtration (8.74g, 2.16 x 10^{-2} mol, 84%, m.p. 96°C).

^{1}H nmr (300 MHz), CD_3OD, δ: 2.17 (m, 4H, 2x-$CH_2\underline{CH_2}CH_2$-), 3.52 (m, 8H, 2x-NCH_2- and 2x-CH_2Br), 7.56 (t, 1H, C-5 H, J=7.8 Hz), 7.94 (d, 2H, C-4 and C-6 H's, J=7.8 Hz), 8.27 (s, 1H, C-2 H).

^{13}C nmr (75.47 MHz), CD_3OD, δ: 31.5 (-$CH_2\underline{C}H_2CH_2$-), 33.5 (-CH_2Br), 39.8 (-CH_2N-), 127.4, 130.0, 131.3, 136.1, 169.6 (C=O).

ms, methane CI: 405, 407 and 409 (M+1), 433, 435, 437 (M+29).

N,N'-Bis (3-thiopropyl) isophthalamide[58] 58

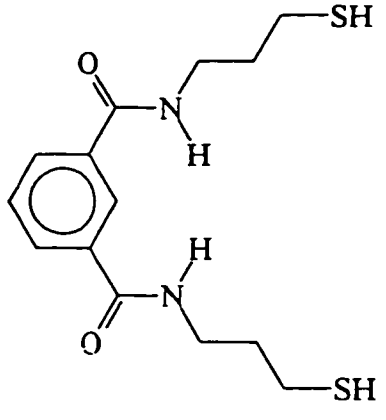

The bisbromo compound **56** (1.20g, 2.96 x 10^{-3}) was dissolved in dry THF (100 mL) and thiourea (0.45g, 5.91 x 10^{-3} mol) was added. The reaction was allowed to reflux overnight under N_2. The resulting thiouronium salt was then taken up in degassed KOH (1g in H_2O, 100mL). The solution was refluxed for 6h. After cooling, a solution of 50% H_2SO_4 was added dropwise to acidify. A white solid precipitated. Attempts at recrystallization failed. ^{13}C nmr appeared messy in the aromatic region but okay in the CH_2 region.

^{13}C nmr (75.47 MHz), $CDCl_3$ and DMSO-d_6, δ: 26.7 (-CH_2SH), 38.3 (-$CH_2\underline{CH_2}CH_2$-), 43.0 (-CH_2N-), 130.5 (C-2), 133.2 (C-5), 135.0 (C-4 and C-6), 139.4 (C-1 and C-3), 171.8 (C=O).

ms (CH_4, CI): 313 (M+1), 341 (M+29), 353 (M+41).

Dimethyl 5-nitroisophthalate[57]

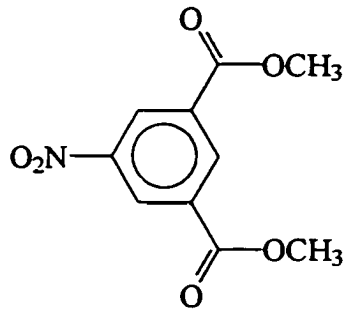

5-Nitroisophthaloyl dichloride **45** (8 g, $3.24x10^{-2}$mol) was added to MeOH slowly. The reaction is very vigorous. A white needle-like solid was filtered off. The reaction was quantitative (7.7 g, $3.24x10^{-2}$mol, m.p. 120°C, lit. m.p. 118-121°C).

^{1}H nmr (300 MHz), $CDCl_3$, δ: 4.0 (s, 6H, 2x-CH_3), 8.85 (s,1H, C-2 H), 8.90 (s,2H, C-4 and C-6 H's).

^{13}C nmr (75.47 MHz), $CDCl_3$, δ: 53.1 (-CH_3), 128.1 (C-4 and C-6), 132.4 (C-1 and C-3), 135.8 (C-2), 148.4 (C-5), 164.1 (C=O).

IR (KBr, cm^{-1}): 1734 (ester C=O), 1537 and 1314 (N=O)

ms (CH_4, CI):240 (M+1), 268 (M+29), 280 (M+41)

General Procedure for the Reduction of Aromatic Nitro groups by H_2/PtO_2

The nitro compound was placed in a Parr hydrogenator with 95% EtOH (~100 mL/0.5g of nitro compound), PtO_2 (20 mol %) and H_2 (25 psi) and shaken for 2 h. When the hydrogenation was complete, the solution was clear except for catalyst. This black particulate was gravity filtered and the solution was evaporated

Dimethyl 5-aminoisophthalate[57]

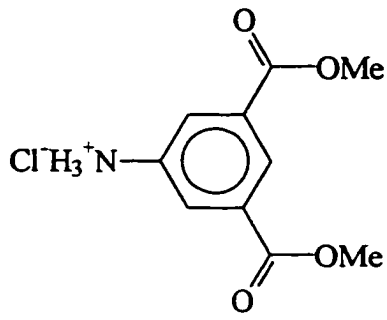

Dimethyl 5-nitroisophthalate (0.98g, 4.10×10^{-3} mol) was reduced as described in the general procedure for the reduction of aromatic nitro groups by H_2/PtO_2 on p. 159. Concentrated HCl (0.35 mL, 4.10×10^{-3} mol) was added so the amine was protonated as it was formed. The reaction was quantitative resulting in a white powder.

^{1}H nmr (300MHz), CD_3OD, δ: 3.97 (s, 6H, 2x-CH_3), 8.23 (d, 2H, C-4 and C-6 H's, J=1.5 Hz), 8.64 (t, 1H, C-2 H, J=1.5 Hz)

^{13}C nmr (75.47 MHz), CD_3OD, δ: 53.4 (-CH_3), 129.0 (C-2)[a], 131.1 (C-1 and C-3), 133.8 (C-4 and C-6)[a], 134.0 (C-5), 166.1 (C=O)

IR (KBr, cm^{-1}): 3455, 3373 and 3257 (-NH_3^+), 1718 (ester C=O), loss of the N=O stretches.

The free amine was generated by extracting with an aqueous solution of NaOH and CH_2Cl_2. The organic layer was collected and dried over $MgSO_4$. An off white solid remained after evaporation (m.p. 148°C, lit[57]. m.p. 176-178°C).

^{1}H nmr (300MHz), CD_3OD, δ: 3.89 (s, 6H, 2x-CH_3), 7.51 (d, 2H, C-4 and C-6 H's, J=1.5 Hz), 8.04 (t, 1H, C-2 H, J=1.5 Hz)

^{13}C nmr (75.47 MHz), CD_3OD, δ: 52.3 (-CH_3), 119.9 (C-4 and C-6), 120.9 (C-2), 131.5 (C-1 and C-3), 146.4 (C-5), 166.0 (C=O).

ms (CI, CH_4): 210 (M+1), 238 (M+29), 250 (M+41), 178 (M-OCH_3).

General Procedure for the Cbz Protection of Aromatic Amines

The amine was dissolved in CH_2Cl_2 (~50 mL/g of amine) and made basic with 2N NaOH. Four equivalents of benzyl chloroformate were added. The reaction was stirred for approximately 1 h. at r.t. after which the organic layer was extracted and washed once with water. The organic layer was dried over $MgSO_4$ and evaporated.

Protection of the amine

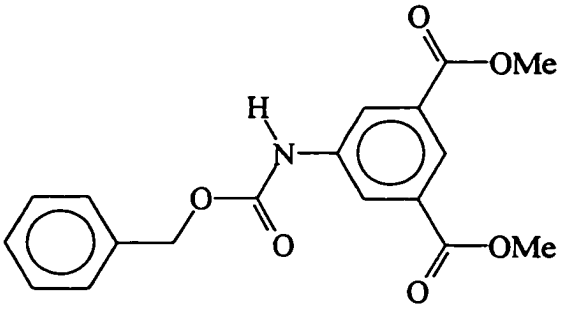

The amine (0.95g, $3.97x10^{-3}$ mol) was dissolved in CH_2Cl_2 (50 mL) and 2N NaOH (25 mL). Benzyl chloroformate was added (4 eq) and the reaction continued as described in the general procedure for the CBz protection of aromatic amines above. The yellow solid was recrystallized using CH_2Cl_2 and 95% EtOH. (0.44g, $1.28x10^{-3}$ mol, 32%, m.p. 178°C). The yield in this preparation was not maximized since it was only a model compound.

^1H nmr (300MHz), 4:1, $CDCl_3$: CD_3OD, δ: 3.82 (s, 6H, 2x-CH_3), 5.12 (s, 2H, Ar-CH_2-), 7.24-7.29 (m, 5H, aromatic H's), 8.20-8.23 (m, 3H, aromatic H's).

^{13}C nmr (75.47 MHz), 4:1, $CDCl_3$: CD_3OD, δ: 52.3 (-CH_3), 66.8 ($ArCH_2$-), 123.5, 124.8, 127.9, 128.1, 128.4, 130.9, 136.0, 139.0, 154.0 (carbamate C=O), 166.3 (amide C=O).

IR (KBr, cm^{-1}): 3328 (N-H), 1717 (ester C=O), 1710 (carbamate C=O).

ms (CH_4, CI): 344 (M+1), 372 (M+29), 384 (M+41).

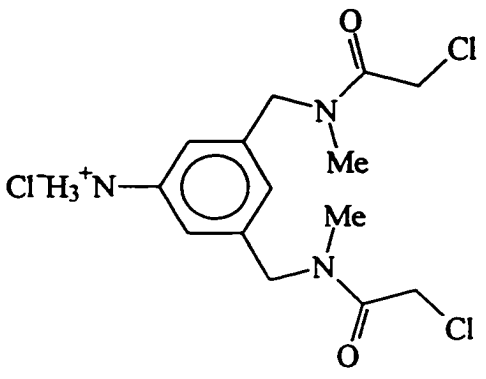

Refer to the general procedure for the reduction of aromatic nitro groups by H_2/PtO_2 p. 159. The nitro compound **43a** (1.80g, $3.99x10^{-3}$ mol) was added to 95% EtOH (100 mL). It did not dissolve. Concentrated HCl (1 eq., 0.35 mL, $3.99x10^{-3}$ mol) was added. A catalytic amount of PtO_2 was added. The mixture was shaken on the hydrogenator at 25 psi of H_2 for 1 h. The reduced compound dissolved in the EtOH. The catalyst was filtered off and the EtOH was evaporated. The compound was dried further on the vacuum line and a white solid resulted. The reaction was quantitative and the compound was used without purification

^{1}H nmr, (300 MHz), CD_3OD, δ: 2.93, 3.10, 3.12 (s, 6H, 2x-CH_3), 4.34, 4.38, 4.39 (s, 4H, 2x-CH_2Cl), 4.65, 4.68 (s, 4H, 2x$ArCH_2$-), 7.28-7.37 (m, 3H, aromatic H's).

free amine, ms (+LSIMS, mNBA): 332 (M+1), 225, 136 (100%), 154.

Protection of 51 to afford 43c

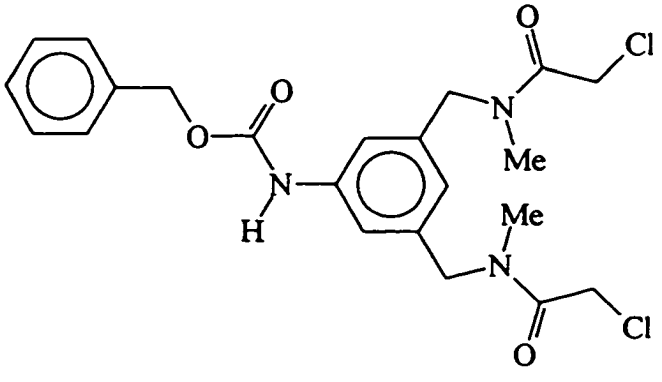

The amine·HCl salt **51** (0.87g, $2.37x10^{-3}$ mol) was dissolved in CH_2Cl_2 (50 mL) and NaOH (2N, 25 mL). Benzyl chloroformate (0.75 mL) was added. Refer to the general procedure for the Cbz protection of aromatic amines p. 161. A thick yellow oil remained. Centrifugal chromatography using first Et_2O and

then gradually increasing the concentration of MeOH. The major band was product, a white solid (0.38g, $8.14x10^{-4}$ mol, 34%).

^{1}H nmr (300 MHz), CD_3OD, δ: 2.90, 3.00, 3.02 (s, 6H, 2x-CH_3), 3.34 (s, 1H, -NH), 4.26, 4.29, 4.30 (s, 4H, 2x-CH_2Cl), 4.53, 4.55, 4.58, 4.61 (m, 4H, 2xAr-CH_2-N-), 5.15 (s, 2H, $ArCH_2O$-), 6.79 (s, 1H, aromatic H), 7.28-7.40 (m, 7H, aromatic H's).

^{13}C nmr (75.47 MHz), CD_3OD, δ: 34.8, 35.7, 35.8 (-CH_3), 42.2, 42.4, 42.5 (-CH_2Cl), 52.2, 54.4 (Ar-CH_2-N-),67.6 (Ar-CH_2-O-), 117.2, 118.3 (C-4 and C-6), 121.4, 122.4 (C-2), 129.0, 129.2, 129.6, 138.1, 139.0, 139.3, 139.7 (other aromatic C's), 141.1, 141.5, 155.7 (carbamate C=O), 169.3, 169.4 (amide C=O).

^{13}C nmr DEPT experiment (75.47 MHz), CD_3OD, δ: 34.8, 35.7, 35.8 were positive indicating -CH_3; 42.2, 42.4, 42.5, 52.2, 54.4, 67.6 are negative indicating -CH_2-'s; 117.2, 118.3, 121.4, 122.4, 129.0, 129.2, 129.6, 138.1 are positive indicating aromatic -CH-'s; 139.0, 139.3, 139.7, 141.1, 141.5, 155.7, 169.3, 169.4 disappear indicating quaternary aromatic C's.

ms (CI, CH_4): 466, 468 (M+1), 494 (M+29).

Synthesis of 60

Isophthaloyl chloride (1.54g, 7.60 x 10^{-3} mol) was dissolved in THF and added slowly to a solution of 1,8-octanediol (2.22g, 1.52 x 10^{-2} mol) in dry THF (1 L) and triethylamine (4 eq).

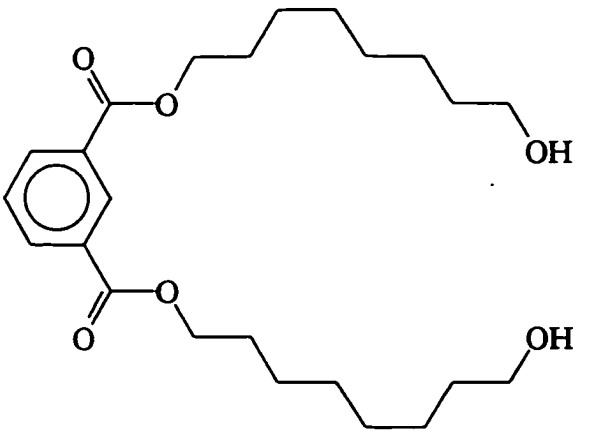

The reaction was stirred for approximately 1h. The triethylamine hydrochloride was filtered off. A second precipitate formed and was filtered off which proved to be the 2+2 macrocycle (1.5% yield). A third precipitate was isolated and appeared to be the 1+1 macrocycle. The diol **60** was isolated by column chromatography on silica gel using Et_2O as the eluent. A clear oil was obtained (1.35g, 3.20x10^{-3} mol, 42%). The diol could also be precipitated by the addition of toluene.

^{1}H nmr (300 MHz), $CDCl_3$, δ: 1.48 (m, 4H), 1.72 (m, 4H), 2.52 (s, 4H), 3.54 (m, 6H), 4.28 (t, 4H, J=6.6 Hz), 7.46 (t, 1H, J=7.8 Hz), 8.16 (d, 2H, J=7.8 Hz), 8.60 (s, 1H),

^{13}C nmr (75.47 MHz), $CDCl_3$, δ: 25.6 (-$\underline{C}H_2CH_2CH_2OH$), 25.9 (-$\underline{C}H_2CH_2CH_2OCO$), 28.6 (-$CH_2\underline{C}H_2CH_2OCO$), 29.2 (-$\underline{C}H_2CH_2CH_2CH_2OCO$), 29.3 (-$\underline{C}H_2CH_2CH_2CH_2OH$), 32.6 (-$\underline{C}H_2CH_2OH$), 62.7 (-$CH_2OH$), 65.5 (-$\underline{C}H_2OCO$, 128.5 (C-5). 130.6 (C-1 and C-3), 130.8 (C-2), 133.7 (C-4 and C-6), 165.9 (C=O).

ms, methane CI: 423 (M+1)(100), 451 (M+29), 463 (M+41), 170, 112, 88.

Exact mass (+LSIMS) calculated for M+1 $C_{24}H_{39}O_6$ m/e 423 2747, found m/e 423.2733.

2+2 macrocycle, **29**

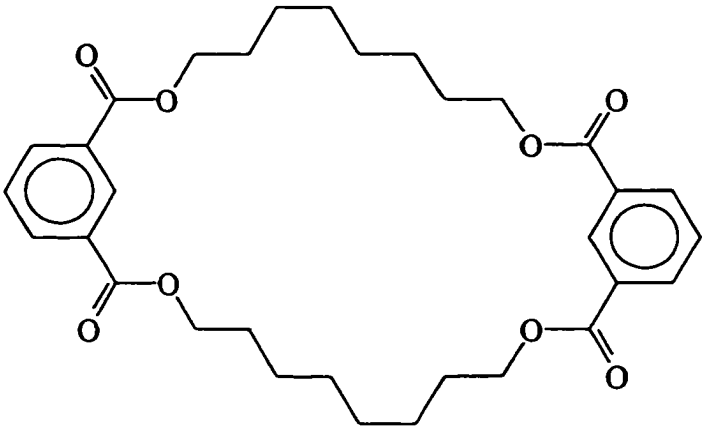

^{1}H nmr (300 MHz),$CDCl_3$, δ: 1.52-1.43 (m, 16H), 1.82-1.73 (m, 8H), 4.33 (t, 8H, J=6 Hz), 7.50 (t, 2H, J=5 Hz), 8.20 (d, 4H, J=6 Hz), 8.60 (s, 2H).

^{13}C nmr (75.47 MHz), $CDCl_3$, δ: 26.0 ($-CH_2\underline{C}H_2CH_2CH_2OCO$), 28.6 ($-\underline{C}H_2CH_2OCO$), 29.1($-\underline{C}H_2CH_2CH_2CH_2OCO$), 65.3 ($-\underline{C}H_2OCO$), 128.7 (C-5), 130.2 (C-1 and C-3), 130.8 (C-2), 133.9 (C-4 and C-6), 165.8 (C=O).

ms, methane CI: 553 (M+1), 581 (M+29), 593 (M+41), 552 ($M^{+\cdot}$), 167.

1+1 macrocycle, **59**

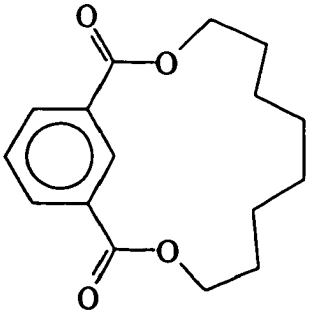

^{13}C nmr (75.47 MHz), $CDCl_3$, δ: 26.0 ($-CH_2\underline{C}H_2CH_2CH_2OCO$), 27.8 ($-\underline{C}H_2CH_2OCO$), 29.3 ($-\underline{C}H_2CH_2CH_2CH_2OCO$), 65.7 ($-\underline{C}H_2OCO$), 128.9, 132.9, 165.3, other aromatic carbons are hidden by impurity peaks. This is contaminated with compound **29**.

Macrocyclic Mixture 61

5-Nitroisophthaloyl dichloride (2.99g, $1.21x10^{-2}$ mol) and the diol (5.65g, $1.21x10^{-2}$ mol) were dissolved in THF (50 mL) and each placed into a separate syringe. They were added slowly overnight via a driver syringe into a 5L rbf charged with freshly distilled THF (2L) and triethylamine hydrochloride (2.44g, $2.42x10^{-2}$ mol). The solution was stirred vigorously with the aid of a high speed stirrer. The reaction was worked up the following day by first filtering off the triethylamine hydrochloride. Evaporation of the THF left an off-white solid. The color was removed from the solid by dissolving in CH_2Cl_2 and then precipitating out with 95% EtOH (7.44g, $1.16x10^{-2}$ mol, 96% yield, m.p. 81-82°C).

^{1}H nmr (300 MHz), $CDCl_3$, δ: 1.41-1.44 (m, 16h, 2x-$OCH_2CH_2CH_2CH_2CH_2CH_2CH_2CH_2O$-), 1.75-1.82 (m, 8H, 4x-OCH_2CH_2-), 4.38 (t, 8H, 4x- OCH_2-, J=6.6 Hz), 8.89-8.98 (m, 6H, aromatic H's).

^{13}C nmr (75.47 MHz), $CDCl_3$, δ: 25.8 (-$OCH_2CH_2CH_2CH_2$-), 28.5 (-$OCH_2CH_2CH_2$-), 29.1 (-OCH_2CH_2-), 66.4 (-OCH_2-), 128.0 (C-4 and C-6), 132.7 (C-1 and C-3), 135.8 (C-2), 148.4 (C-5), 163.8 (C=O).

^{13}C nmr DEPT experiment (75.47 MHz), $CDCl_3$, δ: 25.8 (-$OCH_2CH_2CH_2CH_2$-), 28.5, 29.1, 66.4, 128.0, 132.7, 135.8, 148.4, 163.8

ms (-LSIMS, mNBA): 321.0 (M, 1+1 product), 642.2 (M, 2+2 product), 963.3 (M, 3+3 product), 1284.3 (M, 4+4 product), each molecular ion peak is followed by a loss of 111.

Monotetrahydropyranyl ether of 1,8-octanediol[57] 62

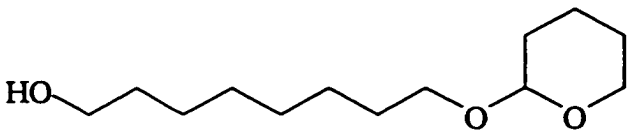

Dihydropyran (4.52 g, 5.38×10^{-2} mol) and p-toluenesulfonic acid (20 mg) were added to a solution of 1,8-octanediol (7.86 g, 5.38×10^{-2} mol) in freshly distilled THF (200 mL) on ice. The reaction was stirred on ice for 1 h. and then allowed to continue stirring at r.t. for 2 h. Pyridine was added to neutralize the acid. The mixture was diluted with diethyl ether at which time the solution became cloudy. The organic mixture was washed with H_2O twice. The organic layer was collected and dried over $MgSO_4$. The solvent was allowed to evaporate and column chromatography on silica gel using 2:1, hexanes:Et_2O as the eluent yielded product **62** as a clear oil (5.94 g, 2.58×10^{-2} mol, 48% yield).

^{1}H nmr (300 MHz), $CDCl_3$, δ: 1.28-1.40 (m, 8H), 1.43-1.85 (m, 10H), 3.28-3.86 (m, 6H), 4.52 (t, 1H, C-2′ H)

^{13}C nmr (75.47 MHz), $CDCl_3$, δ: 19.6, 25.5, 25.7, 26.1, 29.3, 29.4, 29.7, 30.7, 32.7, 62.3 (chain -$\underline{C}H_2O$-), 62.8 (-$\underline{C}H_2OH$), 67.6 (ring -$\underline{C}H_2O$-), 98.8 (-O$\underline{C}$HO-).

ms (CI, CH_4): 231 (M+1), 229 (M-1), 214, 146

Synthesis of 63

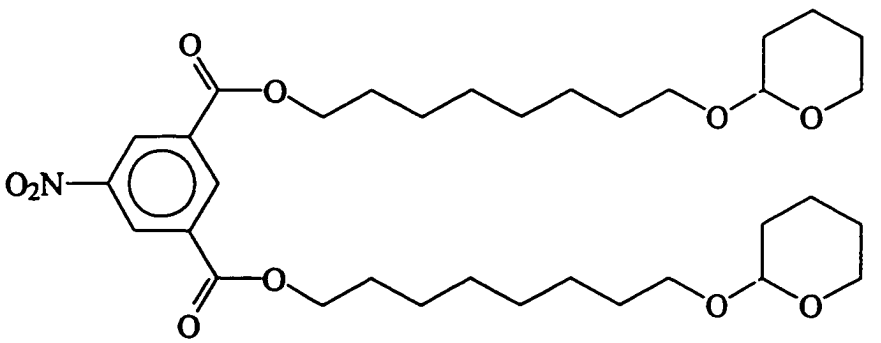

Monosubstituted 1,8-octanediol **62** (4.81 g, 2.09×10^{-2} mol) was dissolved in

freshly distilled THF (200 mL) and stirred on ice. The diacid chloride **45** ($9.95x10^{-3}$ mol) was dissolved in THF (50 mL) and added dropwise to the first solution. Triethylamine (2.11 g, $2.09x10^{-2}$ mol) was also added dropwise simultaneously. The reaction was stirred on ice for 1h. and then allowed to continue stirring at r.t. for an additional 1h. The triethylamine hydrochloride was filtered off and the mother liquor was collected. The THF was allowed to evaporate yielding a yellow oil. Chromatography on silica gel using 3:1, hexanes:Et_2O as the eluent afforded a clear oil. (5.18 g, $8.16x10^{-3}$ mol, 82%). R_f=0.37

^{1}H nmr (300 MHz), $CDCl_3$, δ: 1.25-1.77 (m, 36H), 3.26-3.82 (m , 8 H), 4.33 (t, 4 H), 4.47-4.49 (m, 2 H, C-2′ H's), 8.89 (s, 1 H, Ar C-2 H), 8.92 (d, 2 H, Ar C-4 and C-6 H's, J=1.5 Hz).

^{13}C nmr (75.47 MHz), $CDCl_3$, δ: 19.6 (C-4′), 25.4 (C-6), 25.8 (C-3), 26.1 (C-5′), 28.5 (C-7), 29.1 (C-5), 29.3 (C-4), 29.6 (C-2), 30.7 (C-3′), 62.3 (C-1), 65.3 (C-6′), 67.5 (C-8), 98.7 (C-2′), 127.9 (Ar, C-4 and C-6), 132.7 (Ar, C-1 and C-3), 135.7 (Ar, C-2), 148.4 (Ar, C-5), 163.7 (C=O).

ms (+LSIMS, mNBA): 634.4 (M-1), 468.3 (M+1-2xThp).

Reduction of 63 to 64

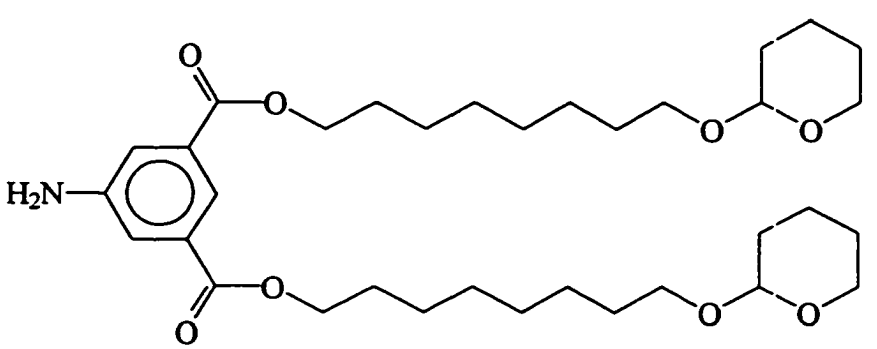

The nitro compound **63** (1.65 g, $2.60x10^{-3}$ mol) was dissolved in 95% EtOH and treated as described

in the general procedure for the reduction of aromatic nitro compounds on p. 159. After the expired catalyst was filtered off and the EtOH was allowed to evaporate, the product remained as a colorless oil (1.57 g, 2.6×10^{-3} mol, quantitative). R_f=0.53 in Et_2O. The spot is fluorescent on silica when detected by UV_{254nm}.

^{13}C nmr (75.47 MHz), $CDCl_3$, δ: 19.7 (C-4'), 25.5 (C-6), 25.9 (C-3), 26.2 (C-5'), 28.6 (C-7), 29.2 (C-5), 29.3 (C-4), 29.7 (C-2), 30.8 (C-3'), 62.4 (C-1), 65.3 (C-6'), 67.6 (C-8), 98.9 (C-2'), 119.6 (Ar C-2), 120.6 (Ar C-4 and C-6), 131.8 (Ar C-1 and C-3), 146.6 (Ar C-5), 166.1 (C=O).

ms (+LSIMS, mNBA) 606.4 (M+1), 438 (-2xThp).

Protection of the Amine 64 to Afford 65

The amine **64** (1.98 g, 3.27×10^{-3} mol) was dissolved in CH_2Cl_2 (8 mL). Di-tert-butyl dicarbonate (0.71 g, 3.27×10^{-3} mol) was added and the reaction was allowed to continue uncovered for 3 d. Column chromatography on silica gel using 1:1, hexanes:Et_2O as the eluent yielded the product as a clear oil (1.59 g, 2.62×10^{-3} mol, 88%) R_f=0.17 in 2:1, hexanes:Et_2O and the spot did not fluoresce.

^{1}H nmr (300 MHz),$CDCl_3$, δ: 1.27-1.82 (m, 45H), 3.31-3.87 (m, 8H), 4.29 (t, 4H), 4.55 (t, 2H), 6.82 (s, 1H, N-H), 8.20 (d, 2H, C-4 and C-6 aromatic H's, J=1.5 Hz), 8.31 (t, 1H, C-2 aromatic H, J=1.5 Hz).

^{13}C nmr (75.47 Mhz), $CDCl_3$, δ: 19.7, 25.5, 25.9, 26.1, 28.3, 28.6, 29.2, 29.3, 29.7, 30.8, 62.3, 65.5, 67.6, 81.1, 98.8, 123.4, 125.0, 131.7, 138.6, 139.0, 152.4, 165.7.

Deprotection of 65 to 66

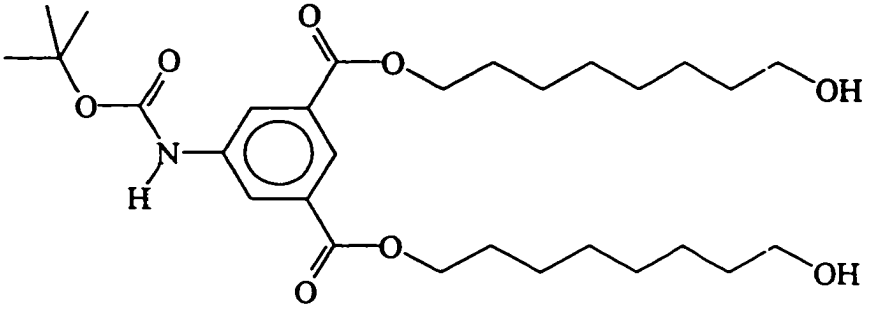

The protected diol **65** (1.33 g, $1.89x10^{-3}$ mol) was dissolved in MeOH (40 mL) and HCl (1 M, 20 mL) was added. The reaction was allowed to continue for 1 h. at r.t. The acid was neutralized with 1 M NaOH and the MeOH was allowed to evaporate. The residue was taken up in CH_2Cl_2 and washed with H_2O twice. The organic layer was collected and dried over $MgSO_4$ and then evaporated. Centrifugal chromatography afforded a white solid (0.71 g, $1.32x10^{-3}$ mol, m.p. 54° 70%) using Et_2O as the eluent.

^{13}H nmr (300 MHz), $CDCl_3$, δ: 1.34-1.45 (m, 16H, $-OCH_2CH_2\underline{CH_2}\underline{CH_2}\underline{CH_2}\underline{CH_2}CH_2CH_2O-$), 1.50 (s, 9H's, 3x-$CH_3$), 1.58 (m, 4H, $-OCH_2\underline{CH_2}CH_2-$), 1.74 (dt, 4H's, $-OCH_2\underline{CH_2}CH_2-$), 3.61 (t, 4H, $HO\underline{CH_2}$, J=6.6 Hz), 4.30 (t, 4H, $-OCH_2$,J=6.6 Hz), 7.01 (s, 1H, N-H, shift varies 6.8-7.5), 8.21 (d, 2H, C-4 and C-6 aromatic H's, J=1.5 Hz), 8.30 (t, 1H, C-2 aromatic H, J=1.5 Hz)

^{13}C nmr (75.47 MHz), $CDCl_3$, δ: 25.6, 25.8, 28.3, 28.6, 29.1, 29.2, 32.7, 63.0, 65.5, 123.4, 124.7, 131.7, 139.6, 152.8 (carbamate, C=O), 165.9 (ester, C=O).

ms (mNBA, +LSIMS): 538.3 (M+1), 482.3, 438.3, 292.1, 208.0

exact mass calculated for $C_{29}H_{48}NO_8$ is 538.3380 found 538.3394

Synthesis of Macrocycle 67

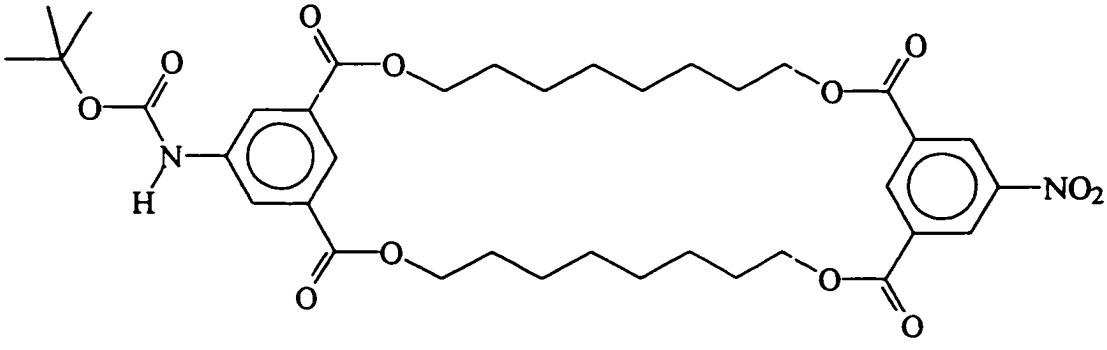

Method 1 High Dilution

5-Nitroisophthaloyl dichloride **45** (0.20g, $7.82x10^{-4}$ mol) and the diol **66** (0.42g, $7.82x10^{-4}$ mol) were dissolved in THF (50 mL) and each placed into a separate syringe. They were added slowly overnight via a driver syringe into a 5L rbf charged with freshly distilled THF (3L) and triethylamine (0.16g, $1.56x10^{-3}$ mol). The solution was stirred vigorously with the aid of a high speed stirrer. The reaction was worked up the following day by first filtering off the TEA·HCl. The THF was evaporated to yield an off-white solid. Centrifugal chromatography using Et_2O as the eluent yielded the product as a white solid. The product was the first band .(0.09g, $1.26x10^{-4}$ mol, 16% yield).

Method 2

5-Nitroisophthaloyl dichloride (0.25g, $1.01x10^{-3}$ mol) and the diol (0.42g, $1.01x10^{-3}$ mol) were each dissolved in THF (50 mL). They were mixed together in an additional 200 mL THF. The solution was stirred vigorously and TEA (0.21g, $2.02x10^{-3}$ mol) was added. The reaction was allowed to continue for 1 h. The triethylamine hydrochloride was removed by filtration. The solvent was evaporated. Centrifugal chromatography using Et_2O as the eluent yielded the product as a white solid. (0.07g, $1.0x10^{-4}$ mol, 10%).

^1H nmr (300 MHz), $CDCl_3$, δ: 1.38-1.52 (m, 25H's), 1.73-1.88 (m, 8H), 4.33 (t, 4H), 4.42 (t, 4H), 6.68 (s, 1H, N-H), 8.18 (2H), 8.25 (1H), 8.83 (1H), 8.89 (2H).

^{13}C nmr(300 MHz), $CDCl_3$, δ: 25.8, 28.3, 28.4, 28.5, 28.9, 65.4, 66.3, 81.2, 123.4, 124.5, 128.2, 131.5, 132.7, 135.3, 139.3, 148.5, 152.4, 163.7, 165.6.

ms (-LSIMS, mNBA): 712.2

Exact mass (-LSIMS, mNBA) calculated for $C_{37}H_{48}N_2O_{12}$ was 712.3208, found 712.3183

5.3 Molecular Mechanics Methodology

The molecular mechanics and dynamics was performed by the CAChe Scientific program suite implemented on a Macintosh IIx. The potential field used in the simulations was the standard MM2 force field[67], including bond stretching, angle bending, stretch-bend, torsion, hydrogen bonding, and Van der Waals terms, where appropriate. The dynamics simulations were done at constant temperature, after an initial equilibration period, and the velocities updated using the Verlet second order numerical integration algorithm[68], forming a

microcannonical ensemble. Starting from a local minimum, each molecule was thermally excited to 100°Cand then allowed to reach a thermal equilibrium over 500 time steps. The actual trajectory was a total of 10,000 time steps, with a sampling every 20 time steps. The sampled geometries were first differentiated by total energy into high, medium and low energy groups. The low energy groups were then inspected in order to assess differences between them. Those which were significantly different were then optimized to the corresponding local minimum using the molecular mechanics modules.

REFERENCES

1. L.M.Mannuzzu, M.M.Moronne, E.Y.Isacoff, *Science*, **1996**, *271*, 213.

2. K.L.Kelner, *Science*, **1996**, *271*, 615.

3. D.P.Corey and J.Garcia-Anoveros, *Science*, **1996**, *273*, 323.

4. C.R.Cantor and P.R.Schimmel, Biophysical Chemistry Part 1: The Conformation of Biological Macromolecules, W.H.Freeman and Company: New York, p.238, 1980.

5. F.M.Menger, D.S.Davis, R.A.Persichetti, J.-J. Lee, *J Am. Chem. Soc.* , **1990**, *112*, 2451.

6. E.Stadler, P.Dedek, K.Yamashita, S.L.Regen, *J. Am. Chem. Soc.*, **1994**, *116*, 6677.

7. T.M.Fyles, K.C.Kaye, T.D.James, D.W.M.Smiley, *Tet. Lett.*, **1990**, *31*, 9, 1233.

8. T.M.Fyles, *Bioorganic Chemistry Frontiers*,1980 pp.71-113.

9. T.M.Fyles and W.F.van Straaten-Nijenhuis, Ion Channel Models, vol. 10, **1996**, pp.53-77.

10. G.W.Gokel and O.Murillo, *Acc. Chem. Res.*, **1996**, *29*, 425

11. a)D.W.Urry, Topics in Current Chemistry, 128, 1985, p.175. b)B.A.Wallace and K.Ravikumar, *Science*, **1988**, *241*, 182.

12. a)A.Finkelstein and R.Holz, Membranes, G.Eisenman ed., M.Dekker, N.Y., vol. 2, p.377, 1973. b)B.deKruiiff and R.A.Demel, *Biochim. Biophys. Acta*, **1974**, *339*, 37.c)J.Bolard, *Biochim. Biophys. Acta*, **1986**, *864*, 257.

13. T.M.Fyles, T.D.James and K.C.Kaye, *J.Am.Chem.Soc.* , **1993**, *115*, 12315.

14. O.Murillo, S.Watanabe, A.Nakano and G.W.Gokel, *J.Am.Chem.Soc.*, **1995**,*117*, 7665.

15. S. H. White Ion Channel Reconstitution, C. Miller, ed., Plenum Press: New York p. 3, 1986.

16. T. M. Fyles, D. Loock, W.F.van Straaten-Nijenhuis, X. Zhou, *J. Org. Chem.*, **1996**, *61*, 8866.

17. I.Tabushi, Y.Kuroda, K.Yokota, *Tet.Lett.*, **1982**, *23*, 44, 4601.

18. Y.Tanaka, Y.Kobuke, M.Sokabe, *Angew.Chem.Int.Ed.Engl.* , **1995**, *34*, 6, 693.

19. G.A.Woolley, A.S.I.Jaikaran, Z.Zhang S.Peng, *J. Am. Chem. Soc.*, **1995**, *117*, 4448.

20. T.M.Fyles, K.C.Kaye, A.Pryhitka, J.Tweddell, M.Zojaji, *Supramolecular Chem.*, **1994**, *3*, 197.

21. V.E.Carmichael, P.J.Dutton, T.M.Fyles, T.D.James, J.A.Swan, M.Zojaji, *J. Am. Chem. Soc.* , **1989**, *111*, 767.

22. T.M.Fyles, T.D.James, K.C.Kaye, *Can. J. Chem.*, **1990**, *68*, 976.

23. Y.Kobuke, K.Ueda and M.Sokabe, *J. Am. Chem. Soc.* , **1992**, *114*, 20, 7618.

24. Y.Kobuke, K.Ueda and M.Sokabe, *Chem. Lett.* , **1995**, *6*, 435.

25. M.R.Ghadiri, J.R.Granja, R.A.Milligan, D.E.McRee, N.Khazanovich, *Nature* , **1993**, *366*, 324.

26. M R.Ghadiri, J.R.Granja, L.K.Buehler, *Nature*, **1994**, *369*, 301.

27. N.Khazanovich, J.R.Granja, D.E.McRee, R.A.Milligan, M.R.Ghadiri, *J. Am. Chem. Soc.*, **1994**, *116*, 6011.

28. a)J.R.Granja, M.R.Ghadiri, *J. Am. Chem. Soc.*, **1994**, *116*, 10785. b) J.D.Hartgerink, J.R.Granja, R.A.Milligan, M.R.Ghadiri, *J. Am. Chem. Soc.* , **1996**, *118*, 43.

29. M.Engels, D.Bashford, M.R.Ghadiri, *J. Am. Chem. Soc.* , **1995**, *117*, 9151.

30. R.J.M.Nolte, A.J.M.Van Beijman, J.G.Neeved, J.W.Zwinker, A.J.Verkley, W.Drenth, *Isr. J. Chem.* , **1984**, *24*, 297.

31. U.Kragten, M.F.M.Roks and R.J.M.Nolte, *J. Chem. Soc., Chem. Commun.*, 1985, *1275*.

32. L.Jullien and J.M.Lehn, *Tet. Lett.* , **1988**, *29*, 31, 3803.

33. J.Canceill, L.Jullien, L.Lacombe and J.M.Lehn, *Helv. Chim. Acta*, **1992**, *75*, 791.

34. M.J.Pregel, L.Jullien, J.Canceill, L.Lacombe and J.M.Lehn, *J. Chem. Soc., Perkin Trans. 2*, **1995**, *3*, 417.

35. M.J.Pregel, L.Jullien and J.M.Lehn, *Angew. Chem. Int. Ed. Engl.*, **1992**, *31*, 12, 1637.

36. A.Nakano, Q.Xie, J.V.Mallen, L.Echegoyen, G.W.Gokel, *J. Am. Chem. Soc.*, **1990**, *112*, 1287.

37. O.Murillo, I.Suzuki, E.Abel, G.W.Gokel, *J. Am. Chem. Soc.*, **1996**, *118*, 7628.

38. N.Voyer, M.Robitaille, *J. Am. Chem. Soc.*, **1995**, *117*, 6599.

39. T.M.Fyles, T.D.James, A.Pryhitka, M.Zojaji, *J. Org. Chem.*, **1993**, *58*, 7456

40. Daniela Loock and Xin Zhou, unpublished results.

41. T.D.James, PhD Thesis, University of Victoria, p. 24.

42. G.W.Gokel, J.C.Medina, C.Li, *Synlett*, **1991**, *10*, 677.

43. J.B.Hendrikson, *J. Am. Chem. Soc.*, **1977**, *99*, 5439.

44. G.J.Powers, R.L.Jones, M.Carruthers, H.van de Fande, H.G.Khorana, *J. Am. Chem. Soc.*, **1975**, *97*, 875.

45. Xin Zhou, Graduate Student, University of Victoria, pore former $A8_2PA8_2A$.

46. C. J. Pedersen, *J. Am. Chem. Soc.*, **1967**, *89*, 7017.

47. One exception to this is found in A.G.Shultz, M.S.Smyth, F.S.Tham, *J. Org. Chem.*, **1991**, *56*, 6952.

48. a)G.Illuminati, L.Mandolini, B.Masci, *J. Am. Chem. Soc.*, **1977**, *99*, 19, 6308. b)C.Galli, L.Mandolini, *J. Chem. Soc. Chem. Commun.*, **1982**, 251. c)R.Cacciapaglia, L.Mandolini, *Chem.Soc. Rev.*, **1993**, *4*, 221. d)G.Illuminati, L.Mandolini, *Acc. Chem. Res.*, **1981**, *14*, 4, 95.

49. K.Ziegler, H.Eberle, H.Ohlinger, *Liebigs Ann. Chem.*, **1933**, *504*, 94.

50. P.G.Owston, R.Peters, E.Ramsammy, P.A.Tasker, J.Trotter, *J.Chem. Soc., Chem. Commun.*, **1980**, 1218.

51. CaCHE program suite, CaCHE Scientific, Inc., Version 3.7, 1994. All molecular mechanics and molecular dynamics computations were done using standard procedures and protocols implemented within the CaCHE program suite. The CaCHE implemented version of the MM2 force field was used throughout.

52. J.S.Bradshaw, K.E.Krakowiak, R.M.Izatt, *J. Heterocyclic Chem.*, **1989**, *26*, 1431.

53. K.E.Krakowiak, J.S.Bradshaw, R.M.Izatt, *J. Heterocyclic Chem.*, **1990**, *27*, 1585.

54. a)M.C.Etter, *Acc. Chem. Res.*, **1990**, *23*, 120. b)J.A.Zerkowski, C.T.Seto, D.A.Wierda, G.M.Whitesides, *J. Am. Chem. Soc.*, **1990**, *112*, 9025. c)J.C.MacDonald, G.M.Whitesides, *Chem. Rev.*, **1994**, *94*, 8, 2383. d)P.Tecilla, V.Jubian, A.D.Hamilton, *Tetrahedron*, **1995**, *51*, 2, 435. e)P.Tecilla, R.P.Dixon, G.Slobodkin, D.S.Alavi, D.H.Waldeck, A.D.Hamilton, *J. Am. Chem. Soc.*, **1990**,*112*, 9408.

55. T.W.G.Solomons, Organic Chemistry, 3rd ed., John Wiley and Sons: New York, p.825, 1984.

56. Aldrich, Catalogue Handbook of Fine Chemicals, 1996-1997.

57. Danny Lau, Graduate Student, University of Victoria.

58. von P.Ruggli, E.Leupin, H.Dahn, *Helv. Chim. Acta.*, **1947**, *XXX*, 1845.

59. The Aldrich Library of ^{13}C and ^{1}H FTNMR Spectra, ed.1, vol.2, p.599C.

60. A. Anantanarayan, P. J. Dutton, T. M. Fyles, M. J. Pitre, *J. Org. Chem.*, **1986**, *51*, 752.

61. S. Buckler, summer student, University of Victoria, 1996.

62. C. Xu, A. McAuley, unpublished results.

63. W.S.Reich, G.G.Rose, W.Wilson, *J. Chem. Soc.*, **1947**, 1234.

64. K.Saigo, N.Kihara, Y.Hashimoto, R-J. Lin, H.Fujimura, Y.Suzuki, M.Hasegawa, *J. Am. Chem. Soc.*, **1990**, *112*, 1144.

65. M.N.Bogdanov, A.U.Leshchiner, L.A.Plyashkevich, A.B.Raskine, *Vysokomol. Soedin., Ser A*, **1967**, *9*, 2198.

66. M.Kato, M.Kageyama, R.Tanaka, K.Kuwahara, A.Yoshikoshi, *J. Org. Chem.*, **1975**, *40*, 1932.

67. N.L.Allinger *J. Am. Chem. Soc.* **1977**, *99*, 8127.

68. M.P.Allen, D.J.Tildesley "Computer Simulation of Liquids", Oxford, Claredon Press, **1991**.